

Predicting the Initial Retroreflectivity of Pavement Markings from Glass Bead Quality

DETAILS

74 pages | 8.5 x 11 | PAPERBACK

ISBN 978-0-309-25890-6 | DOI 10.17226/22639

AUTHORS

Smadi, Omar; Hawkins, Neal; Aldemir-Bektas, Basak; Carlson, Paul; Pike, Adam; and Davies, Chris

BUY THIS BOOK

FIND RELATED TITLES

Visit the National Academies Press at NAP.edu and login or register to get:

- Access to free PDF downloads of thousands of scientific reports
- 10% off the price of print titles
- Email or social media notifications of new titles related to your interests
- Special offers and discounts



Distribution, posting, or copying of this PDF is strictly prohibited without written permission of the National Academies Press. (Request Permission) Unless otherwise indicated, all materials in this PDF are copyrighted by the National Academy of Sciences.

NATIONAL COOPERATIVE HIGHWAY RESEARCH PROGRAM

NCHRP REPORT 743

**Predicting the Initial
Retroreflectivity of
Pavement Markings from
Glass Bead Quality**

Omar Smadi

Neal Hawkins

Basak Aldemir-Bektas

CENTER FOR TRANSPORTATION RESEARCH AND EDUCATION, IOWA STATE UNIVERSITY
Ames, IA

Paul Carlson

Adam Pike

TEXAS A&M TRANSPORTATION INSTITUTE, TEXAS A&M UNIVERSITY
College Station, TX

Chris Davies

POTTERS INDUSTRIES LLC

Conshohocken, PA

Subscriber Categories

Highways • Materials

Research sponsored by the American Association of State Highway and Transportation Officials
in cooperation with the Federal Highway Administration

TRANSPORTATION RESEARCH BOARD

WASHINGTON, D.C.

2013

www.TRB.org

NATIONAL COOPERATIVE HIGHWAY RESEARCH PROGRAM

Systematic, well-designed research provides the most effective approach to the solution of many problems facing highway administrators and engineers. Often, highway problems are of local interest and can best be studied by highway departments individually or in cooperation with their state universities and others. However, the accelerating growth of highway transportation develops increasingly complex problems of wide interest to highway authorities. These problems are best studied through a coordinated program of cooperative research.

In recognition of these needs, the highway administrators of the American Association of State Highway and Transportation Officials initiated in 1962 an objective national highway research program employing modern scientific techniques. This program is supported on a continuing basis by funds from participating member states of the Association and it receives the full cooperation and support of the Federal Highway Administration, United States Department of Transportation.

The Transportation Research Board of the National Academies was requested by the Association to administer the research program because of the Board's recognized objectivity and understanding of modern research practices. The Board is uniquely suited for this purpose as it maintains an extensive committee structure from which authorities on any highway transportation subject may be drawn; it possesses avenues of communications and cooperation with federal, state and local governmental agencies, universities, and industry; its relationship to the National Research Council is an insurance of objectivity; it maintains a full-time research correlation staff of specialists in highway transportation matters to bring the findings of research directly to those who are in a position to use them.

The program is developed on the basis of research needs identified by chief administrators of the highway and transportation departments and by committees of AASHTO. Each year, specific areas of research needs to be included in the program are proposed to the National Research Council and the Board by the American Association of State Highway and Transportation Officials. Research projects to fulfill these needs are defined by the Board, and qualified research agencies are selected from those that have submitted proposals. Administration and surveillance of research contracts are the responsibilities of the National Research Council and the Transportation Research Board.

The needs for highway research are many, and the National Cooperative Highway Research Program can make significant contributions to the solution of highway transportation problems of mutual concern to many responsible groups. The program, however, is intended to complement rather than to substitute for or duplicate other highway research programs.

NCHRP REPORT 743

Project 04-38
ISSN 0077-5614
ISBN 978-0-309-25890-6
Library of Congress Control Number 2013931636

© 2013 National Academy of Sciences. All rights reserved.

COPYRIGHT INFORMATION

Authors herein are responsible for the authenticity of their materials and for obtaining written permissions from publishers or persons who own the copyright to any previously published or copyrighted material used herein.

Cooperative Research Programs (CRP) grants permission to reproduce material in this publication for classroom and not-for-profit purposes. Permission is given with the understanding that none of the material will be used to imply TRB, AASHTO, FAA, FHWA, FMCSA, FTA, or Transit Development Corporation endorsement of a particular product, method, or practice. It is expected that those reproducing the material in this document for educational and not-for-profit uses will give appropriate acknowledgment of the source of any reprinted or reproduced material. For other uses of the material, request permission from CRP.

NOTICE

The project that is the subject of this report was a part of the National Cooperative Highway Research Program, conducted by the Transportation Research Board with the approval of the Governing Board of the National Research Council.

The members of the technical panel selected to monitor this project and to review this report were chosen for their special competencies and with regard for appropriate balance. The report was reviewed by the technical panel and accepted for publication according to procedures established and overseen by the Transportation Research Board and approved by the Governing Board of the National Research Council.

The opinions and conclusions expressed or implied in this report are those of the researchers who performed the research and are not necessarily those of the Transportation Research Board, the National Research Council, or the program sponsors.

The Transportation Research Board of the National Academies, the National Research Council, and the sponsors of the National Cooperative Highway Research Program do not endorse products or manufacturers. Trade or manufacturers' names appear herein solely because they are considered essential to the object of the report.

Published reports of the

NATIONAL COOPERATIVE HIGHWAY RESEARCH PROGRAM

are available from:

Transportation Research Board
Business Office
500 Fifth Street, NW
Washington, DC 20001

and can be ordered through the Internet at:

<http://www.national-academies.org/trb/bookstore>

Printed in the United States of America

THE NATIONAL ACADEMIES

Advisers to the Nation on Science, Engineering, and Medicine

The **National Academy of Sciences** is a private, nonprofit, self-perpetuating society of distinguished scholars engaged in scientific and engineering research, dedicated to the furtherance of science and technology and to their use for the general welfare. On the authority of the charter granted to it by the Congress in 1863, the Academy has a mandate that requires it to advise the federal government on scientific and technical matters. Dr. Ralph J. Cicerone is president of the National Academy of Sciences.

The **National Academy of Engineering** was established in 1964, under the charter of the National Academy of Sciences, as a parallel organization of outstanding engineers. It is autonomous in its administration and in the selection of its members, sharing with the National Academy of Sciences the responsibility for advising the federal government. The National Academy of Engineering also sponsors engineering programs aimed at meeting national needs, encourages education and research, and recognizes the superior achievements of engineers. Dr. Charles M. Vest is president of the National Academy of Engineering.

The **Institute of Medicine** was established in 1970 by the National Academy of Sciences to secure the services of eminent members of appropriate professions in the examination of policy matters pertaining to the health of the public. The Institute acts under the responsibility given to the National Academy of Sciences by its congressional charter to be an adviser to the federal government and, on its own initiative, to identify issues of medical care, research, and education. Dr. Harvey V. Fineberg is president of the Institute of Medicine.

The **National Research Council** was organized by the National Academy of Sciences in 1916 to associate the broad community of science and technology with the Academy's purposes of furthering knowledge and advising the federal government. Functioning in accordance with general policies determined by the Academy, the Council has become the principal operating agency of both the National Academy of Sciences and the National Academy of Engineering in providing services to the government, the public, and the scientific and engineering communities. The Council is administered jointly by both Academies and the Institute of Medicine. Dr. Ralph J. Cicerone and Dr. Charles M. Vest are chair and vice chair, respectively, of the National Research Council.

The **Transportation Research Board** is one of six major divisions of the National Research Council. The mission of the Transportation Research Board is to provide leadership in transportation innovation and progress through research and information exchange, conducted within a setting that is objective, interdisciplinary, and multimodal. The Board's varied activities annually engage about 7,000 engineers, scientists, and other transportation researchers and practitioners from the public and private sectors and academia, all of whom contribute their expertise in the public interest. The program is supported by state transportation departments, federal agencies including the component administrations of the U.S. Department of Transportation, and other organizations and individuals interested in the development of transportation. **www.TRB.org**

www.national-academies.org

COOPERATIVE RESEARCH PROGRAMS

CRP STAFF FOR NCHRP REPORT 743

Christopher W. Jenks, *Director, Cooperative Research Programs*
Crawford F. Jencks, *Deputy Director, Cooperative Research Programs*
Edward T. Harrigan, *Senior Program Officer*
Anthony Avery, *Senior Program Assistant*
Eileen P. Delaney, *Director of Publications*
Doug English, *Editor*

NCHRP PROJECT 04-38 PANEL Materials and Construction—General Materials

Mitch Gipson, *California DOT, Sacramento, CA (Chair)*
Kurtis A. Younkin, *Iowa DOT, Ames, IA*
David Kuniega, *Pennsylvania DOT, Harrisburg, PA*
Xuedong “Vincent” Liu, *Utah DOT, Salt Lake City, UT*
James “Jim” McGraw, *Minnesota DOT, Maplewood, MN*
Masha B. Wilson, *Nevada Department of Public Safety, Carson City, NV*
Carl K. Andersen, *FHWA Liaison*

AUTHOR ACKNOWLEDGMENTS

The authors would like to acknowledge the project panel members for their input and feedback throughout the research project. In addition, we would like to thank the Iowa Department of Transportation for their laboratory assistance. The authors would also like to acknowledge a number of glass bead manufacturers (Greenstar, Potters Industries, and Weissker) for their glass bead donations, without which the project would not have been successful.

FOREWORD

By Edward T. Harrigan

Staff Officer

Transportation Research Board

This report describes a proposed laboratory test method to predict the initial retroreflectivity of pavement markings in the field based on the quality of the applied glass beads. Thus, the report will be of immediate interest to state materials and maintenance engineers with responsibility for specification and placement of pavement marking materials.

NCHRP Project 4-38, “Recommended Laboratory Test for Predicting the Initial Retroreflectivity of Pavement Markings from Glass Bead Quality,” was conducted by Iowa State University, Ames, Iowa, with participation by Texas A&M Transportation Institute, College Station, Texas, and Potters Industries LLC, Conshohocken, Pennsylvania.

The objective of the project was to develop a laboratory test to predict the initial retroreflectivity of pavement markings in the field based on the quality of the glass beads. The test would be rapid (i.e., preparation and testing complete in 24 hours or less); repeatable and reproducible; cost-effective; practical (i.e., suitable for routine use in a state materials testing laboratory); and verified and validated through measurements of the initial retroreflectivity of pavement markings applied in the field.

The initial retroreflectivity of pavement markings depends greatly on the quality of the applied glass beads. Specifications for glass beads usually include percent rounds, gradation, coatings, and refractive index as measures of quality. In the past, field measurements of the initial retroreflectivity of pavement markings prepared with glass beads meeting the same specifications and applied by the same paint crew with identical equipment have substantially varied, suggesting that other bead qualities have a substantial impact on initial retroreflectivity. Differences in initial retroreflectivity of this magnitude can lead to a gain or loss of a year or more in the useful life of a marking.

The project team conducted a combined laboratory and field experiment to develop, verify, and validate the proposed test method. The laboratory experiment addressed the characterization of glass beads and identified a drawdown test as a promising method to relate the laboratory retroreflectivity of glass beads to initial pavement marking retroreflectivity. The field experiment successfully verified and validated the laboratory results through a series of pilot- and full-scale pavement marking applications. Finally, the variability of the drawdown test method was estimated through a modified interlaboratory study. The study included five laboratories, which used the same set of beads and the same paint to conduct the drawdown test independently. Analysis of the results demonstrated that the test method is repeatable and reproducible.

The report fully documents the research; a proposed laboratory test method in AASHTO standard format is presented in Chapter 5: Findings and Recommendations. In addition, the report includes Appendix A: Explanation for Statistical Graphing.

C O N T E N T S

1	Summary
3	Chapter 1 Introduction
3	Project Background
3	Project Objectives
4	Literature Review
5	Application of Bead Properties to Retroreflectivity and Pavement Marking Durability
7	Pavement Marking Installation and Its Impact on Retroreflectivity
8	Bead and Pavement Marking Interaction Using Embedment and Bead Roll
10	Industry Bead Testing Practices
11	Evaluation Tools and Testing Equipment
11	State Department of Transportation Bead Testing Practices
14	Research Approach
14	Background
16	Laboratory Testing
17	Field Testing
18	Proof-of-Concept Testing
19	Field Implementation
19	Report Organization
20	Chapter 2 Experimental Design
20	Proof-of-Concept Testing
20	Introduction
20	Experimental Design
20	Laboratory Testing
22	Field Testing
22	Lab and Field Data
22	Statistical Analysis
33	Field Stripes
34	Comparing Retroreflectivity (Laboratory Test Plates to Field Stripes)
38	Proof-of-Concept Findings and Conclusions
38	Laboratory Testing
38	Materials
40	Physical Characteristics
42	Image Analysis for Air Inclusions
44	Drawdown Sample Preparation
44	Drawdown Procedure
45	Environmental Lab Conditions
45	Retroreflectivity Measurements
47	Bead Embedment and Distribution
47	Results

48	Field Testing
49	Calibration
52	Installation
52	Measurement
53	Laboratory Versus Field Testing
53	Analysis
57	Chapter 3 Field Implementation
57	Calibration
57	Installation
58	Measurement
58	Drawdown Work
58	Drawdown Lab Plates
59	Statistical Analysis
59	Drawdown Plates
61	Field Stripes
61	Results
63	Chapter 4 Drawdown Interlaboratory Study
63	Background
63	Precision Analysis for Five Labs
63	Calculation of the Statistics
63	Precision Statistics
65	Summary of Results
67	Precision Analysis for Three Labs
69	Chapter 5 Findings and Recommendations
69	Findings
69	Proposed Drawdown Test Procedure
73	References
74	Appendix A Explanation for Statistical Graphing
74	Visual Comparison of Group Means

S U M M A R Y

Predicting the Initial Retroreflectivity of Pavement Markings from Glass Bead Quality

Pavement markings contribute to motorist safety by providing much needed guidance along the roadway under both daytime and nighttime conditions. Basic pavement marking characteristics such as color, width, and placement are defined clearly in the current *Manual on Uniform Traffic Control Devices* (MUTCD). However, roadway authorities are left to decide the minimum retroreflectivity (nighttime visibility) thresholds with which they are comfortable, if retroreflectivity is monitored at all, and achieving these thresholds is an ongoing challenge.

This project developed a recommended laboratory test to predict the initial retroreflectivity of pavement markings in the field based on the quality of the glass beads. The test was expected to be rapid (i.e., preparation and testing complete in 24 hours or less), repeatable and reproducible, cost-effective, practical (i.e., suitable for routine use in a state materials testing laboratory), and verified and validated through measurements of the initial retroreflectivity of pavement markings applied in the field.

The work plan for this research included two key components: a laboratory test and a field verification test, along with the necessary data collection efforts for monitoring and evaluation purposes. The laboratory component addressed the characterization of glass beads and the development of a test method to determine potential initial retroreflectivity. This process included identifying key issues that relate specific bead properties to pavement marking retroreflectivity. The field component served as a verification of the laboratory test results. The field component addressed in-place initial retroreflectivity as a function of bead properties, placement, and the interaction of beads and paint. Data collection included bead and paint properties, pavement marking installation information, retroreflectivity measurements, pavement marking images, and video from a high-speed camera.

The research effort was categorized by the following major tasks:

- Proof-of-concept testing
- Laboratory testing procedures
- Field testing procedures
- Laboratory versus field analysis
- Field implementation
- Interlaboratory study
- Drawdown testing procedure

A proof-of-concept test consisted of conducting a small-scale experiment using the recommended drawdown laboratory test procedure on two bead samples. This work was completed prior to the full-scale laboratory evaluation. Each bead sample was evaluated at two laboratories in terms of gradation, roundness, coating, color, and air inclusions. The two

bead samples were used in a small-scale field test to compare lab and field retroreflectivity and to determine optimal installation requirements. Modifications to both the laboratory and field test procedures were considered based on the results from the proof-of-concept testing.

The laboratory portion of this project consisted of using the drawdown method to produce sample plates for a number of different bead packages, which, after 24 hours, were measured in terms of resulting retroreflectivity. The overall goal was to assemble bead packages that give a wide range of gradation, color, presence of coating, and air inclusions, which should result in a wide range of retroreflectivity values. The research team worked with industry to obtain 30 bead packages, which originated from seven manufacturing sources. This was done to create a range of bead quality and physical characteristics. The bead characteristics evaluated included the following:

- Gradation
- Roundness
- Color
- Air inclusions
- Coating

The 30 bead packages had a wide range of rounds (68% to 90%), a range of color (26 to 38 in terms of luminance or L values), a range of air inclusions (0.95% to 7.78%), and very different gradations. The resulting retroreflectivity ranged from a minimum of 290 millicandela (mcd) to a maximum of 680 mcd.

The field testing portion of the research was conducted using 15 different bead packages (as recommended from the laboratory testing) applied on both concrete and asphalt surfaces. The retroreflectivity of these stripes was measured after 24 hours.

A comparison of retroreflectivity readings for the 15 bead packages was completed based on the laboratory and field testing results. A statistical analysis was completed to compare the laboratory and field retroreflectivity data. With two exceptions on concrete, all of the field values were lower than those in the laboratory, which is intuitive given that the laboratory represents ideal conditions. Retroreflectivity values for the markings on concrete were closer to the laboratory values (averaged 17% lower) as opposed to asphalt (averaged 26% lower).

At the completion of the laboratory and field testing, the research team worked with a striping contractor to apply the developed drawdown test procedure using a long-line paint truck. The predicted laboratory pavement marking retroreflectivity values were checked against initial field retroreflectivity, with the difference between the predicted versus observed retroreflectivity values being only 13 mcd in both cases. These results verify that the developed drawdown procedure can predict the retroreflectivity potential of a bead package. This information was used to assist in finalizing the recommended laboratory test procedure.

The variability of the developed drawdown test method was investigated using a modified interlaboratory analysis. This included five different laboratories, which used the same set of beads and the same paint to conduct the drawdown test independently. The drawdown test method developed was proven to be repeatable and reproducible based on an interlaboratory study of five labs.

The research team developed a drawdown laboratory test to determine potential retroreflectivity. The test was calibrated and validated by conducting a field test. The drawdown procedure met the project objectives given that it was rapid (preparation and testing is 24 hours), repeatable and reproducible, cost effective, and easy to use.

CHAPTER 1

Introduction

Project Background

Pavement markings contribute to motorist safety by providing much needed guidance along the roadway under both daytime and nighttime conditions. Basic pavement marking characteristics such as color, width, and placement are defined clearly in the current *Manual on Uniform Traffic Control Devices* (MUTCD).

However, nighttime visibility [generally termed *retroreflectivity* and described in units of millicandela (mcd) per meter squared per lux] is not defined clearly in the current MUTCD. Roadway authorities are left to decide the minimum retroreflectivity thresholds with which they are comfortable (if retroreflectivity is monitored at all), and achieving these thresholds is an ongoing challenge.

Agencies today face an expanding market in choosing pavement marking materials, yet few are as inexpensive and heavily relied upon as latex paint. As an example, the Iowa Department of Transportation (DOT) paints approximately 95% of its system using waterborne paint and AASHTO Type I beads. The placement of these markings can be described as a moving manufacturing process, with outcomes that are highly dependent on a variety of factors.

Through the monitoring of statewide pavement marking performance since 2004, the Center for Transportation Research and Education (CTRE) and the Iowa DOT became aware of the need to record the initial pavement marking retroreflectivity values for the purposes of adjustments to operations, overall quality control, and compliance, with self-imposed minimum initial values.

The Iowa DOT currently uses initial values of 300 mcd for white and 200 mcd for yellow waterborne materials. Requiring high initial retroreflectivity values has generally proved to be a good indicator of bead embedment and effective service life.

For the Iowa DOT, this information is recorded continuously for new markings by positioning an employee roughly 2 miles behind the moving paint operation. An employee uses

a handheld retroreflectometer to record initial values and relay the information up to the paint truck for adjustments when necessary.

These values are also recorded via the global positioning system (GPS) and associated with the roadway segments within a statewide pavement marking management system, which includes both a paint and retroreflectivity database.

In the fall of 2011, 15 samples of AASHTO M247 Type I glass beads were acquired from state DOT material laboratories for testing of heavy metals (not reported here) and retroreflectivity [by the Texas Transportation Institute (TTI)]. The retroreflective performance was measured by creating draw-downs using the same standardized drawdown procedure for each set of beads.

Three replicates were made of each bead sample using a typical white waterborne paint at 15 mil. After the markings cured for 24 hours, a 30-m geometry handheld retroreflectometer was used to measure the retroreflectivity of the pavement marking samples. Retroreflectivity was measured five times in both directions, and an overall average and standard deviation were calculated as shown in Figure 1.

Many specifications require a minimum retroreflectivity of 250 mcd for white pavement markings. While most of the 15 samples met that common specification level, two of the samples did not. This indicates that the AASHTO M247 specification does not include all of the factors that are needed to have confidence in the retroreflective performance of the beads and demonstrates the potential wide range of resulting retroreflectivity values (170 to 475 mcd), reinforcing the need to conduct this research.

Project Objectives

The objective of this project was to develop a recommended laboratory test to predict the initial retroreflectivity of pavement markings in the field based on the quality of the glass beads. The test needed to be rapid (i.e., preparation and

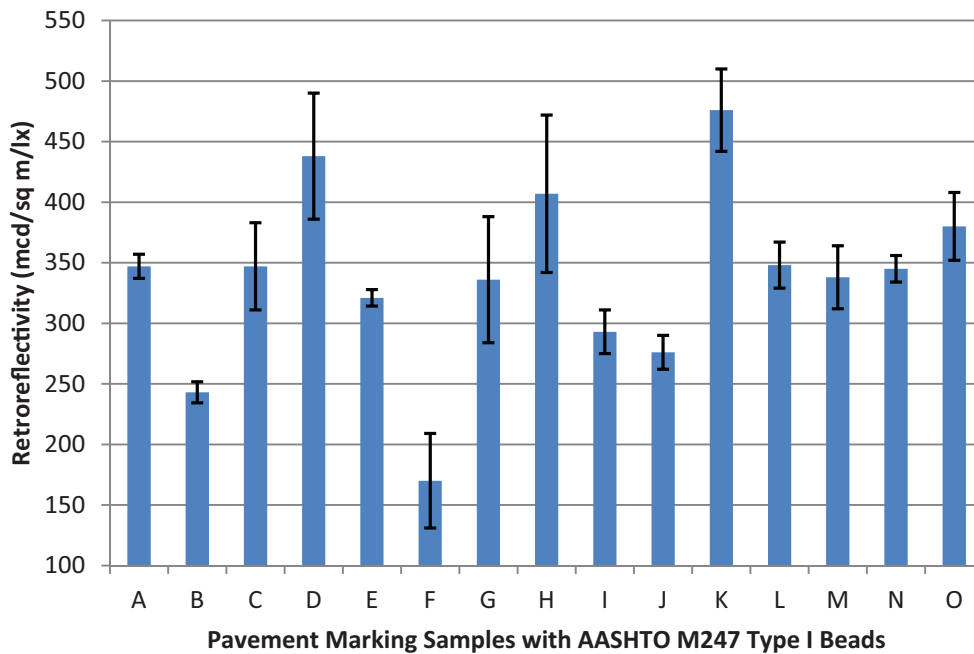


Figure 1. Retroreflectivity from 15 different M247 bead samples.

testing complete in 24 hours or less), repeatable and reproducible, cost-effective, practical (i.e., suitable for routine use in a state materials testing laboratory), and verified and validated through measurements of the initial retroreflectivity of pavement markings applied in the field.

Achieving this objective was dependent on an understanding of glass bead properties and associating these properties with retroreflectivity as a function of proper placement. The research approach combined bead properties, proper placement, monitoring, and assessments of pavement marking performance.

Our conceptual approach is summarized in Figure 2, which shows the interaction between the three different components (beads, placement, and retroreflectivity). As shown, achieving

optimal retroreflectivity requires both good quality beads and proper installation.

Literature Review

The research team divided the literature review task into four different areas: general pavement marking information related to the impact that bead properties, binder quality, and binder and bead interaction have on retroreflectivity; industry practices in the United States and abroad regarding bead testing; evaluation tools and testing equipment; and DOT practices for testing and evaluation of beads. The following sections describe the findings of our literature search related to these four areas.

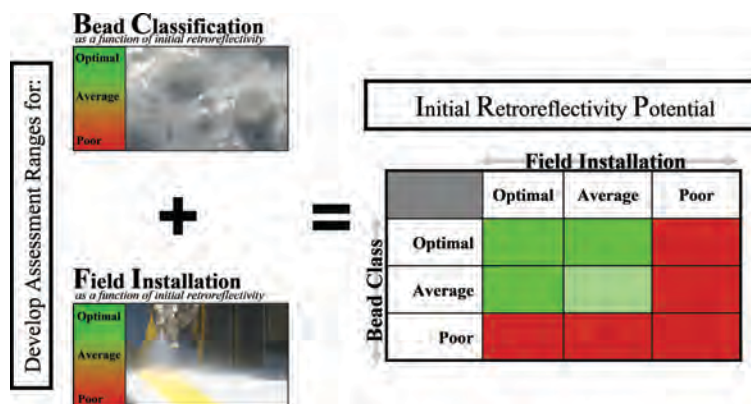


Figure 2. Conceptual research approach.

Application of Bead Properties to Retroreflectivity and Pavement Marking Durability

The ability of pavement marking glass beads to reflect light depends on several factors, including the properties of the glass beads themselves. The properties of the beads are controlled during the bead manufacturing process. These properties can be tested and evaluated prior to installing a pavement marking to make sure acceptable beads are being used.

Several bead properties that can affect retroreflectivity are bead size (gradation), refractive index, roundness, clarity, and coatings on the beads (Gates et al. 2003, McGinnis 2001, Migletz et al. 1994, Texas DOT 2004).

Gradation

Glass bead gradation refers to the size of the beads in a bead mix. When beads are manufactured, they have many different sizes. Bead size is measured and must meet requirements or specifications. Different gradations may be called for, depending on the pavement marking binder used or the desired characteristics of the pavement marking.

Gradations are typically referred to by mesh or sieve size unless standards exist for certain gradations of mixes, such as AASHTO M247 or DOT-specific bead types. A typical gradation is 20 to 80 or 100 mesh, which will contain a certain percentage of beads of different sizes within the range (Austin and Schultz 2006, Migletz et al. 1994, O'Brien 1989, Virginia DOT 2009).

A range of bead sizes is recommended to achieve a good marking initially and to maintain an adequate retroreflectivity level for as long as possible. This recommendation is based on the following (Austin and Schultz 2006, Migletz et al. 1994, O'Brien 1989, Virginia DOT 2009):

- Changing weather conditions can affect drying time, which can affect bead embedment depths. Changes in marking temperature can have the same effect on drying time.
- Changes in marking application speed or pressure may vary the marking thickness, which may not allow enough marking for the large beads to embed properly or may result in too much marking material, resulting in over-embedding small beads. Changing road surface textures can have the same effect on varying marking thickness.
- Beads over-embedded initially may become exposed as the marking wears, renewing retroreflectivity as the marking ages.

Large Beads. Large beads are larger than the standard beads applied to markings; typically, the standard bead is the AASHTO M247 bead gradation. These larger beads may be applied in addition to the standard bead gradation as a double

drop or as part of a larger bead gradation. The development of thicker paint marking systems has allowed an increase in the use of larger glass beads.

Larger glass beads have been found to provide improved wet-weather retroreflectivity over standard glass beads (Carnaby 2006, Kalchbrenner 1989, Texas DOT 2004). This improved retroreflectivity in wet conditions is possible because the larger bead is less likely to be submerged in water and thus is able to offer some retroreflective properties; in contrast, a smaller glass bead that gets covered in water is no longer able to provide any retroreflection.

Larger glass beads are also able to recover retroreflectivity more quickly than smaller glass beads after the rain has stopped. If there is enough water, larger glass beads can still become submerged and will provide little or no retroreflectivity, similar to smaller glass beads.

Larger beads have also been found to provide higher dry retroreflectivity than standard glass beads (Gates et al. 2003, O'Brien 1989, Texas DOT 2004). A Texas DOT study found that Type III beads provided higher levels of dry retroreflectivity for white and yellow markings on a sealcoat road surface than Type II beads (Gates et al. 2003). Type III beads are a larger gradation bead mix, whereas Type II beads are a smaller gradation bead mix.

Refractive Index

Refractive index (RI) is a measure of the speed of light in a medium. The RIs of air and water are approximately 1.0 and 1.3, respectively. The RI is a function of the chemical makeup of the beads, which is determined by the raw material used to make the beads. The RI of pavement marking beads ranges from 1.5 to 2.4 (Benz et al. 2009, Burns et al. 2007, Burns et al. 2008, Migletz et al. 1994).

Refraction is the bending of light as it passes from one medium to another. As the light from a headlamp beam enters a pavement marking bead, the light is refracted downward toward the marking binder material. The light then reflects off the binder material and is refracted back out of the bead. The light that is reflected back toward the light source is the retroreflected light. The RI of the bead determines how much the light will bend and where the light will be focused on the binder behind the marking.

The maximum optical efficiency of a pavement marking bead occurs at an RI of approximately 1.9 under dry conditions (Burns et al. 2007). The reason for this is that a spherical lens is most efficient at reflecting incident light when it focuses the light at the equator of the bead. A bead with an RI of 1.9 will refract the light near the equator of the bead, while a 1.5-RI bead will focus the light above the bead's equator, and a 2.4-RI bead will focus the light below the equator.

Beads that have an RI of 1.5 are made from a hard soda lime glass consisting of crushed scrap windowpane glass, called

cullet. Beads with an RI of 1.9 are made from virgin glass and have a different chemical makeup. Beads with an RI of 1.5 are most commonly used on roadway pavement markings. Cost and durability are the main reasons for using the less efficient 1.5-RI beads instead of the 1.9-RI beads (Austin and Schultz 2006, Burns et al. 2008, Migletz et al. 1994, Texas DOT 2004).

The 1.5-RI beads are less expensive because they are a recycled material with a well-established production technology. The 1.5-RI beads also require fewer pounds of beads to be applied than higher RI beads because the lower RI beads are less dense.

Improvements in glass and ceramic technology could solve the durability issues associated with higher RI beads. The use of 1.9-RI beads should be expected to grow as technology to mass produce them improves (Burns et al. 2008). Currently, beads with an RI of 1.9 are used frequently in airport markings (Austin and Schultz 2006, Migletz et al. 1994).

Roundness and Clarity

Roundness and clarity are two important factors for a glass bead to be highly retroreflective (Austin and Schultz 2006, Benz et al. 2009, Migletz et al. 1994, Texas DOT 2004, Virginia DOT 2009). Beads that are perfectly spherical and clear will reflect better than beads that are not perfectly spherical or are not clear.

The need for roundness can be explained by noting that a round surface will more efficiently bend incoming light downward to the pavement marking material in which the bead is embedded. This light is then reflected off the marking material and back out of the bead, and some of the light is directed back toward the light source. Roundness requirements typically range from 70% to 80% rounded. This would indicate that 70% to 80% of the beads applied to the marking are required to be spherical in shape (McGinnis 2001).

Roundness is influenced greatly by the properties of the blast furnace and the manufacturing process. While the manufacturing process generally produces round glass beads, some of them are not round. Some of the glass beads take on an oval or football shape. Some beads may also adhere to each other in the solidifying process. (Texas DOT 2004, Virginia DOT 2009)

The need for clarity can be explained by noting that if there are particles or air bubbles within or on the bead (large or small) or if there are surface abrasions on beads, they will decrease the amount of light that the bead is able to transmit. Clarity is affected significantly by the manufacturing process and type of raw material used.

Coatings

Bead coatings are used to make beads easier to dispense, increase adhesion to the binder material, and improve embedment and, therefore, retroreflectivity. The three most

common forms of bead coatings are moistureproof coating, adhesion coating, and flotation coating.

Moistureproof Coating. Pavement marking beads can be effective without any coatings. However, in some humid locations, it is difficult to apply the beads because they clump in the bead hopper or tank of the striping machines. To address this problem, a moistureproof coating can be applied to the beads, allowing them to remain free-flowing under all striping conditions.

This coating alleviates problems during application, but it was not designed to improve wet-weather visibility. The moistureproof coating allows the beads to be stored, handled, and applied without clumping. Each manufacturer has its own system to make the beads flow without clumping. Some may use silicone oils or add inorganic particles such as China clay (Virginia DOT 2009).

Adhesion Coating. With some types of beads and marking materials, optimal bead application may be difficult to achieve. Specially formulated bead coatings are available that can assist in achieving proper bead embedment depths. Larger glass beads are often more difficult to embed properly than smaller beads. To help overcome this problem, larger beads are typically coated with an adhesion coating prior to application (Texas DOT 2004, Virginia DOT 2009).

With the development of higher-build materials (epoxy, high-build paints), a number of approaches to improve performance have been taken with the standard 20- to 80-mesh beads that have been the standard gradation. Typical wicking around a 20-mesh bead would increase embedment depth beneficially from 30% to 60%. On the other hand, that same wicking phenomenon would totally submerge an 80-mesh bead in the binder.

Coating all of the beads with a non-adherent silicon coating would prevent wicking but would also result in poor durability. As a result, silane coupling agents (adhesion coatings) were developed that resulted in controlled wicking as well as good bead adhesion to the binder system for the 20- to 80-mesh beads. Silane adhesion coatings are specific to each binder system (Kalchbrenner 1989).

To evaluate the impact of adhesion coatings, a study was conducted to compare markings that had beads applied with and without adhesion coatings. Four pavement markings were applied with uncoated large-sized glass beads, while four more markings were applied with large-sized glass beads with an adhesion coating. Methyl methacrylate (MMA or cold-applied plastic) was the binder material tested.

The pavement markings were installed in a curved area to get more tire wear on the markings for a form of accelerated wear that would not be possible with a marking in a tangent. After 6 months of testing, the adhesion-coated beads remained, whereas most of the non-adhesion-coated beads

were gone. Likewise, a second test using thermoplastic and large-sized beads proved the benefit of adhesion coatings. The bead loss was not so dramatic in this case, although, over years of testing, the adhesion-coated section of the marking has provided a significantly better result (Carnaby 2006).

Flotation Coating. Standard glass beads can be treated with a coating that causes all of them, large and small, to float in wet paint rather than sink completely. Theoretically, because all the beads are exposed, a brighter marking is obtained. Two major advantages associated with flotation beads involve application and performance.

Flotation beads provide a more consistent level of brightness because embedment is more consistent. All beads float, so half of the bead is exposed regardless of variations in paint thickness. With standard beads, if too much paint is applied, a large portion of the beads will sink, reducing initial brightness.

However, given that no flotation beads are sunk under the surface of the marking, a flotation bead marking is often not as durable as a standard beaded marking. As the paint wears, the larger beads will be lost and no new beads will be exposed. As a result of this flotation, coated beads are often used when long-term durability is not as important as initial retroreflectivity (Migletz et al. 1994).

Impact of Binder Quality on Pavement Marking Retroreflectivity

An effective pavement marking system not only requires quality beads but also a quality binder. If either part of the system is not good, or they are not installed properly, then the marking system will not perform as well as it could.

The type of binder used can vary depending on the roads to which the markings are applied or the state in which they are applied.

Binder Material. The components differ depending on the type of pavement marking material used, but all markings have a binder and pigment. The binder is the resin that holds the marking together and creates the bond with the road and the beads, whereas the pigment is what gives the marking its color. Many markings also have fillers or solvents to increase yield or workability. The type and quantity of binder, pigmentation, and filler play an important role in the retroreflectivity of the beads, as well as the daylight appearance of the line (Migletz et al. 1994, Smith and Yin 2005, Virginia DOT 2009).

For example, the National Transportation Product Evaluation Program (NTPEP) found average initial retroreflectivity values for paint and thermoplastic markings to be 250 and 500 mcd per meter squared per lux, respectively, while the maximum values found were 450 and 850 mcd per meter squared per lux for the same paint and thermoplastic markings (NTPEP 1989–1996).

Titanium dioxide (TiO_2) is a common reflective pigment in white pavement markings. Typically, more TiO_2 in a marking allows it to reach a higher retroreflectivity level, but the cost of the pigment needs to be taken into account. While TiO_2 is also present in yellow markings to help improve their retroreflective properties, too much of it has an impact on the color of the marking.

Other pigments exist and may provide better retroreflectivity and color capabilities for marking materials. In a recent study, an engineered pigment was shown to be 50% brighter than TiO_2 (Burns et al. 2007).

Marking binder thickness also has an impact on retroreflectivity and durability (Gates et al. 2003). All pavement marking systems deteriorate over time with exposure to traffic and weather. Typical waterborne paints often have a lower initial retroreflectivity value and degrade at a faster rate than other marking materials. This is partially due to the thin application thickness.

Newer high-build paints allow the paint to be applied more thickly and, therefore, hold larger glass beads for higher retroreflectivity and maintain greater durability (Texas DOT 2004). A thicker application of paint will be effective only if the marking stays adhered to the road surface and maintains a strong bond with the beads. Research indicates that the precise composition of paint is not as important as the precise application of the paint (Migletz et al. 1994).

Binder Color. The color of the pavement marking material can affect how retroreflective the marking will be. It is commonly accepted that yellow markings will have approximately 70% to 80% of the retroreflectivity of white markings (NTPEP 1989–1996). Yellow is less reflective than white because the yellow pigments absorb more of the light than the white pigments. In addition, the thick applications of paint markings and lack of opacity in the pigments often cause yellow paints to have a dull or faded appearance compared to other marking materials (Texas DOT 2004).

However, the retroreflectivity degradation rate has been found to be similar for the two colors (Scheuer et al. 1997).

Pavement Marking Installation and Its Impact on Retroreflectivity

The proper installation of beads and pavement marking materials on a road surface is the most important step in obtaining a pavement marking that will be durable and retroreflective. Improved marking visibility and service life have been demonstrated by properly sizing and treating beads for the thickness and type of binder used (Kalchbrenner 1989).

The road surface to which the pavement marking material is applied and the application of the beads can also have an impact on the quality of the marking.

Road Surface

Depending on where the marking is being applied, the road surface may be asphalt cement concrete (ACC), Portland cement concrete (PCC), or sealcoat surface treatments. Each surface has its own set of problems that affect pavement marking applications. With ACC and PCC, creating a bond between the marking and the road surface is the most prevalent surface-related issue.

The bond can be affected by dirt, texture, chemical or mechanical properties, curing compounds, and road surface oils in new hot-mix asphalt (HMA) (Virginia DOT 2009). However, with proper preparation, a good bond can be obtained on these surfaces.

Markings applied to sealcoat surface treatments face a more difficult scenario. The surface of the sealcoat is not smooth like HMA and PCC surfaces. Less smoothness helps create a mechanical bond between the surface and the marking but hurts retroreflectivity. Pavement markings on rough surfaces commonly have lower retroreflectivity and shorter service lives than identical markings on smooth surfaces (Gates et al. 2003, Texas DOT 2004). Both paints and thicker thermoplastic markings are affected by the surface irregularities.

Two major reasons for lower performance of markings on sealcoat surfaces are that (1) many of the beads fall between aggregates and are not exposed to vehicle lights and (2) the thin binder material on the top of the aggregate results in poor bead adhesion on top, where most vehicle illumination falls (Gates et al. 2003).

Direction of application is also a factor on sealcoat surfaces since the back sides of aggregates tend to receive less binder material and fewer beads. This fact plays a significant role for yellow centerline pavement markings on undivided roads (Texas DOT 2004). Direction of application is also a factor when evaluating the retroreflectivity of markings applied to smooth road surfaces, as described in part of the next section.

Research has been conducted to try to improve paint performance on sealcoat road surfaces (Carnaby 2006). The research used a dual spray system for applying the binder, with the nozzles angled toward one another so the paint streams would intersect with one another at the pavement at approximately a 60-degree angle. By using two binder applicators, the pressure could be reduced. Coupled with the interaction of the paint streams, it was hypothesized that the material was more likely to stay on the top of the markings (Carnaby 2006). This method produced favorable results similar to those of a marking applied on a smooth road surface.

Bead Application

Beads are applied to pavement markings in the field by either spraying under pressure or dropping by gravity onto the wet marking material (Migletz et al. 1994, Texas DOT 2004).

Bead application properties are controlled during striping through adjustments made by the applicator in the field.

The two most important field-controlled properties are bead embedment and the amount and dispersion of the beads on the line. The embedment and dispersion are influenced by characteristics such as bead drop rate, speed of the striping truck, distance between binder applicator and bead applicator, ambient temperature, and viscosity of the binder material. In general, the more beads on a surface, the greater the retroreflectivity, although too many beads may cause retroreflectivity to decrease. Beads should be uniformly applied over the surface of the markings (Texas DOT 2004).

Bead drop rates usually range from 6 to 12 lbs per 100 square feet for thermoplastics and are often higher for paints and epoxies (Texas DOT 2004). The *Standard Specifications for Construction of Roads and Bridges on Federal Highway Projects* (FHWA 2003) specifies that glass beads be applied at a rate of 6 lbs per gallon or 12 lbs per gallon for waterborne paint, depending on the type of glass bead used, and at 12 lbs per 100 square feet for thermoplastics (FHWA 2003). These application rates usually provide optimal coverage.

Yellow centerline pavement markings on undivided roads need to be retroreflective in both directions. Field research on this topic has found that the direction of application has a significant impact on the retroreflectivity of a paint marking. Markings measured in the direction of application had significantly higher retroreflectivity values (Rasdorf et al. 2009). Similar results have been found on thermoplastic markings (Gates et al. 2003).

The differing retroreflectivity by direction can be explained partially due to the striping vehicle imparting forward velocity on the drop-on glass beads, causing them to either roll or burrow into the binder. When the markings burrow into the binder, the opposite direction will have lower retroreflectivity. When the beads bounce and roll, both directions are likely to have lower retroreflectivity.

In either scenario, the retroreflectivity is affected negatively for at least one direction of travel. The faster the application vehicle travels, the higher the likelihood that the beads will either burrow or roll on the marking. Ideally, the beads would drop onto the marking with zero velocity and embed properly so that the beads don't burrow or roll.

Bead and Pavement Marking Interaction Using Embedment and Bead Roll

Two factors that can greatly affect the initial and long-term retroreflectivity of a marking system are bead embedment and bead roll. Bead embedment is how deep the beads sink initially into the binder material when they are applied. Bead roll is a phenomenon caused by the forward velocity of the striping vehicle while applying the pavement markings, which

causes the beads to roll as they hit the binder material. Both of these factors are described in further detail in the following.

Embedment

Pavement marking retroreflectivity and durability are dependent on the embedment depth of the beads in the pavement marking material. Optimum embedment depth of a standard 1.5-RI drop-on glass bead is approximately 60% of the bead diameter (Austin and Schultz 2006, Burns et al. 2007, Dale 1967, McGinnis 2001, O'Brien 1989, Texas DOT 2004, Virginia DOT 2009). Based on the RI of the bead, the optimal embedment depth can vary slightly.

As indicated in the section on refractive index, a 1.9-RI bead focuses the light near its equator, whereas a 1.5-RI bead focuses it above the equator, and beads above 1.9 RI focus it below the equator. Beads with a 1.9 RI only need to be embedded approximately 50%, but for better adhesion to the marking and longer life, an embedment of 60% may be more optimal. Beads that are not embedded properly are either over- or under-embedded; the effects of both are described in the following.

An under-embedded bead is a bead that does not sink deep enough into the binder material. When pavement marking beads are under-embedded, it decreases retroreflectivity and can lead to premature bead loss. Embedment of less than 50% can lead to premature bead loss because of the lack of bonding area between the bead and the binder (Dale 1967, O'Brien 1989, Virginia DOT 2009). This loss of beads can lead to accelerated degradation in the marking retroreflectivity due to fewer retroreflective beads on the marking (Benz et al. 2009).

Even if the beads remain on the marking, the retroreflectivity will not be as high as it would have been with beads embedded properly because some of the light that enters the beads exits out the back and does not reflect off the binder. A common cause for under-embedment with paint pavement markings is when the marking is not applied thickly enough, not allowing the beads to sink in far enough (Austin and Schultz 2006). Figure 3 illustrates under-embedded bead retroreflectivity on the left side.

In other cases, beads may be over-embedded, with beads sinking too deep into the binder material. Over-embedment can cause very low initial retroreflectivity, but the beads are not subject to premature bead loss (Benz et al. 2009, Dale

1967). As the marking wears, the beads actually may become more exposed, providing better retroreflectivity.

Beads typically start to see retroreflectivity levels decrease when embedment goes over 60%, and a sharp decrease occurs when embedment is more than 75% (O'Brien 1989, Virginia DOT 2009).

Too much paint is often a reason for over-embedment of beads in pavement markings (Austin and Schultz 2006). Figure 3 displays over-embedded beads on the right. The over-embedded beads look almost as bright as the properly-embedded beads in the middle, but there is much less area of bead exposed and less light retroreflected with the over-embedded beads on the right. Figure 3 illustrates that, if embedment errors are made, it is better to over-embed the beads than to under-embed them.

Even though an approximately 60% embedment is optimal, not all beads can or will be embedded at this level. Some beads will be embedded completely and others will be loose on top. A new marking will generally have 70% of all the beads embedded completely and the remaining 30% exposed for retroreflection (Burns et al. 2007, Virginia DOT 2009).

There are several ways to make sure beads are applied at the proper embedment depth. Bead coatings can help control the embedment depths of beads in paint or other diffuse reflective binder material. However, proper coatings need to be used based on the marking material, beads, and application thickness to achieve proper embedment and good retroreflectivity and adhesion to the marking. Improper coatings can be counterproductive, resulting in poor pavement marking performance (Burns et al. 2007).

Research by O'Brien (1989) studied the effects of different glass beads in thermoplastic marking materials only. Moistureproof, coated beads were embedded 60% to 65% in thermoplastic drawdown lab testing, whereas uncoated beads were over-embedded at 75% to 90%.

Application of beads at the correct rate is also necessary to get adequate coverage and embedment because many of the beads will sink. Enough beads need to be applied to make sure some remain on top (O'Brien 1989).

Bead embedment in hot-applied materials, such as thermoplastic, can be affected by the material temperature. A hotter binder will allow the beads to sink deeper into it. The pressure of the bead applicator, the distance at which the beads are applied behind the binder, the height of the bead applicator, and the angle of the bead applicator can also affect bead embedment (Texas DOT 2004).

Bead Roll

When installing thin-film markings (such as water-based paint or epoxy), an issue that may cause lower initial retroreflectivity is bead roll. The forward velocity of the striping



Figure 3. Glass bead embedment depth retroreflectivity comparison (Texas DOT 2004).

vehicle will impart a forward velocity on the drop-on glass beads that are applied to the marking. This forward velocity may cause the beads to bounce or roll when they contact the paint surface. The faster the striping vehicle is traveling, the greater the chances of bead roll. When beads roll through a wet thin-film marking material, they can become coated with the binder material, making them useless as retroreflectors, at least initially (Texas DOT 2004).

A method to counteract bead roll is to use a bead application system that can produce a static drop of beads that have little or no forward velocity. Previous research into this type of beading system found that the resulting marking had a much higher initial retroreflectivity measurement. The static drop system resulted in a retroreflectivity average exceeding 500 mcd per meter squared per lux, compared to an approximate average of 300 mcd per meter squared per lux with the standard system (Carnaby 2006).

Summary Information

In summary, the retroreflectivity that a glass bead can provide is affected by many parameters:

- Gradation or size
- RI
- Roundness and clarity
- Coatings on the beads
- Type of marking material binder used
- Road surface conditions
- Quantity and distribution of glass beads on the marking material
- Embedment and roll

The first four parameters listed are controlled during the manufacturing process of glass beads. These parameters can be tested and evaluated prior to installation of pavement markings. The last four parameters are related to the application of the pavement marking system. It takes both good beads and a good application to result in a good pavement marking system that is both retroreflective and durable.

Industry Bead Testing Practices

Because most industry bead-testing practices are considered proprietary and trade secrets, this section examines potential laboratory tests to be considered in this research.

Potential Laboratory Tests and Procedures

Glass Drawdown Test. This is the industry test for determining retroreflectivity of glass beads in paint. The test consists of drawing a controlled thickness of paint onto a flat object (glass plate) and then dropping glass beads onto the

wet paint in a consistent manner. This test is fairly repeatable depending on how much experience the tester has.

Color Patty Test. This test is used in the plastics industry to illustrate the color of the glass when it is used as filler. Glass beads are mixed with a clear binder and allowed to harden in a mold. The cured patty is then measured for color on a colorimeter. Some highway agencies have focused on glass color as a reason for lower field retroreflectivity and, as such, have begun to try to set limits or windows for glass bead color. This test is an attempt to measure that color. Our initial thinking is that this test will not be a good predictor of field retroreflectivity.

Color Ease Drawdown Test. This is a less expensive version of the laboratory drawdown test. It consists of a plastic drawdown bar and cardboard cards. It is not as repeatable as the standard drawdown.

Dipstick Test. This is a field test. One simply dips a tongue depressor into the paint and then dips the tongue depressor covered with wet paint into a bucket of glass beads. The paint is allowed to dry and placed in a fixture to measure retroreflectivity.

90-Degree Double-Sided Tape Test. This test involves dropping glass beads onto white double-sided tape. The beaded tape is then placed into a fixture to measure retroreflectivity at a 90-degree angle.

Beads into Dimpled Aluminum Plate Test. In this test, usually for large beads, a plate of aluminum is prepared with dimples to accept the glass beads. Once the glass beads fill the dimples, retroreflectivity is measured.

Colorimeter Beads in Oil Test. This test involves dropping glass beads into a cuvette of oil and measuring the light transmitted through the cuvette.

Digital Camera Test. This test fabricates a fixture to hold a digital camera at a fixed angle to a drawdown sample and then takes a photo and processes that photo to get retroreflectivity using image analysis. This test can possibly involve infrared (IR) lens filters.

Transparency Test. The concept for this test is to measure glass bead transparency and correlate that value to loss of retroreflectivity due to air inclusions, surface hazing, and/or imperfections.

Digital Photo of Drawdown Filter Test. This test involves taking a picture of a laboratory drawdown of field pavement markings and using digital filters to process the image to view, and possibly count, air inclusions in the glass beads.

The research team focused on the drawdown test as part of a proof of concept to develop the laboratory test to measure potential bead retroreflectivity.

Evaluation Tools and Testing Equipment

The section provides background information on state-of-the-practice tools and equipment used in the analysis of pavement marking installations.

Bead Gun Delivery and Analysis Using High-Speed Video

A recent study by CTRE in Iowa provides an analysis of pavement marking quality versus bead gun delivery (Mizera et al. 2009). The Iowa DOT relies heavily on the performance of waterborne pavement markings in providing guidance to motorists. Waterborne markings are installed by Iowa DOT crews at the district level and cover roughly 95% of the state-maintained system of 9,000 centerline miles. Paint operations within each of the six Iowa DOT districts include both long-line and curb marking crews and equipment.

The Iowa DOT is continually seeking opportunities to improve crew-applied waterborne marking performance in terms of durability and retroreflectivity. Specific to nighttime performance, proper placement (proper embedment, good distribution, and no or minimum bead roll) of the glass beads within the waterborne paint is critical to maximizing retroreflectivity. One of the ways the Iowa DOT improved retroreflectivity was to improve bead placement through slowing its trucks down from around 14 mph to 8 mph.

With a limited painting season and slower truck speeds, the Iowa DOT found it difficult to achieve its desired annual paint coverage. In an effort to increase application speed and yet achieve good bead placement (and resulting retroreflectivity), the Iowa DOT investigated the option of using a new style of bead gun. Mizera et al. (2009) present the findings of a field study that contrasted the use of two different (higher application speed) bead guns and report on their overall effectiveness in balancing proper bead placement over various application speeds from 8 mph to 14 mph. To contrast the different bead delivery systems, the researchers used a high-speed video camera. The high-speed camera and study findings are described in the following.

Data collection took place on the side of the roadway as the striping truck passed by. A Photron Fastcam SA-1 high-speed camera and appropriate lighting were set up along the roadway to capture bead trajectory. The camera is capable of capturing high-speed video with megapixel resolution at 5,000 frames per second (Photron 2010). The camera was set up perpendicular to the direction of the truck to obtain footage that would allow the subjective evaluation of the horizon-



Figure 4. High-speed camera setup on side of roadway.

tal and vertical velocity of the glass beads. Additional video captured footage at an angle that showed the distribution of glass beads as they exited the bead gun. This video footage showed bead gun distribution across the width of the stripe before the beads reached the paint. Figure 4 shows the setup used. Notice the test panel in front of the camera that was collected for each run.

Figure 5 shows the observed bead roll between the two guns, contrasted for the varying application speeds.

The number of beads observed to roll was calculated based on four 1-in. by 1-in. squares, where the number of beads rolling was divided by the total number of beads on each sample.

Figure 6 shows that retroreflectivity was found to decrease with increased bead roll due to higher application speeds (see percent of rolled beads). Higher application speeds were shown to produce less distribution and more bead roll, as represented by the percentages shown.

State Department of Transportation Bead Testing Practices

The second area of the literature review covered current state DOT practices in the area of bead property testing and specifications. We were able to get information from 20 states regarding their bead testing information. Table 1 shows the different states and the bead property tests they conduct or specify.

As Table 1 shows, the majority of the states use gradation, roundness, index of refraction, and clarity as their basic testing criteria. Few states test for chemical content or stability. In addition, less than 50% of the responding states test for the

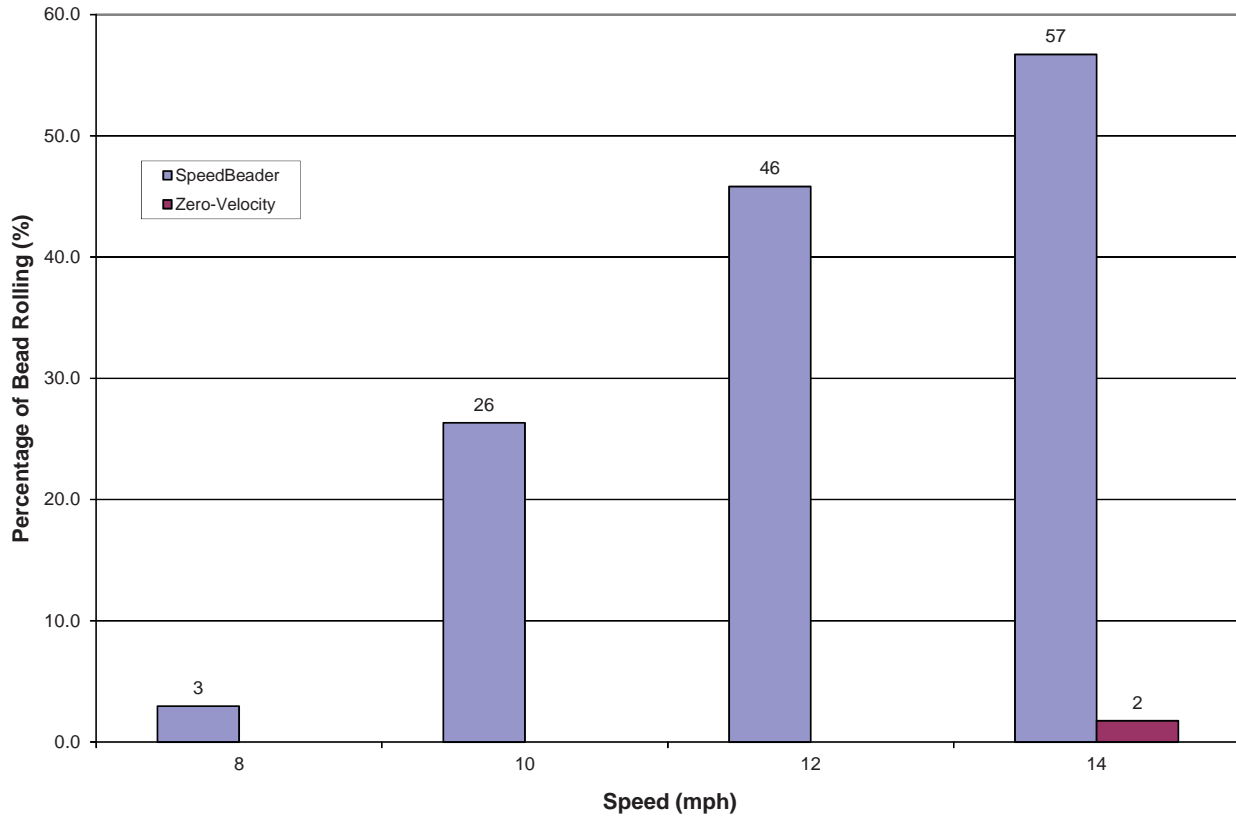


Figure 5. Average distribution of SpeedBead and Zero-Velocity bead guns.

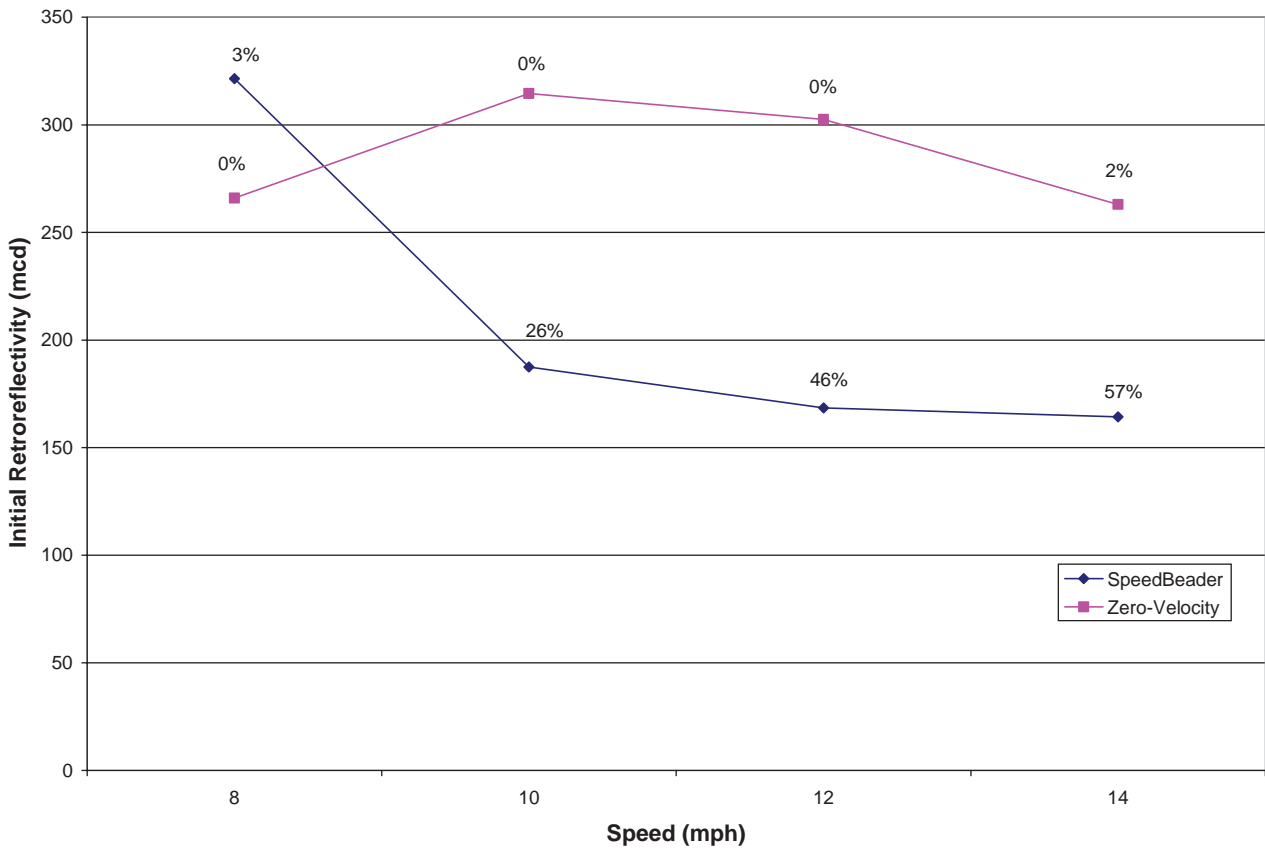


Figure 6. Relationship between initial retroreflectivity and striping truck speed.

Table 1. State DOTs bead testing information.

Highway Agency	Property / Test Method												
	Gradation	Imperfections / Roundness	Index of Refraction	Chemical (Silica) Content	Chemical Stability	Flowing Properties / Moisture Resistance		Adhesive Bead Coating	Clarity	Bulk Color	Specific Gravity	Bead Embedment	References AASHTO M-247
	Sieve Analysis	Vibratile Inclined Plate (ASTM D-1155)	Becke Line / Immersion Method (ASTM D-1214)		Fed Spec TT-B-1325B	Uncoated	Coated	Dansyl Chloride Test			ASTM D-153		
Alaska DOT	X	X	X						X				X
Arizona DOT	X	X	X		X		X		X		X		
California DOT	X	X	X		X		X		X	X	X	X	
Florida DOT	X	X	X						X				X
Georgia DOT													
Illinois DOT	X	X	X	X	X	X	X		X				
Indiana DOT	X	X							X				X
Kansas DOT	X	X							X			X	X
Maryland SHA													
Michigan DOT	X	X	X		X				X				X
Minnesota DOT	X	X						X	X				X
Nebraska DOR			X										
North Carolina DOT	X	X	X	X	X		X		X			X	X
Ohio DOT	X	X	X	X			X	X	X				X
Pennsylvania DOT	X	X							X				X
South Carolina DOT	X	X	X	X			X	X	X				X
Virginia DOT	X	X							X				X
Washington DOT	X	X							X				X
Wisconsin DOT	X	X							X				X

Alaska DOT: Spec Sec 712-2.08 Glass Beads: Only requirement is to meet AASHTO M247 Type I.

California DOT: State Spec 8010-004: Requirement to be “free of air inclusions when viewed under 20X magnification.”

Georgia DOT: Special Provision 657 (preformed plastic): beads shall be “free from air inclusions.” Also, perform Sieve Analysis and Oil Immersion (for Index of Refraction).

Kansas DOT: Requirement for dual coating (moisture-resistant coating and a silane coating for adhesion) but no test specified.

Maryland SHA: Spec Sec 549 Pavement Markings: No Requirements for glass beads. Just requirements for min retroreflectivity.

Michigan DOT: Requirement for dual coating (moisture-resistant coating and a silane coating for adhesion) but no test specified.

Minnesota DOT: Requirement for dual coating—must meet M247 Section 4.4.2 and pass Dansyl Chloride Test. Epoxy: requirement for moisture-resistant coating—must meet M247 Section 4.2.2.

North Carolina DOT: Spec Sec 1087-4: Requirement for 100% North American recycled glass cullet.

Ohio DOT: Beads shall be “free from air inclusions.” Epoxy: Requirement for coating—pass Dansyl Chloride Test (emit yellow-green florescence).

South Carolina DOT: Requirement for 100% recycled glass cullet. Requirement: “free from excessive air bubbles.”

Washington DOT: Spec Sec 9-34.4: Requirement for dual coating (silicone and silane) for beads in waterborne paint.

Wisconsin DOT: Spec Sec 646.2.3: Requirement for dual coating (moisture resistance and adherence).

presence of coating, while only three states test for the type of coating (moisture, adhesion, or flotation). Three states (California, Georgia, and South Carolina) have air inclusion requirements but do not specify a test. As noted previously, air inclusions (or air bubbles) in the beads may be one of the important properties affecting retroreflectivity.

Australia/New Zealand Standards' "Glass Beads for Pavement Marking Materials" (2006) provides a sample specification to analyze air inclusions or optical quality. This standard is summarized as follows.

When a minimum of 200 beads are examined under magnification, the beads shall comply with the following:

- a. Beads shall be clear and shall not show opacity greater than 2% by count. NOTE: Some adhesion-coated beads may be semi-transparent, and this should be taken into account when assessing opacity.
- b. Beads with greater than 25% of the visible area affected by gas inclusions (bubbles) shall be considered defective, and no more than 2% by count shall exhibit this defect.
- c. Bead surfaces shall be smooth and no more than 2% by count shall exhibit surface crazing.

To facilitate counting of the beads, they may be spread in a single layer over the base of a clear, colorless watch glass or recessed microscope slide and placed over a sheet of 1-mm graph paper to allow segmenting of the beads into manageable groups. Petroleum jelly or a similar substance may be used to prevent the beads from moving around during examination.

The research team worked on a procedure to use digital images of beads immersed in oil at 30 times (30×) magnification to quantify air inclusions. These results are discussed in Chapter 2 of this report.

Research Approach

The work plan for this research included two key components: a laboratory test and a field verification test, along with the necessary data collection efforts for monitoring and evaluation purposes (see Figure 7).

The laboratory component addressed the characterization of glass beads and the development of a test method to determine potential initial retroreflectivity. This process included identifying key issues that relate specific bead properties to pavement marking retroreflectivity.

The field component served as a verification of the laboratory test results. The field component addressed in-place initial retroreflectivity as a function of bead properties, placement, and the interaction of beads and paint.

Data collection included bead and paint properties, pavement marking installation information, retroreflectivity

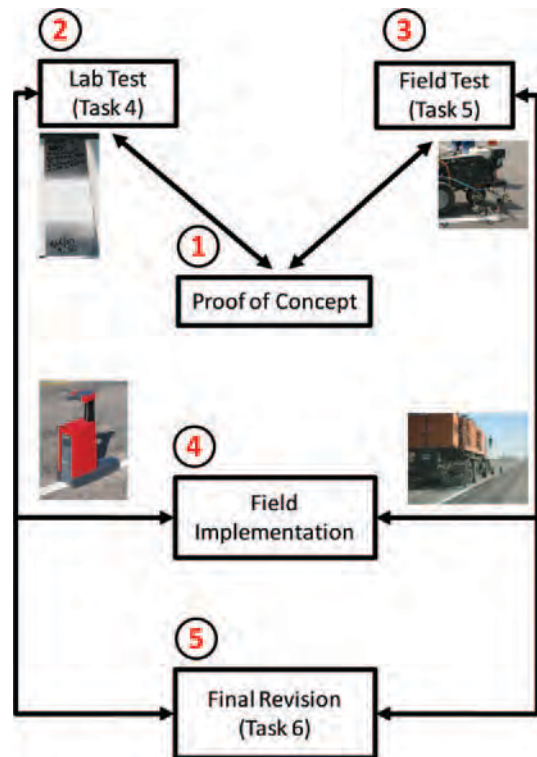


Figure 7. Work plan process overview.

measurements, pavement marking images, and video from the high-speed camera. The following sections identify the details of the work plan.

Background

The objective of this project was to develop a recommended laboratory test to predict the initial retroreflectivity of pavement markings in the field based on the quality of the glass beads. The focus of the research was AASHTO Type I beads in 15-mil waterborne paint.

Typical state DOT practice is to perform physical bead characteristic tests on gradation, roundness, and presence of coating. However, even when beads meet the acceptable ranges within AASHTO specifications, a wide retroreflectivity range can still exist (variations of over 300 mcd, as shown in Figure 1). There are a number of ways to address this variability, with two practical options:

1. **Additional bead testing:** Increasing the number of tests conducted on glass bead physical characteristics could help further illustrate their impact on retroreflectivity. Less common tests are air inclusion, milkiness, color, surface characteristics, chemical composition, and so forth, most of which are mentioned within the AASHTO M247 and federal (TT-B-1325C 2007) specifications under

general requirements: “The beads shall be transparent, clean, colorless glass, smooth and spherically shaped, free from milkiness, pits, or excessive air bubbles.” However, there are neither standardized test methods nor acceptable ranges established for most of these characteristics. In addition, this approach would require an exhaustive sensitivity analysis and the development of multiple standard tests and equipment.

2. **Drawdown testing:** The laboratory drawdown test is a common industry test for determining retroreflectivity of glass beads in paint. It consists of drawing a controlled thickness of standard paint onto a flat object or test panel and then dropping glass beads onto the wet paint in a controlled manner. Once dry, a retroreflectometer is used to measure the resulting retroreflectivity. This test can provide immediate feedback on the retroreflective potential of the glass beads. Data provided by Potters Industries, Inc., demonstrates the utility in using the drawdown test method:

- Laboratory drawdown tests were used to evaluate samples from 10 different sources of glass beads, all of which met the AASHTO Type I specification for gradation and roundness (see Table 2).
- Additional physical characteristics of the glass beads were also measured in terms of color, coatings, and a microscopic evaluation for air inclusions. Rating sys-

tems were applied to the color and air inclusion analysis as a way to rank the sampled M247 beads.

- CIELAB color readings were taken, with each color precisely designated using its specific letter *a* and *b* values and its brightness, *L*. The three parameters in the model represent the luminance of the color, *L* (with the smallest *L* yielding black), its position between red and green, *a* (with the smallest *a* yielding green), and its position between yellow and blue, *b* (with the smallest *b* yielding blue), scaled to a white reference point.
- Retroreflectivity: Drawdown tests were made for each sample at the same time using the same equipment and materials (15 mil of white waterborne latex paint and 8 lbs of glass beads per gallon of latex white paint). Several retroreflectivity readings were taken for each drawdown sample, and an average was computed.
- Results: Retroreflectivity values were contrasted to different parameters, with three examples noted in the following:
 - A. Retroreflectivity by sample: As shown in Table 3, even though each bead sample met current AASHTO specifications, the average retroreflectivity varied from a low of 285 mcd to a high of 445 mcd (160 mcd variation).
 - B. Retroreflectivity versus brightness, *L*: Figure 8 shows the relationship between *L* or brightness and

Table 2. Gradation and rounds by sample.

Gradation & Overall Rounds (by Camsizer)							
	U.S. Sieve / Micron	16 / 1180	20 / 850	30 / 600	50 / 300	100 / 150	Overall Rounds
Sample	Specification (% Passing thru)	100	95-100	75-95	15-35	0-5	80% Min.
1		100.0	99.9	91.6	17.8	0.3	83.4
2		100.0	99.6	90.6	18.0	0.0	83.5
3		100.0	99.6	90.1	19.6	0.8	81.2
4		100.0	99.0	87.3	18.9	0.0	83.0
5		100.0	100.0	91.9	17.4	0.1	82.5
6		100.0	99.6	84.1	23.7	0.1	83.0
7		100.0	99.7	85.3	18.1	0.2	84.7
8		100.0	99.7	86.4	21.7	0.1	81.0
9		100.0	99.4	88.9	17.8	0.2	82.2
10		100.0	99.3	82.3	27.5	0.1	86.2

Table 3. Retroreflectivity by sample.

Sample ID	Average Retroreflectivity (mcd)
1	370
2	285
3	431
4	417
5	398
6	339
7	445
8	328
9	389
10	356

measured retroreflectivity. As can be seen, retroreflectivity improves with increasing bead sample brightness.

- C. Retroreflectivity versus air inclusions rating: Figure 9 shows the relationship between the air inclusions rating and measured retroreflectivity. As can be seen, retroreflectivity declines as air inclusions increase.

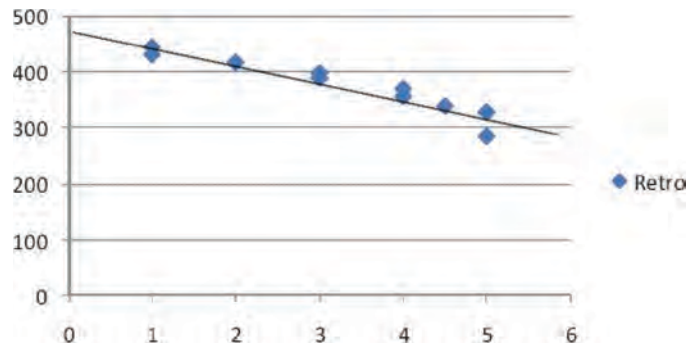


Figure 9. Retroreflectivity versus air inclusions rating.

Experimental Plan.

1. Obtain four bead sources, all matching AASHTO Type I specifications concerning gradation, roundness, and coating. The four bead sources will be selected to give a range of color and air inclusions to allow testing on the impact each of these items has on initial retroreflectivity.
2. Each bead source will consist of 18 different bead packages according to the following:
 - a. Roundness: High, moderate, and low.
 - b. Gradation: High (more large beads), moderate, and low (more fines).
 - c. Coating: Dual and none.

Table 4 represents 25% of the testing plan, given that four bead sources would be used. The quantities show either 2 lbs or 100 lbs, with the larger quantity to be used in the field evaluation (12 bead packages). In total, there would be 72 bead packages for drawdown testing. Repeatability testing would

Laboratory Testing

Based on the potential laboratory tests and procedures, literature reviews, team discussions, and industry information, the research team recommended the following testing approach.

Recommended Laboratory Test

Use the drawdown test method to explore the sensitivity of the initial retroreflectivity to varying glass bead characteristics, as detailed in the following.

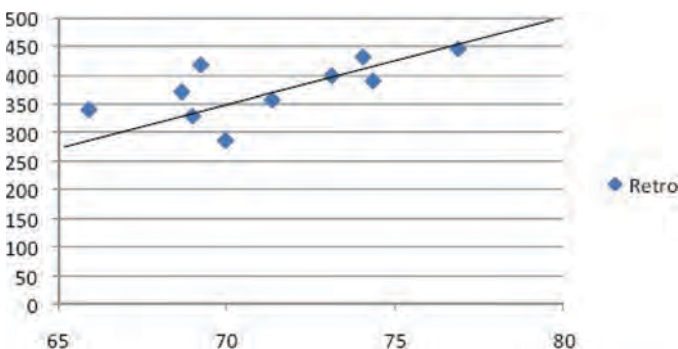


Figure 8. Retroreflectivity versus brightness, L.

Table 4. Laboratory test matrix.

Source	Bead Package	% Rounds	Gradation	Coating	QTY (lbs)
A	1	60	low	none	100
A	2	70	low	none	2
A	3	80	low	none	2
A	4	60	med	none	2
A	5	70	med	none	2
A	6	80	med	none	2
A	7	60	high	none	2
A	8	70	high	none	2
A	9	80	high	none	2
A	10	60	low	dual	2
A	11	70	low	dual	2
A	12	80	low	dual	2
A	13	60	med	dual	2
A	14	70	med	dual	100
A	15	80	med	dual	2
A	16	60	high	dual	2
A	17	70	high	dual	2
A	18	80	high	dual	100

bring the total number of drawdown tests to 80 (four bead packages will have three drawdown tests).

Experimental Procedure.

1. For each bead package from each source:
 - a. Measure rounds, gradation, air inclusions, and color.
 - b. Develop a drawdown with standard (to be determined) white latex paint at 15 mil.
2. Randomly choose four bead packages (5%) to conduct repeatability testing (three drawdowns for each package).
3. Drawdown standard:
 - a. Create a daily drawdown standard with a controlled bead sample for quality control purposes.
 - b. Sample plates: glass substrate (standard size used in the Potters Industries, Inc., research and development lab).
 - c. Bead load rate: equivalent of 8 lbs per gallon.
 - d. Binder: latex paint (control paint, such as Sherwin-Williams).
 - e. Drawdown rate for 15 mil wet (control application speed and pressure).
 - f. Sample line width: 4-in. lines.
4. Drawdown retroreflectivity measurement technique:
 - a. Time before retroreflectivity measurement: 24-h cure time ± 4 h.
 - b. Tip and brush excess beads.
 - c. Use 30-m geometry handheld device.
 - d. Take five readings from five different locations in each direction (total of 10 readings per drawdown).

Field Testing

The field component serves as a verification of the laboratory test results. The field component addressed in-place initial retroreflectivity as a function of bead properties, placement, and the interaction of beads and paint.

Testing Facilities

The field portion of this research effort required dedicated facilities and equipment to control the evaluation of initial retroreflectivity. This testing was completed at the Texas A&M University Riverside Campus, shown in Figure 10.

The Riverside Campus is currently home to the TTI/Texas DOT mobile retroreflectivity certification course. The course has 37 different pavement marking lanes ranging in length from 0.4 to 0.5 miles. Figure 11 shows a portion of the certification course. This same area of the facility, as well as an adjacent asphalt area, provided sufficiently large areas where pavement markings could be applied to compare the controlled field application to the laboratory portion of the research.



Figure 10. Texas A&M University Riverside Campus.

Equipment

A self-propelled paint striper was used to apply markings. The striper is capable of applying standard pavement marking paint and beads at standard rates. The striper also has the ability to vary the speed of application or bead drop rate to levels desired for the testing. Measurement equipment applicable to the research is as follows (also see Figure 12):

- Pavement marking retroreflectometer: LTL-X.
- Luminance meter: Prometric PM-1600 series CCD photometer.
- Pavement marking applicator: Graco LineLazer striper.

Figure 13 shows the Graco LineLazer IV 5900 striper used, which has an EZ Bead glass bead applicator and LineDriver ride-on drive system. The LineLazer IV 5900 can output up to 1.6 gallons per minute of paint with a maximum pressure of 3,300 psi. All forms of standard traffic paint can be applied using the system. The drive system and pump engine use an advanced vibration reduction system to eliminate engine vibrations for improved line quality. The digital display on the striper outputs psi, mil instant average, lineal foot, gallons, and mil total. The LineDriver system can maintain forward



Figure 11. Mobile retroreflectivity certification course.



Figure 12. Pavement marking evaluation equipment.

speeds of up to 10 mph. Supplementary drive systems may be used to provide higher speeds than those provided by the LineDrive system.

Field Testing Plan

The research plan included a field evaluation of 12 different bead packages, as shown in Table 5. As shown, the bead rate and paint thickness would remain constant. Application speed, bead characteristics (bead package), and surface type would be varied to determine these variables' impact on initial retroreflectivity. In total, there would be a maximum of 72 field tests. Repeatability testing would bring the total number to 80 (four bead packages would be installed three different times). The final number of field tests would be dependent on the outcome of the drawdown laboratory tests.

Field Testing Procedure.

1. Each field test consisted of placing a 20-ft-long stripe in addition to a 2-ft sample plate.
2. High-speed video was filmed during each installation.
3. After placement, digital (macro) images were taken.



Figure 13. Striping equipment (Graco 2010).

Field Test Retroreflectivity Measurement Technique.

1. Allow time before retroreflectivity measurement: 24-h cure time ± 4 h.
2. Brush excess beads.
3. Use 30-m geometry handheld device.
4. For each 20-ft stripe, take 16 readings in each direction (total of 32 readings per stripe).
5. For each 2-ft sample plate, use the drawdown retroreflectivity technique as discussed in the laboratory test method procedure.

Proof-of-Concept Testing

The proof-of-concept testing consisted of conducting a small-scale experiment using the recommended drawdown laboratory test procedure on two bead samples. This work was completed prior to the full-scale laboratory evaluation. Each bead sample was evaluated in terms of gradation, roundness, coating, color, and air inclusions at two laboratories. The two bead samples were used in a small-scale field test to compare lab and field retroreflectivity and to determine optimal installation requirements. Modifications to both the laboratory and field test procedures were considered based on the results from the proof-of-concept testing.

Proof-of-Concept Testing Procedure

1. Acquire two bead packages of 200 pounds each (high-/low-end beads) that meet AASHTO Type I specifications.
2. Measure bead physical characteristics.
3. Perform three drawdowns per bead package, as specified in the recommended laboratory test.
4. Compare retroreflectivity measurements of drawdowns.

Table 5. Field testing plan.

Source	Bead package	Speed (mph)			Bead Rate 8 lbs/gal	Paint Thickness 15-mil	Surface	
		low	mid (opt)	high			Asphalt	Concrete
A	1	x	x	x	x	x	x	x
A	14	x	x	x	x	x	x	x
A	18	x	x	x	x	x	x	x
B	1	x	x	x	x	x	x	x
B	14	x	x	x	x	x	x	x
B	18	x	x	x	x	x	x	x
C	1	x	x	x	x	x	x	x
C	14	x	x	x	x	x	x	x
C	18	x	x	x	x	x	x	x
D	1	x	x	x	x	x	x	x
D	14	x	x	x	x	x	x	x
D	18	x	x	x	x	x	x	x

5. Establish optimal installation settings and complete field installation for the two bead packages.
6. Conduct field retroreflectivity measurements.
7. Conduct an analysis of the proof-of-concept data.

Field Implementation

At the completion of both the laboratory and field testing, the research team worked with a striping contractor in Texas to apply the developed drawdown test procedure using a long-line paint truck. The predicted laboratory pavement marking retroreflectivity values were checked against initial field retroreflectivity. The field-applied pavement markings were installed using a long-line paint truck under normal field conditions. This information was used to assist in finalizing the recommended laboratory test procedure.

Report Organization

The remainder of this report is organized as follows. Chapter 2 summarizes the experimental design and provides:

- Proof of concept;
- Laboratory testing procedures, data, and results;
- Field testing procedures, data, and results; and
- Laboratory versus field analysis.

Chapter 3 covers the field implementation, with a focus on calibration, installation, and retroreflectivity measurements.

Chapter 4 provides the results from the drawdown inter-laboratory study (ILS).

Chapter 5 contains the overall findings and recommendations, including the drawdown testing procedure in the format of a proposed AASHTO standard method of test.

CHAPTER 2

Experimental Design

Proof-of-Concept Testing

Introduction

The proof-of-concept testing included conducting a small-scale experiment using the recommended drawdown laboratory test procedure on several bead packages. This work was completed prior to the full-scale laboratory evaluation. Each bead package was evaluated in terms of gradation, roundness, coating, and color. The bead samples were used in a small-scale field test to compare lab and field retroreflectivity and to determine optimal installation requirements. Modifications to the laboratory and field test procedures were considered based on the results from the proof-of-concept testing.

Proposed proof-of-concept testing procedure:

1. Acquire five bead packages (high-/low-end beads) that meet AASTHO Type I specifications.
2. Measure bead physical characteristics.
3. Perform two drawdowns per bead package, as specified in the recommended laboratory test.
4. Compare retroreflectivity measurements of drawdowns.
5. Establish optimal installation settings and complete field installation for the five bead packages.
6. Conduct field retroreflectivity measurements.
7. Conduct an analysis of the proof-of-concept data.

Experimental Design

The laboratory portion of this proof of concept consisted of using the drawdown method to produce two sample plates for each of the five bead packages and, after 24 hours, to measure the resulting retroreflectivity for each plate. Two additional sample plates were produced for bead packages 2 (lowest retroreflectivity) and 4 (highest retroreflectivity).

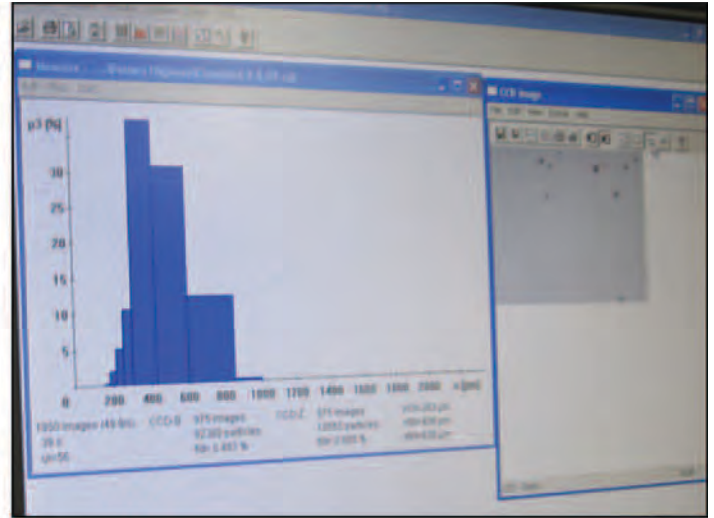
The field activities included placement of two 20-ft stripes for each of the five bead packages using a small-scale paint

striper. Retroreflectivity measurements were measured for each stripe after 24 hours. The lab and field retroreflectivity measurements were then compared for each bead package, and a statistical analysis was conducted.

Laboratory Testing

With a few exceptions, the research team followed the proposed proof-of-concept procedure; it evaluated five bead packages as opposed to two and produced two drawdown sample plates per bead package as opposed to three. A description of the laboratory testing activities follows, and Figure 14 provides photos of the process.

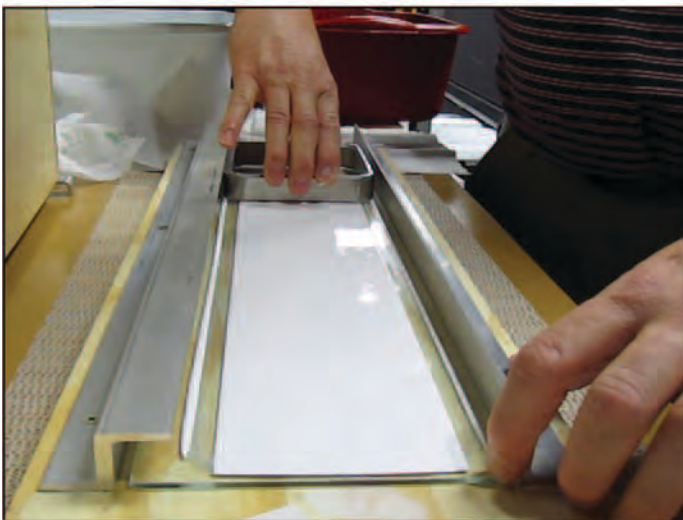
1. Acquired five (200-lb) bead packages (labeled 1 through 5) in an attempt to cover a range of bead characteristics that would deliver different retroreflectivity ranges. All bead packages met the AASHTO M247 specifications for both roundness and gradation.
2. Measured the bead characteristics for each bead package, including gradation, roundness, coating, color, and air inclusion. All bead samples for the proof-of-concept testing had a dual coating (of silicone and silane, which provides both anti-wetting and adherence properties).
3. Bead samples were prepared for the drawdowns using the following procedure:
 - a. Beginning with a 50-lb bag for each of five bead packages, a 16:1 splitter was used to obtain a 3-lb sample for each bead package.
 - b. Each 3-lb sample was further reduced (four times) using a 1:1 splitter to obtain a small enough sample (80 to 90 g) to be used in the lab for the drawdowns.
4. Performed drawdowns for each bead package as noted:
 - a. Equipment: Bead delivery box, wet film applicator to deliver 15 mil of paint with a width of 4 in., bucket of water.



Five bead types in 50-pound bags. Camsizer being used to measure bead characteristics.



Using a 16:1 splitter to get a 3-pound sample and a 1:1 splitter for drawdown sample size.



Delivering paint on the sample plate and measuring retroreflectivity after 24 hours.

Figure 14. Laboratory testing images.

- b. Materials:
 - i. Sample plate: 24 in. long by 6 in. wide (glass).
 - ii. Paint: Sherwin-Williams TM2152 White (from a small, airtight container), see <http://www.paintdocs.com/webmsds/webPDF.jsp?SITEID=STORECAT&doctype=PDS&lang=E&prodno=TM2152>.
 - iii. Beads: 17 g per drawdown plate (for each of the five bead packages).
 - c. Procedure:
 - i. Labeled the sample plate using bead package, sample number, and date.
 - ii. Applied paint using the wet film applicator.
 - iii. Dropped the applicator in water to clean.
 - iv. Positioned the bead delivery box over the sample plate and dropped the beads.
 - v. Removed the sample plate and allowed to dry for 24 hours.
 - vi. Repeated for each bead package.
 5. Retroreflectivity measurements:
 - a. After 24 hours, lightly brushed the excess beads off each sample plate.
 - b. Using a handheld 30-m geometry device, measured retroreflectivity at five random locations in both directions (forward and reverse) for each sample plate.
 - c. Repeated for a second set of retroreflectivity measurements per plate.
 - d. Recorded all readings and calculated averages.
2. Captured beads from the striper bead gun for a set time interval and weighed the sample to calibrate to 8 lbs of beads per gallon of paint.
 3. Checked bead distribution and embedment.
 4. Captured bead and paint interaction using the high-speed camera.
 - ii. Placed two 20-ft stripes with a 20-ft gap.
 - iii. Repeated for each bead package.
 2. Retroreflectivity measurements:
 - a. After 24 hours, swept each line to remove excess beads.
 - b. Using a handheld 30-m geometry device, measured retroreflectivity at 16 random locations in both directions (forward and reverse) for each stripe.
 - c. Repeated for a second set of retroreflectivity measurements per stripe.
 - d. Recorded all readings and calculated averages.

Lab and Field Data

This section documents the data obtained during the proof-of-concept testing (physical bead properties and lab and field retroreflectivity measurements).

Bead Properties

Table 6 shows the physical bead properties measured for each of the five bead packages.

A Camsizer was used to obtain the gradation and roundness measurements. CIELAB color readings were measured for the color of each bead package. Percent air inclusions were determined using image analysis (see the Image Analysis section later in this chapter).

Laboratory Retroreflectivity

Table 7 shows the average retroreflectivity numbers for each bead package per sample plate and direction.

Field Retroreflectivity

Table 8 shows the average retroreflectivity values for each bead package per stripe, set, and direction. The data show that bead package 4 has the highest retroreflectivity level and that bead package 2 has the lowest, which matches the laboratory measurements.

Statistical Analysis

This section summarizes the statistical analysis completed for the lab and field retroreflectivity data. The statistical analysis was completed using JMP base version 8.0.1.

Field Testing

The research team followed the proposed proof-of-concept procedure as detailed in the following. Figure 15 provides photos of the process.

1. Placed two 20-ft-long field stripes for each bead package as noted:
 - a. Equipment: TTI's striper is a Graco LineLazer IV 5900 with EZ Bead glass bead applicator and LineDriver ride-on drive system.
 - b. Materials:
 - i. Paint: Sherwin-Williams TM2152 White.
 - ii. Bead: 50-lb bag for each of the five bead packages.
 - c. Procedure:
 - i. Calibrated paint striper in terms of applied paint thickness (15 mil wet) and bead delivery (8 lbs per gallon).
 1. Using sample plates and a weight scale, calibrated the paint striper speed and paint gun position to achieve a 4-in. wide stripe at 15-mil wet thickness based on delivered paint weight.



Calibrating the striper using a scale to ensure a delivered thickness of 15 mil wet.



Using a scale to calibrate bead delivery rate to 8 pounds per gallon.



Placing two 20-foot stripes for each of the 5 bead packages. Measuring retroreflectivity after 24 hours.

Figure 15. Field testing images.

Table 6. Bead properties.

U.S. Sieve	AASHTO M247 % Passing Through	Bead Package				
		1	2	3	4	5
18	100	99.9	99.9	99.63	99.97	99.99
20	95–100	99.77	99.72	98.52	99.83	99.78
30	75–95	86.45	89.27	88.55	90.04	88.47
40		67.53	53.44	60.23	61.49	46.42
50	15–35	30.99	20.4	19.37	27.27	21.1
80		4.68	3.12	1.73	4.15	1.31
100	0–5	1.34	0.82	0.47	1.43	0.23

% Rounds	80 min	82.3	78	85	75.5	80
Color, L	White = 89.17	59.3	59.9	59.57	61.78	56.39

Air inclusions (AI)	% of sample area with AI	8.3	4.1	6.5	2.8	8.2
---------------------	--------------------------	-----	-----	-----	-----	-----

Table 7. Laboratory retroreflectivity measurements.

Lab Drawdowns May 20th, 2010 @ TTI		Measurements at 10 a.m.			
		Measurement Set 1		Measurement Set 2	
Bead Package	Sample	Forward	Reverse	Forward	Reverse
1	A	407	403	405	404
	B	397	389	396	388
2	A	372	327	369	326
	B	346	349	344	352
3	A	387	377	387	376
	B	386	380	388	378
4	A	426	424	434	421
	B	427	416	427	419
5	A	385	382	384	377
	B	384	382	379	389

Table 8. Field retroreflectivity measurements.

Field Striping May 20th, 2010 @ TTI		Measurements after 18 hours				Measurements after 24 hours	
		Measurement Set 1		Measurement Set 2		Measurement Set 3	
Bead Package	Sample	Forward	Reverse	Forward	Reverse	Forward	Reverse
1	A	364	305	367	306	375	311
	B	356	304	359	303	371	317
2	A	310	277	312	276	316	280
	B	321	264	325	262	326	263
3	A	346	309	349	311	359	312
	B	349	305	353	303	358	307
4	A	373	326	378	322	383	325
	B	392	340	391	339	396	346
5	A	335	287	337	281	337	289
	B	345	306	343	309	349	315

Laboratory Sample Plates

Figure 16 shows the laboratory plates and retroreflectivity measurement procedures.

The designations used within the statistical analysis were as follows:

- RL: Retroreflected luminance (millicandelas per meter squared per lux).
- Bead package: Numbers that designate five different bead packages used in the study (1 through 5).
- Sample plate: Two drawdown sample plates for each bead package (A and B).

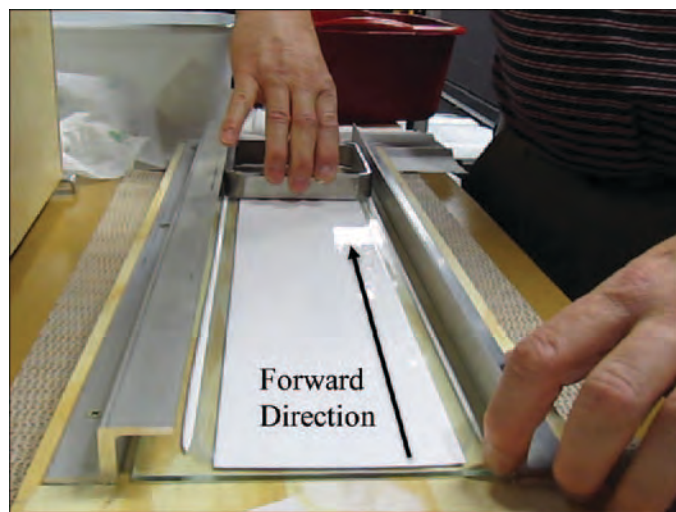
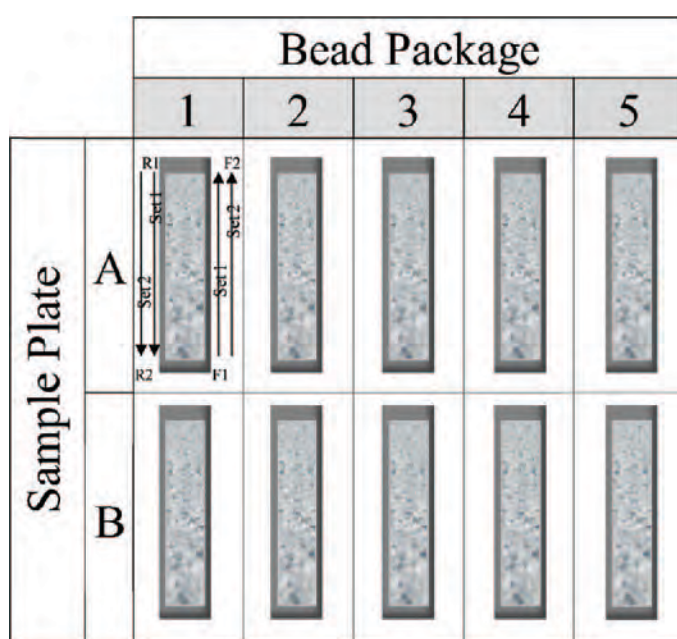


Figure 16. Laboratory drawdown designations.

- Direction: The direction of retroreflectivity readings (*F* for forward and *R* for reverse, with *forward* defined as the direction in which the paint was applied to the sample plate).
- Set: Retroreflectivity measurement set (Set 1 and Set 2) with retroreflectivity readings taken twice for each sample plate and direction (e.g., Plate 1A forward direction was measured twice as Set 1 and Set 2), and each measurement set consisted of five readings.

Effect of Bead Package on Retroreflectivity

Figure 17 shows the retroreflectivity measurements by bead package, direction measured, and set and also includes summary statistics for the data.

One-way analysis of variance (ANOVA) was used to compare the mean retroreflectivity values of different beads. Figure 18 summarizes the results. The ANOVA here tests the null hypothesis that the mean retroreflectivity values of different beads are the same. (In other words, bead type does not have an effect on retroreflectivity readings in this data set.) The coefficient of determination (R^2) is over 85%, which can be interpreted as more than 85% of the variation being accounted for by fitting means to each bead type.

The *F*-statistic of the ANOVA, which is smaller than 0.001, provides significant evidence to reject the null hypothesis. Therefore, bead type in this data set has an effect on mean retroreflectivity value, and the mean retroreflectivity value from at least one bead type is different from the other groups.

The mean retroreflectivity between bead pairs was compared by Tukey-Kramer comparison. Figure 19 summarizes the results.

At the 95% confidence level, the mean retroreflectivity values from beads 1, 2, and 4 are significantly different, while the mean retroreflectivity from beads 3 and 5 cannot be distinguished.

Effect of Sample Plate on Retroreflectivity

Figure 20 of the one-way ANOVA results for the sample effect shows that the variation in the retroreflectivity values cannot be attributed to sample effect. The high *F*-statistic value of 0.38 indicates that we do not have significant evidence to reject the null hypothesis (that the two retroreflectivity mean values are the same). Comparing the means by the Tukey-Kramer test also supports the same conclusion that the means of retroreflectivity values from different samples are not statistically different from each other.

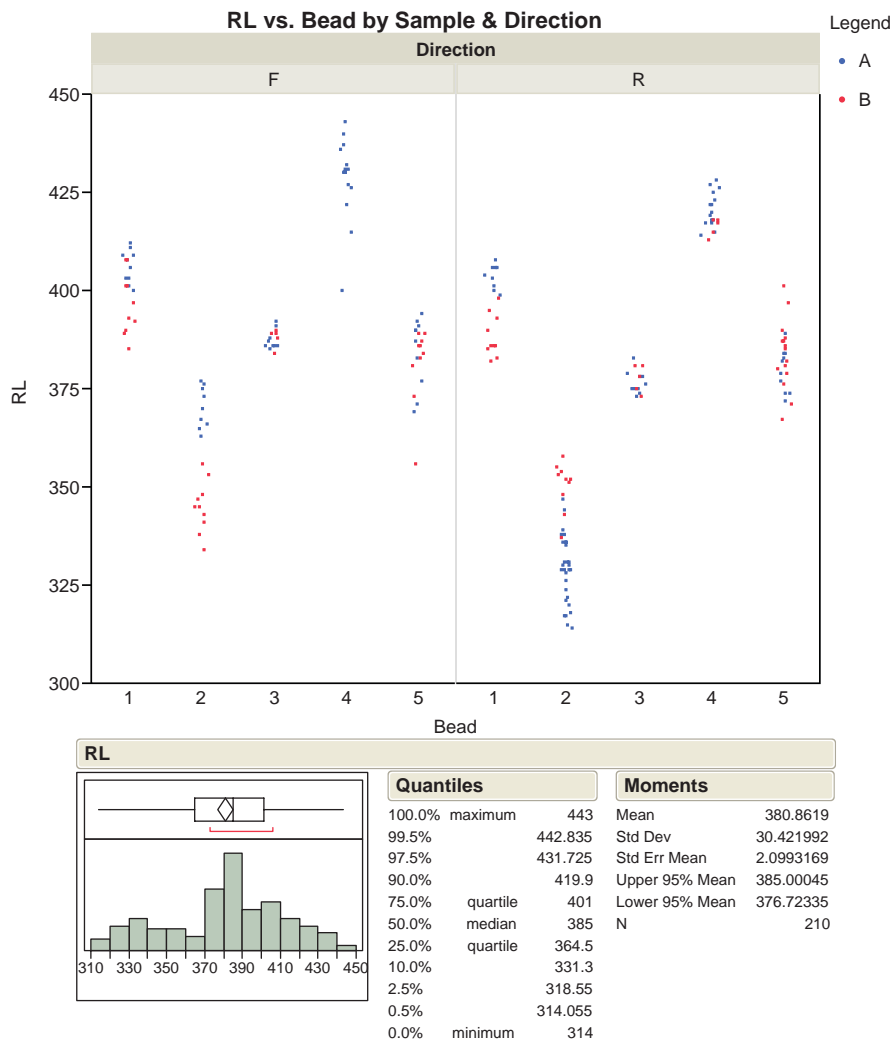


Figure 17. Retroreflectivity by bead, direction, and set and summary statistics—lab.

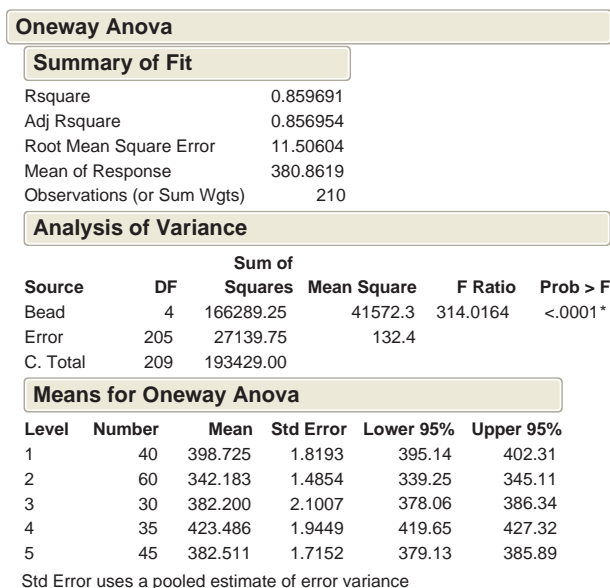
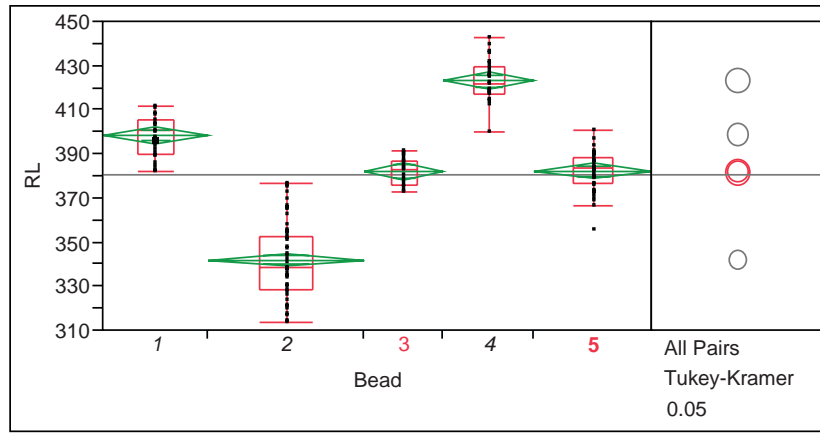


Figure 18. ANOVA of retroreflectivity by bead package—lab.

Effect of Measurement Direction on Retroreflectivity

Figure 21 of the one-way ANOVA results for the direction effect shows that a part of the variation in the retroreflectivity values can be attributed to direction. However, unlike bead effect, the coefficient of determination is low (~6%).

The low *F*-statistic value, smaller than 0.002, indicates that we have significant evidence to reject the null hypothesis, and the mean retroreflectivity values of the data sets from reverse and forward readings are not the same. The result of the Tukey-Kramer test also shows that the mean retroreflectivity values from different directions are significantly different from one another. Based on these results, the research team identified the specific direction (forward) for which to take retroreflectivity measurements for draw-down plates.



Means Comparisons

Comparisons for all pairs using Tukey-Kramer HSD

	q*	Alpha
	2.75222	0.05
Abs(Dif)-LSD		
	4	1
4	-7.56989	17.4312
1	17.4312	-7.08098
5	33.83765	9.332413
3	33.40673	8.876667
2	74.56703	50.07765

Positive values show pairs of means that are significantly different.

Level	Mean
4	A 423.48571
1	B 398.72500
5	C 382.51111
3	C 382.20000
2	D 342.18333

Levels not connected by same letter are significantly different.

Level	- Level	Difference	Std Err Dif	Lower CL	Upper CL	p-Value
4	2	81.30238	2.447249	74.5670	88.03774	0.0000*
1	2	56.54167	2.348661	50.0776	63.00569	0.0000*
4	3	41.28571	2.862780	33.4067	49.16470	0.0000*
4	5	40.97460	2.593168	33.8376	48.11156	0.0000*
5	2	40.32778	2.269022	34.0829	46.57262	0.0000*
3	2	40.01667	2.572829	32.9357	47.09765	0.0000*
4	1	24.76071	2.663131	17.4312	32.09023	0.0000*
1	3	16.52500	2.778973	8.8767	24.17333	<.0001*
1	5	16.21389	2.500341	9.3324	23.09536	<.0001*
5	3	0.31111	2.712000	-7.1529	7.77512	1.0000

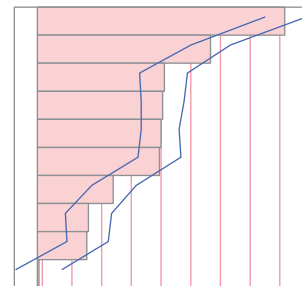


Figure 19. Tukey-Kramer result by bead packages—lab.

Effect of Set on Retroreflectivity

Figure 22 of the one-way ANOVA results for the measurement set effect shows that almost no variation in the retroreflectivity values can be attributed to different sets.

Tukey-Kramer comparison of the means shows a near match for the two sets. Therefore, it can be concluded that different measurement sets do not have a significant effect on retroreflectivity readings. This confirms that taking five

readings randomly across the plate is feasible and that there is no need to establish fixed areas for measurement.

Lab Plates Regression Model

A least squares regression model was run with the data from the lab plates and with the variables, which were significant in one-way ANOVA. Three independent variables

Oneway Anova

Summary of Fit

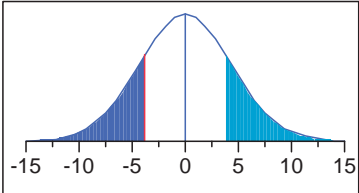
Rsquare	0.003688
Adj Rsquare	-0.0011
Root Mean Square Error	30.43875
Mean of Response	380.8619
Observations (or Sum Wgts)	210

t Test

B-A

Assuming equal variances

Difference	-3.795	t Ratio	-0.87743
Std Err Dif	4.325	DF	208
Upper CL Dif	4.732	Prob > t	0.3813
Lower CL Dif	-12.322	Prob > t	0.8094
Confidence	0.95	Prob < t	0.1906



Analysis of Variance

Source	DF	Sum of Squares	Mean Square	F Ratio	Prob > F
Sample	1	713.32	713.315	0.7699	0.3813
Error	208	192715.68	926.518		
C. Total	209	193429.00			

Means for Oneway Anova

Level	Number	Mean	Std Error	Lower 95%	Upper 95%
A	130	382.308	2.6697	377.04	387.57
B	80	378.513	3.4032	371.80	385.22

Std Error uses a pooled estimate of error variance

Oneway Analysis of RL By Sample

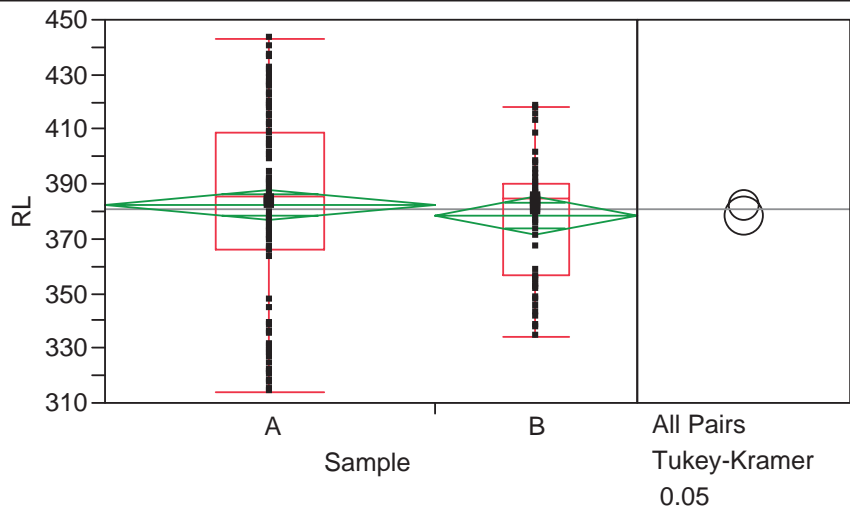


Figure 20. ANOVA and Tukey-Kramer for retroreflectivity by sample—lab.

Oneway Anova

Summary of Fit

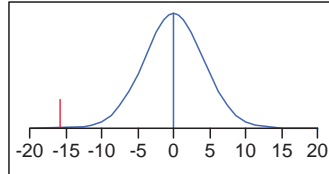
Rsquare	0.065536
Adj Rsquare	0.061044
Root Mean Square Error	29.47884
Mean of Response	380.8619
Observations (or Sum Wgts)	210

t Test

R-F

Assuming equal variances

Difference	-15.700	t Ratio	-3.81937
Std Err Dif	4.111	DF	208
Upper CL Dif	-7.596	Prob > t	0.0002*
Lower CL Dif	-23.804	Prob > t	0.9999
Confidence	0.95	Prob < t	<.0001*



Analysis of Variance

Source	DF	Sum of Squares	Mean Square	F Ratio	Prob > F
Direction	1	12676.63	12676.6	14.5876	0.0002*
Error	208	180752.37	869.0		
C. Total	209	193429.00			

Means for Oneway Anova

Level	Number	Mean	Std Error	Lower 95%	Upper 95%
F	90	389.833	3.1073	383.71	395.96
R	120	374.133	2.6910	368.83	379.44

Std Error uses a pooled estimate of error variance

Oneway Analysis of RL By Direction

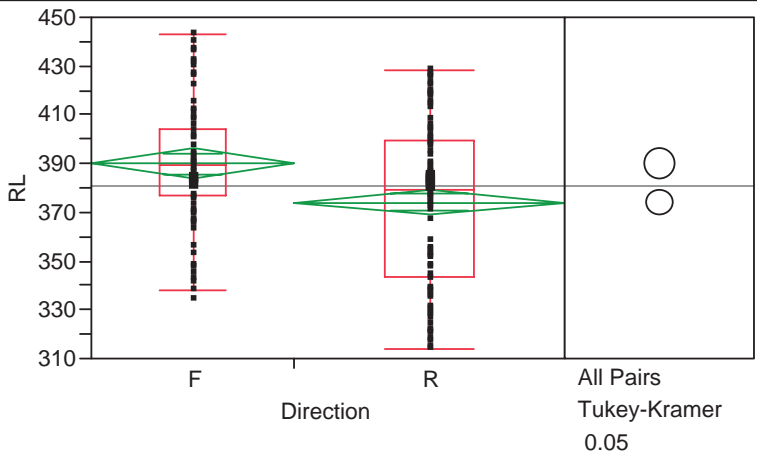


Figure 21. ANOVA and Tukey-Kramer for retroreflectivity by direction—lab.

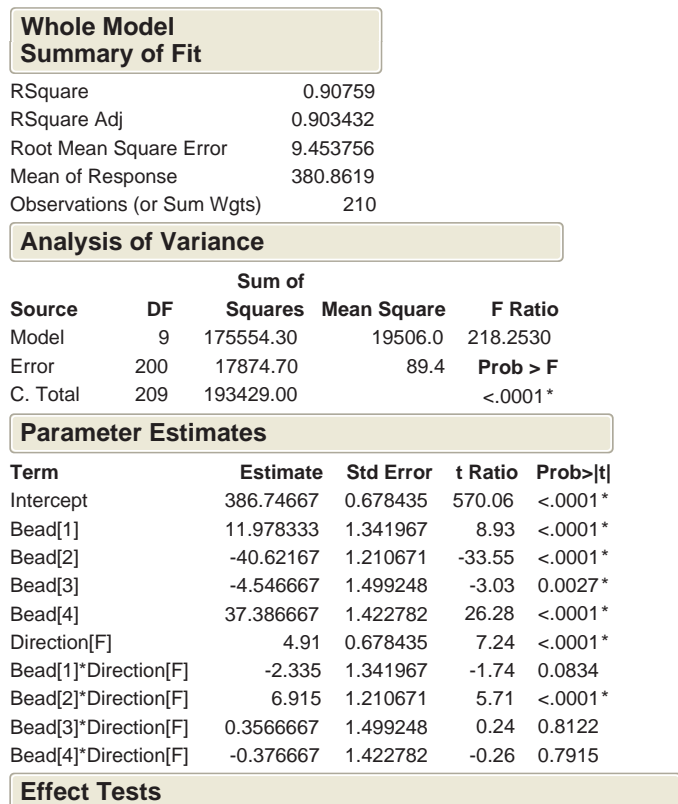
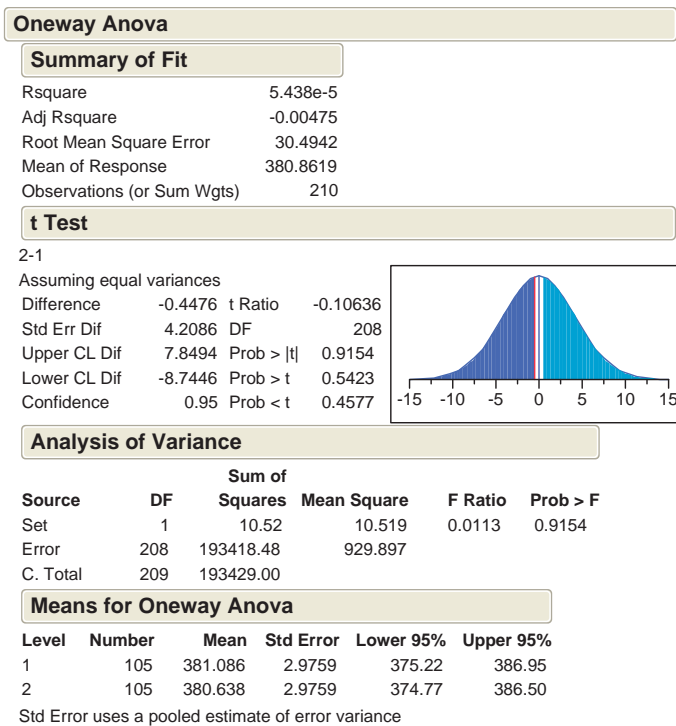


Figure 23. Lab plates regression model—lab.

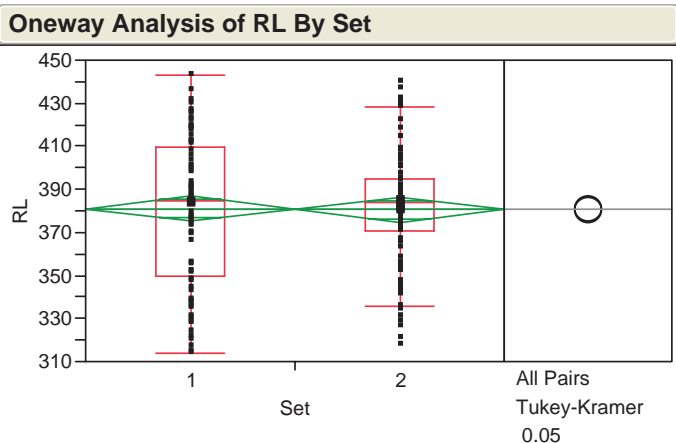


Figure 22. ANOVA and Tukey-Kramer for retroreflectivity by measurement set—lab.

included in the regression were bead type, direction, and an interaction term of bead type and direction. The regression model (see Figure 23) was significant with an almost 91% R^2 . Tukey-Kramer comparisons were also done at each variable level.

Figure 24 shows leverage plots for the two variables of bead and direction.

A leverage plot is a graphical representation of an effect's significance test. The effect in the model (bead and direction) for the plots in Figure 24 is tested for significance by comparing the sum of squared residuals to the sum of squared residuals of the model with that effect removed. This type of

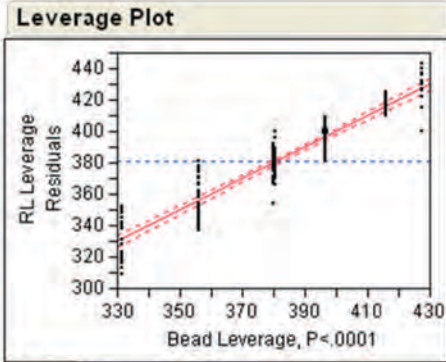
plot shows for each point what the residual would be both with and without that effect in the model.

The distance from a point to the line of fit (red line) shows the actual residual. The distance from the point to the horizontal line of the mean (blue line) shows what the residual error would be without the effect in the model. In other words, the mean line in this leverage plot represents the model where the hypothesized value of the parameter (effect) is constrained to zero.

Figure 24 shows that the least square means of retroreflectivity values for bead packages 1, 2, and 4 are significantly different, while the means from packages 3 and 5 are not. The least square means for forward and reverse directions are also significantly different.

Tukey-Kramer comparison at the interaction level term shows how the least square mean retroreflectivity is different for each bead type and reading direction combination (Figure 25). In the comparison matrix, the difference between means, the standard error of difference, and the upper to lower confidence levels are presented.

Bead



Least Squares Means Table

Level	Sq Mean	Std Error	Mean
1	398.72500	1.4947700	398.725
2	346.12500	1.2945088	342.183
3	382.20000	1.7260118	382.200
4	424.13333	1.6145362	423.486
5	382.55000	1.4180634	382.511

LSMeans Differences Tukey HSD

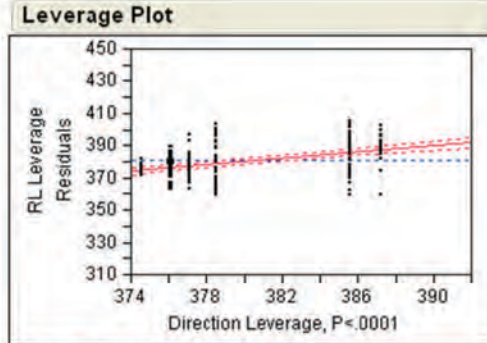
$\alpha = 0.050$ $Q = 2.75283$

LSMean[i]	LSMean[j]				
	1	2	3	4	5
Mean[i]-Mean[j]					
Std Err Dif					
Lower CL Dif					
Upper CL Dif					
1		52.6	16.525	-25.408	16.175
		1.97739	2.2833	2.20024	2.0604
		47.1566	10.2395	-31.465	10.5031
		58.0434	22.8105	-19.351	21.8469
2	-52.6		-36.075	-78.008	-36.425
	1.97739		2.15751	2.08942	1.92007
	-58.043		-42.014	-83.705	-41.711
	-47.157		-30.136	-72.312	-31.139
3	-16.525	36.075		-41.933	-0.35
	2.2833	2.15751		2.36344	2.23384
	-22.811	30.1357		-48.439	-6.4994
	-10.239	42.0143		-35.427	5.79937
4	25.4083	78.0083	41.9333		41.5833
	2.20024	2.08942	2.36344		2.14887
	19.3514	72.3116	35.4272		35.6679
	31.4652	83.7051	48.4395		47.4988
5	-16.175	36.425	0.35	-41.583	
	2.0604	1.92007	2.23384	2.14887	
	-21.847	31.1394	-5.7994	-47.499	
	-10.503	41.7106	6.49937	-35.668	

Level	Sq Mean
4	A 424.13333
1	B 398.72500
5	C 382.55000
3	C 382.20000
2	D 346.12500

Levels not connected by same letter are significantly different.

Direction



Least Squares Means Table

Level	Sq Mean	Std Error	Mean
F	391.65667	1.0064292	389.833
R	381.83667	0.9100519	374.133

LSMeans Differences Student's t

$\alpha = 0.050$ $t = 1.9719$

LSMean[i]	LSMean[j]	
	F	R
Mean[i]-Mean[j]		
Std Err Dif		
Lower CL Dif		
Upper CL Dif		
F	0	9.82
	0	1.35687
	0	7.14439
	0	12.4956
R	-9.82	0
	1.35687	0
	-12.496	0
	-7.1444	0

Level	Sq Mean
F	A 391.65667
R	B 381.83667

Levels not connected by same letter are significantly different.

Figure 24. Least squares analysis for bead and direction—lab.

LSMeans Differences Tukey HSD

a= 0.050 Q= 3.19981

		LSMean[j]									
Mean[i]-Mean[j]	1,F	1,R	2,F	2,R	3,F	3,R	4,F	4,R	5,F	5,R	
Std Err Dif											
Lower CL Dif											
Upper CL Dif											
1,F	0	5.15	43.35	67	13.8333	24.3667	-27.367	-18.3	18.4	19.1	
	0	2.98954	2.98954	2.58902	3.22907	3.22907	3.22907	2.98954	2.98954	2.83613	
	0	-4.416	33.784	58.7156	3.50091	14.0342	-37.699	-27.866	8.83404	10.0249	
	0	14.716	52.916	75.2844	24.1658	34.6991	-17.034	-8.734	27.966	28.1751	
1,R	-5.15	0	38.2	61.85	8.68333	19.2167	-32.517	-23.45	13.25	13.95	
	2.98954	0	2.98954	2.58902	3.22907	3.22907	3.22907	2.98954	2.98954	2.83613	
	-14.716	0	28.634	53.5656	-1.6491	8.88425	-42.849	-33.016	3.68404	4.87493	
	4.41596	0	47.766	70.1344	19.0158	29.5491	-22.184	-13.884	22.816	23.0251	
2,F	-43.35	-38.2	0	23.65	-29.517	-18.983	-70.717	-61.65	-24.95	-24.25	
	2.98954	2.98954	0	2.58902	3.22907	3.22907	3.22907	2.98954	2.98954	2.83613	
	-52.916	-47.766	0	15.3656	-39.849	-29.316	-81.049	-71.216	-34.516	-33.325	
	-33.784	-28.634	0	31.9344	-19.184	-8.6509	-60.384	-52.084	-15.384	-15.175	
2,R	-67	-61.85	-23.65	0	-53.167	-42.633	-94.367	-85.3	-48.6	-47.9	
	2.58902	2.58902	2.58902	0	2.86227	2.86227	2.86227	2.58902	2.58902	2.41024	
	-75.284	-70.134	-31.934	0	-62.325	-51.792	-103.53	-93.584	-56.884	-55.612	
	-58.716	-53.566	-15.366	0	-44.008	-33.475	-85.208	-77.016	-40.316	-40.188	
3,F	-13.833	-8.6833	29.5167	53.1667	0	10.5333	-41.2	-32.133	4.56667	5.26667	
	3.22907	3.22907	3.22907	2.86227	0	3.45202	3.45202	3.22907	3.22907	3.08758	
	-24.166	-19.016	19.1842	44.008	0	-0.5125	-52.246	-42.466	-5.7658	-4.613	
	-3.5009	1.64909	39.8491	62.3254	0	21.5792	-30.154	-21.801	14.8991	15.1463	
3,R	-24.367	-19.217	18.9833	42.6333	-10.533	0	-51.733	-42.667	-5.9667	-5.2667	
	3.22907	3.22907	3.22907	2.86227	3.45202	0	3.45202	3.22907	3.22907	3.08758	
	-34.699	-29.549	8.65091	33.4746	-21.579	0	-62.779	-52.999	-16.299	-15.146	
	-14.034	-8.8842	29.3158	51.792	0.51249	0	-40.688	-32.334	4.36575	4.61302	
4,F	27.3667	32.5167	70.7167	94.3667	41.2	51.7333	0	9.06667	45.7667	46.4667	
	3.22907	3.22907	3.22907	2.86227	3.45202	3.45202	0	3.22907	3.22907	3.08758	
	17.0342	22.1842	60.3842	85.208	30.1542	40.6875	0	-1.2658	35.4342	36.587	
	37.6991	42.8491	81.0491	103.525	52.2458	62.7792	0	19.3991	56.0991	56.3463	
4,R	18.3	23.45	61.65	85.3	32.1333	42.6667	-9.0667	0	36.7	37.4	
	2.98954	2.98954	2.98954	2.58902	3.22907	3.22907	3.22907	0	2.98954	2.83613	
	8.73404	13.884	52.084	77.0156	21.8009	32.3342	-19.399	0	27.134	28.3249	
	27.866	33.016	71.216	93.5844	42.4658	52.9991	1.26575	0	46.266	46.4751	
5,F	-18.4	-13.25	24.95	48.6	-4.5667	5.96667	-45.767	-36.7	0	0.7	
	2.98954	2.98954	2.98954	2.58902	3.22907	3.22907	3.22907	2.98954	0	2.83613	
	-27.866	-22.816	15.384	40.3156	-14.899	-4.3658	-56.099	-46.266	0	-8.3751	
	-8.834	-3.684	34.516	56.8844	5.76575	16.2991	-35.434	-27.134	0	9.77507	
5,R	-19.1	-13.95	24.25	47.9	-5.2667	5.26667	-46.467	-37.4	-0.7	0	
	2.83613	2.83613	2.83613	2.41024	3.08758	3.08758	3.08758	2.83613	2.83613	0	
	-28.175	-23.025	15.1749	40.1877	-15.146	-4.613	-56.346	-46.475	-9.7751	0	
	-10.025	-4.8749	33.3251	55.6123	4.61302	15.1463	-36.587	-28.325	8.37507	0	

Level	Least Sq Mean
4,F A	428.66667
4,R A	419.60000
1,F B	401.30000
1,R B C	396.15000
3,F C D	387.46667
5,F D	382.90000
5,R D	382.20000
3,R D	376.93333
2,F E	357.95000
2,R F	334.30000

Levels not connected by same letter are significantly different.

Figure 25. Tukey-Kramer comparisons—lab.

Field Stripes

Figure 26 shows the field stripes and retroreflectivity measurement procedures.

The designations used within the statistical analysis were as follows:

- RL: Retroreflectivity value (mcd per meter squared per lux).
- Bead package: Numbers that designate five different bead packages used in the study (1 through 5).
- Sample: Two different field stripes installed per bead type (A and B).
- Direction: The direction of retroreflectivity readings (*F* for forward and *R* for reverse, with *forward* defined as the direction in which the paint striper traveled to install the lines).

		Bead Package				
		1	2	3	4	5
Field Stripe	A 20'					
	B 20'					

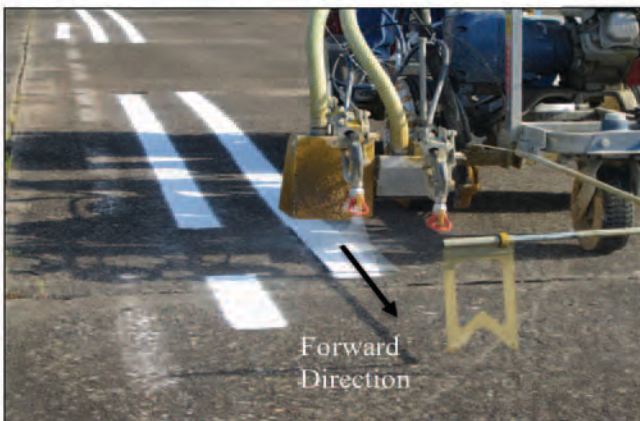


Figure 26. Field installation designations.

- Set: Retroreflectivity measurement set (Set 1 and Set 2) with retroreflectivity readings taken twice for each field stripe sample (e.g., field stripe 1A forward direction was measured twice as Set 1 and Set 2), and each measurement set consisting of 16 readings.

Effect of Bead Package on Retroreflectivity

Figure 27 shows the retroreflectivity measurements by bead package, direction measured, and set and also includes summary statistics for the data.

ANOVA was used to compare the means of retroreflectivity values of different beads (see Figure 28). The ANOVA here tests the null hypothesis that the mean retroreflectivity values of different beads are the same. (In other words, bead type does not have an effect on retroreflectivity reading in this data set.) The coefficient of determination (R^2) is over 85%, which can be interpreted as more than 85% of the variation being accounted for by fitting means to each bead type.

The *F*-statistic of the ANOVA, which is smaller than 0.001, provides significant evidence to reject the null hypothesis. Therefore, bead type in this data set has an effect on mean retroreflectivity value, and the mean retroreflectivity value from at least one bead type is different from the other groups.

The mean retroreflectivity between bead pairs was compared by a Tukey-Kramer comparison (see Figure 29). At the 95% confidence level, the mean retroreflectivity values from beads 1, 2, and 4 are significantly different, while the mean retroreflectivity from beads 3 and 5 cannot be distinguished.

Effect of Sample Plate on Retroreflectivity

Figure 30 shows that, as was the case for the lab plates, the sample effect was again insignificant in the mean retroreflectivity values for the field stripes with an *F*-value of 0.16. The Tukey-Kramer comparison also suggested that the means from different samples were not statistically different.

Effect of Measurement Direction on Retroreflectivity

Figure 31 shows that the effect of direction on the mean retroreflectivity values in the field stripes was again coherent, even though larger when compared with the lab plates, and was significant. The mean retroreflectivity values for the two directions were significantly different from each other at the 95% confidence level.

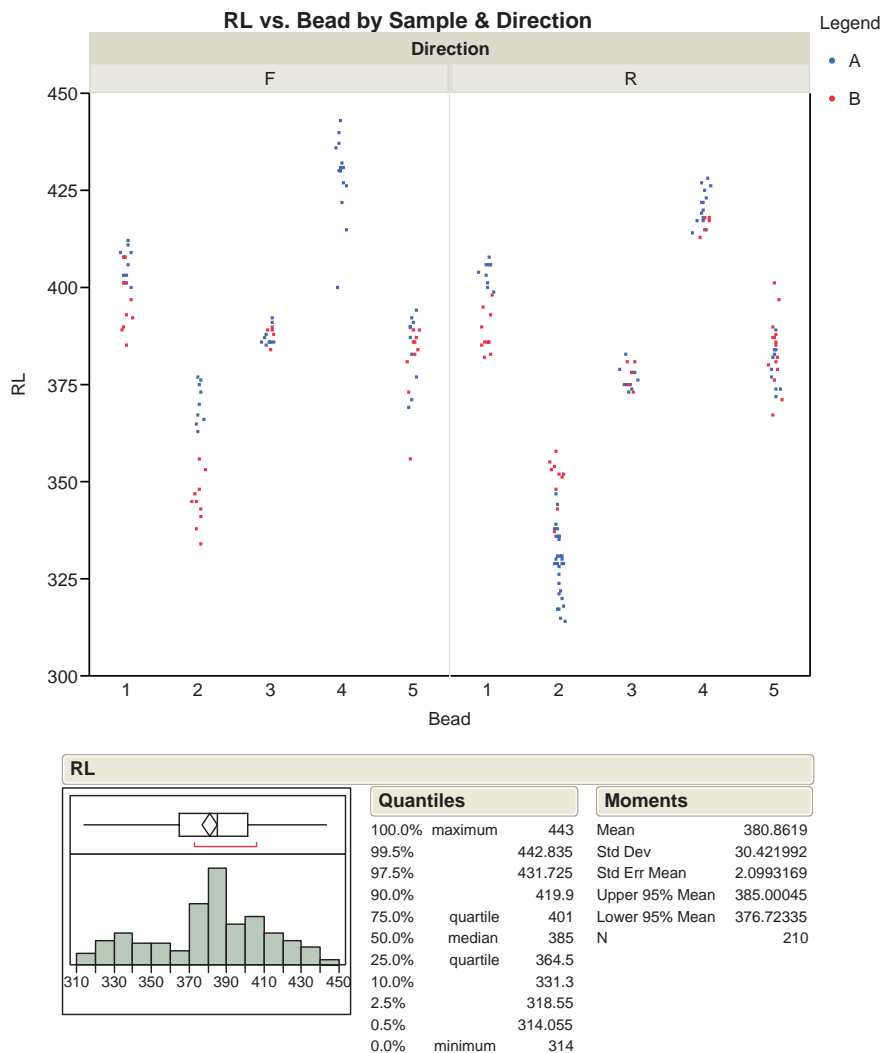


Figure 27. Retroreflectivity by bead package, direction, summary statistics—field.

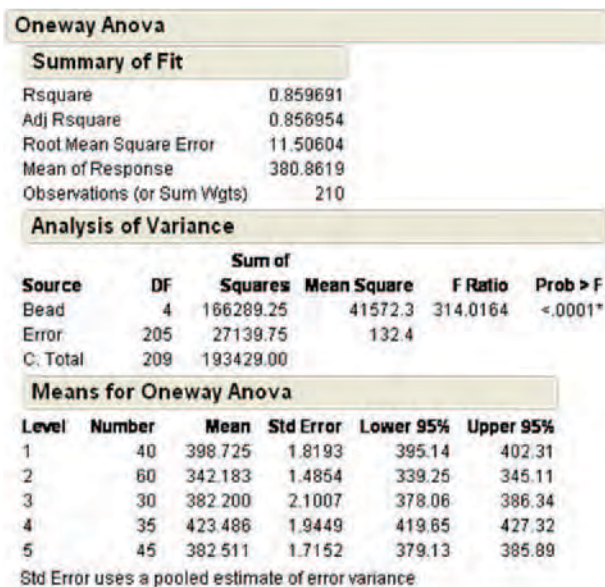


Figure 28. ANOVA of retroreflectivity by bead package—field.

Comparing Retroreflectivity (Laboratory Test Plates to Field Stripes)

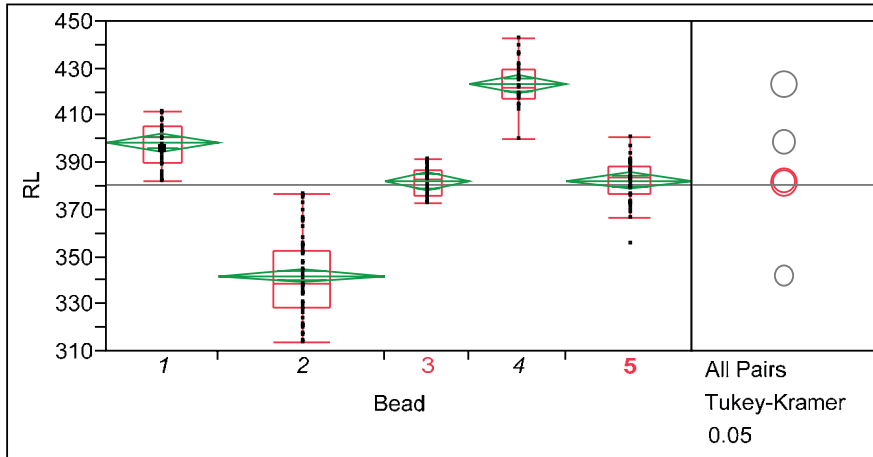
Figure 32 illustrates the laboratory test plates and field stripes.

Designations used in the analysis included the following:

- Type was used as a variable for lab plates (*P*) and field stripes (*S*).
- Direction: The directions of retroreflectivity readings were *F* for forward and *R* for reverse, with *forward* defined as the direction in which the paint was applied to the sample plate or field stripe.

Comparison Regression Model

A regression model (Figure 33) was fit for the combined data set where bead, type, and their two-way interaction were the investigated model effects. The regression was significant, with a coefficient of determination of 84%. Bead and type



Means Comparisons

Comparisons for all pairs using Tukey-Kramer HSD

	q*	Alpha			
	2.75222	0.05			
Abs(Dif)-LSD					
	4	1	5	3	2
4	-7.56989	17.4312	33.83765	33.40673	74.56703
1	17.4312	-7.08098	9.332413	8.876667	50.07765
5	33.83765	9.332413	-6.67601	-7.1529	34.08294
3	33.40673	8.876667	-7.1529	-8.17641	32.93569
2	74.56703	50.07765	34.08294	32.93569	-5.7816

Positive values show pairs of means that are significantly different.

Level	Mean
4	A 423.48571
1	B 398.72500
5	C 382.51111
3	C 382.20000
2	D 342.18333

Levels not connected by same letter are significantly different.

Level	- Level	Difference	Std Err Dif	Lower CL	Upper CL	p-Value
4	2	81.30238	2.447249	74.5670	88.03774	0.0000*
1	2	56.54167	2.348661	50.0776	63.00569	0.0000*
4	3	41.28571	2.862780	33.4067	49.16470	0.0000*
4	5	40.97460	2.593168	33.8376	48.11156	0.0000*
5	2	40.32778	2.269022	34.0829	46.57262	0.0000*
3	2	40.01667	2.572829	32.9357	47.09765	0.0000*
4	1	24.76071	2.663131	17.4312	32.09023	0.0000*
1	3	16.52500	2.778973	8.8767	24.17333	<.0001*
1	5	16.21389	2.500341	9.3324	23.09536	<.0001*
5	3	0.31111	2.712000	-7.1529	7.77512	1.0000

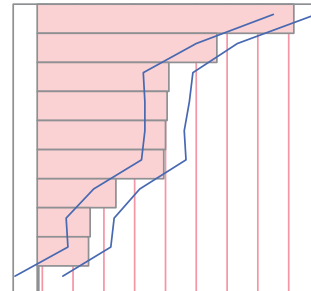


Figure 29. Tukey-Kramer result by bead package—field.

Oneway Anova

Summary of Fit

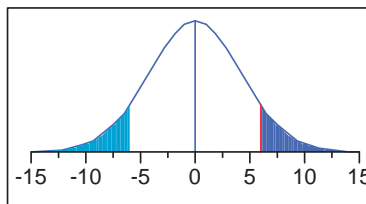
Rsquare	0.006326
Adj Rsquare	0.003201
Root Mean Square Error	37.48282
Mean of Response	331.6375
Observations (or Sum Wgts)	320

t Test

B-A

Assuming equal variances

Difference	5.962	t Ratio	1.422791
Std Err Dif	4.191	DF	318
Upper CL Dif	14.208	Prob > t	0.1558
Lower CL Dif	-2.283	Prob > t	0.0779
Confidence	0.95	Prob < t	0.9221



Analysis of Variance

Source	DF	Sum of Squares	Mean Square	F Ratio	Prob > F
Sample	1	2844.11	2844.11	2.0243	0.1558
Error	318	446777.84	1404.96		
C. Total	319	449621.95			

Means for Oneway Anova

Level	Number	Mean	Std Error	Lower 95%	Upper 95%
A	160	328.656	2.9633	322.83	334.49
B	160	334.619	2.9633	328.79	340.45

Std Error uses a pooled estimate of error variance

Oneway Analysis of RL By Sample

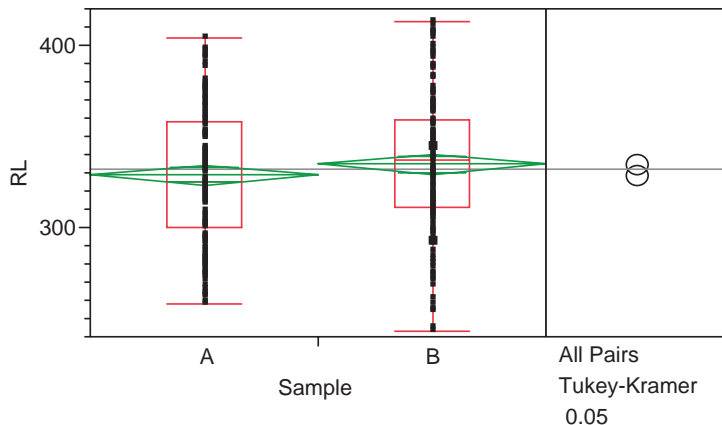


Figure 30. ANOVA and Tukey-Kramer for retroreflectivity by sample—field.

Oneway Anova

Summary of Fit

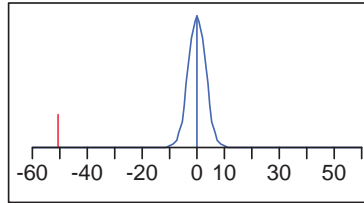
Rsquare	0.453984
Adj Rsquare	0.452267
Root Mean Square Error	27.78517
Mean of Response	331.6375
Observations (or Sum Wgts)	320

t Test

R-F

Assuming equal variances

Difference	-50.512	t Ratio	-16.2604
Std Err Dif	3.106	DF	318
Upper CL Dif	-44.401	Prob > t	0.0000*
Lower CL Dif	-56.624	Prob > t	1.0000
Confidence	0.95	Prob < t	0.0000*



Analysis of Variance

Source	DF	Sum of Squares	Mean Square	F Ratio	Prob > F
Direction	1	204121.01	204121	264.4001	<.0001*
Error	318	245500.94	772		
C. Total	319	449621.95			

Means for Oneway Anova

Level	Number	Mean	Std Error	Lower 95%	Upper 95%
F	160	356.894	2.1966	352.57	361.22
R	160	306.381	2.1966	302.06	310.70

Std Error uses a pooled estimate of error variance

Oneway Analysis of RL By Direction

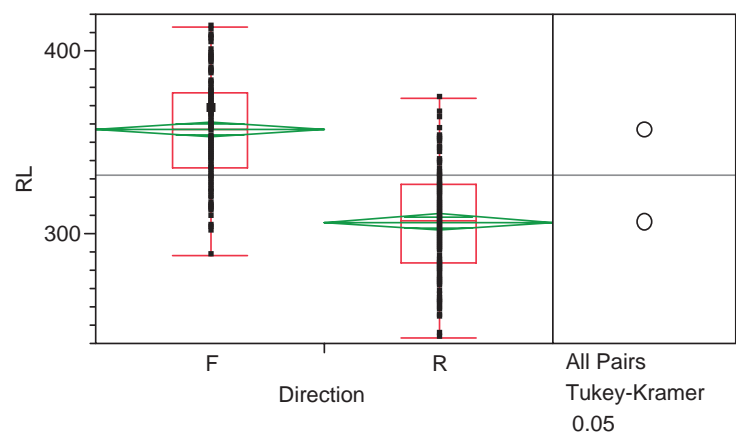


Figure 31. ANOVA and Tukey-Kramer for retroreflectivity by direction—field.

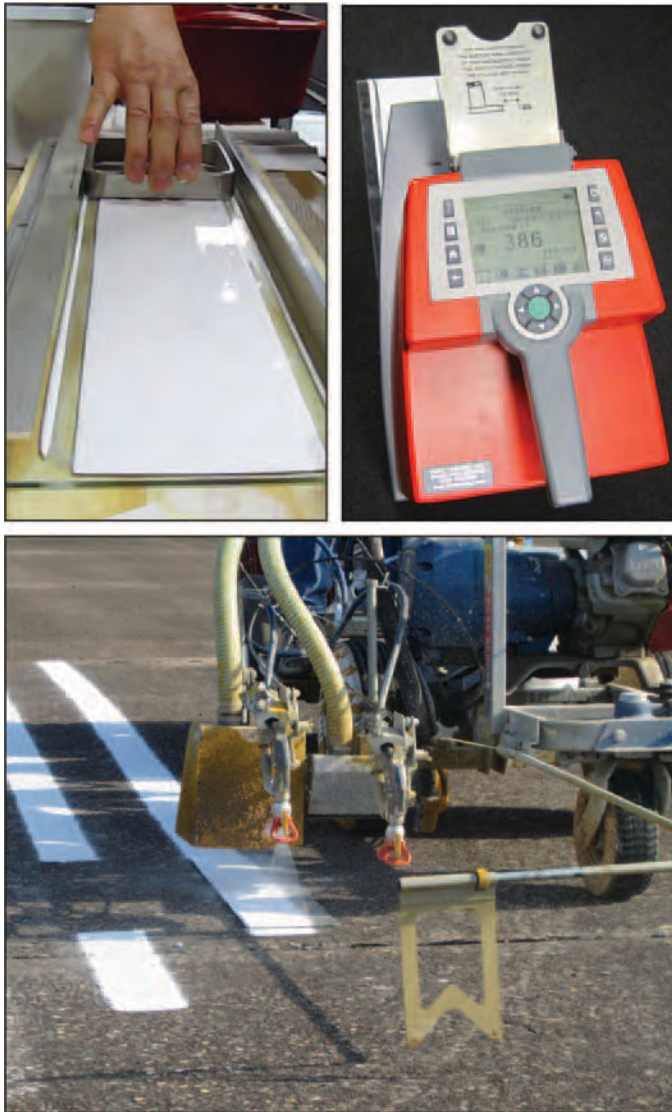


Figure 32. Laboratory (top left) versus field (bottom) comparison.

effects were very convincingly significant, while their two-way interaction was significantly weak.

The leverage plot for type further displays the significance of this effect. Comparison of means by the Tukey Honestly Significant Difference (HSD) test shows that mean retroreflectivity for each bead type is significantly different. The mean retroreflectivity values from lab plates and field stripes are also significantly different. On average, lab plates are 35 mcd higher in retroreflectivity than the field stripes.

Proof-of-Concept Findings and Conclusions

Laboratory Portion

The results show that the drawdown method is sensitive to the different bead packages used, even though, in some cases,

the retroreflectivity measurements only differed by 20 or 30 mcd. The maximum and minimum retroreflectivity values for the lab sample plates were 434 and 326 mcd, respectively.

The statistical analysis demonstrated that both the sample plate and measurement set did not produce statistically significant retroreflectivity means for the drawdown plates. This ensures that the drawdown method is consistent and objective and not sensitive to factors other than bead type when standard procedures are followed.

The statistical analysis demonstrated a significant relationship, even though low at only 6%, between resulting retroreflectivity and direction of measurements. Based on that, the drawdown procedure was adjusted by choosing the forward direction to take retroreflectivity measurements for the laboratory portion of the experiment.

Field Portion

The statistical analysis demonstrated that field stripe retroreflectivity is not affected by either stripe sample or measurement set. For field stripes, the maximum and minimum retroreflectivity values for the lab sample plates were 396 and 263 mcd, respectively.

The striper was calibrated to deliver a 15-mil wet thickness and 8 lbs per gallon of beads at 2.5 mph. This optimal speed produced proper bead embedment and distribution. This optimal speed was used to install the field stripes as part of the field portion of the experiment.

The statistical analysis demonstrated a significant relationship between retroreflectivity and measurement direction, as expected in field installations. Based on these results, the research team identified a measurement direction (forward) to measure the retroreflectivity of the field stripes during field testing.

Laboratory Testing

The laboratory portion of this project consisted of using the drawdown method to produce sample plates for a number of different bead packages, which, after 24 hours, were measured in terms of resulting retroreflectivity. The overall goal was to assemble bead packages that give a wide range of gradation, color, presence of coating, and air inclusions, which should result in a wide range of retroreflectivity values.

Materials

Paint: The source of paint (Sherwin-Williams TM2152 White) for all lab testing was the same as that used in the proof-of-concept testing as discussed and approved by the research panel. Table 9 shows the paint properties and standard tests completed.

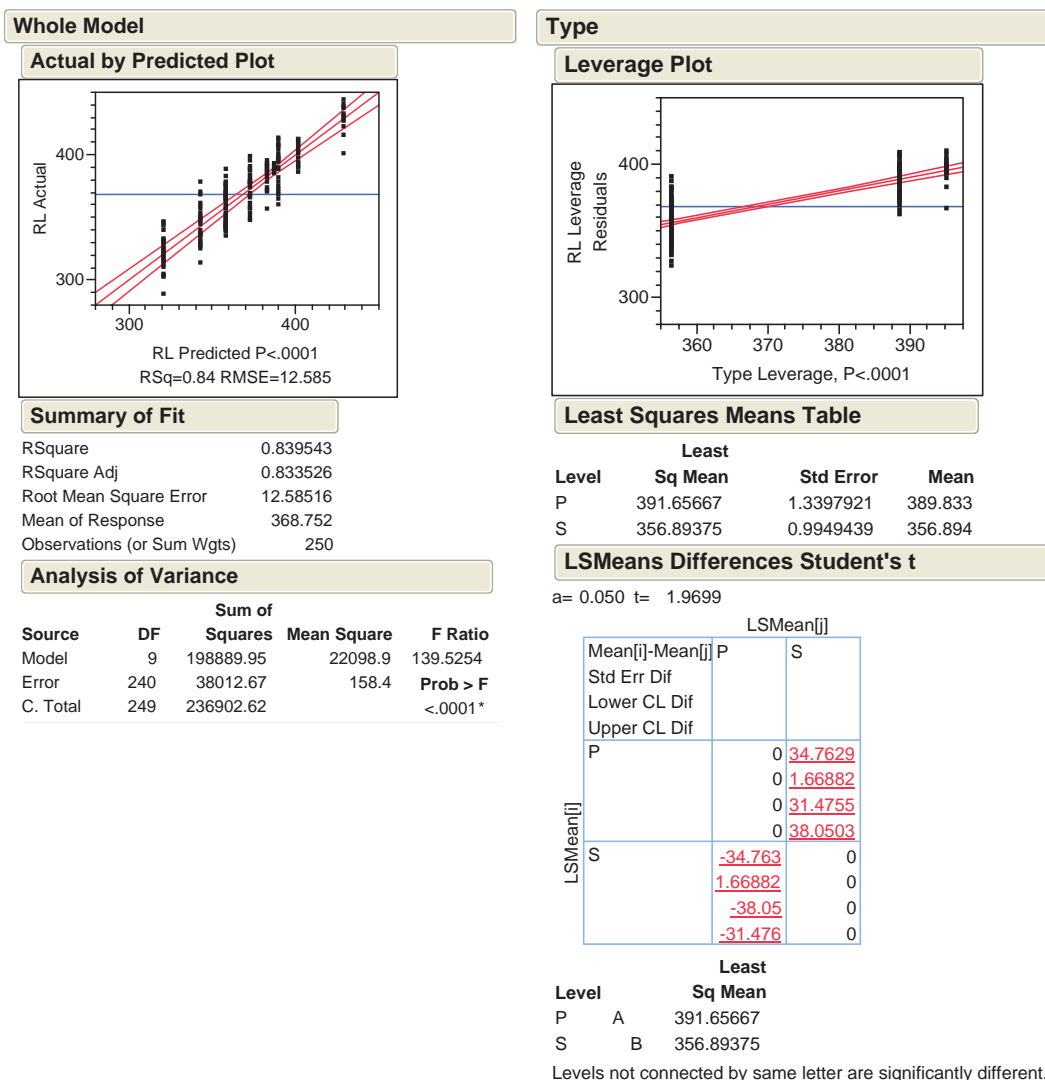


Figure 33. Comparison regression model results.

Table 10 shows the results of independent laboratory testing using Fourier transform-infrared spectroscopy (FTIR) on the extracted resin from the product received.

A variation of ASTM D2372 was followed to extract the resin, and a variation of ASTM D2621 was followed in run-

ning the FTIR scan. The FTIR analysis, along with spectral analysis, indicates the resin system of the Sherwin-Williams traffic paint received has a 99% probability of being Dow/Rohm & Haas HD-21 and can be assumed to be 100% acrylic.

Beads: The research team worked with industry to obtain 15 bead packages from seven manufacturing sources for the laboratory testing. Table 11 shows the different bead sources and packages supplied.

Fifteen additional samples were created (only for Potters Industries, given that the research team had a large quantity of beads for each bead package) through adding beads to or removing beads from the original #30 mesh (large beads) and #100 mesh (fines) bead packages. This was done to create a range of gradation (low, medium, and high) for different bead packages. When combined with the original 15, this resulted in 30 unique bead packages for testing.

Table 9. Paint testing—properties and methods.

Paint Property	Test Method
Viscosity at 25 ± 1°C (Stormer)	ASTM D562A
Density/wt per gal, g/ml @ 25°C (or lb/gal)	ASTM D1475
Fineness of grind/dispersion, Hegman	ASTM D1210
Nonvolatile/total solids, by weight %	ASTM D2369
Pigment content, by weight %	ASTM D3723
% nonvolatile in vehicle (vehicle solids)	ASTM D2369
Dry to no pickup time, without beads	ASTM D711
Initial daytime color, D65/2°, Y, x, y, & YI (E313)	ASTM D1729
Dry opacity @ 10 mil wet (or 5 mil dry)	Fed 141/4121.1

Table 10. Independent paint testing results.

Paint Property	Test Method	Results
Viscosity at 25 ± 1°C (Stormer)	ASTM D562A	81 KU
Density/wt per gal, g/ml @ 25°C (or lb/gal)	ASTM D1475	14.2 lb/gal
Fineness of grind/dispersion, Hegman	ASTM D1210	4
Nonvolatile/total solids, by weight %	ASTM D2369	0.781
Pigment content, by weight %	ASTM D3723	0.6195
% nonvolatile in vehicle (vehicle solids)	ASTM D2369	NC
Dry to no pickup time, without beads	ASTM D711	<10 min
Initial daytime color, D65/2°, Y, x, y, & YI (E313)	ASTM D1729	Y-89.1, YI-1.9, x-0.314, y-0.321
Dry opacity @ 10 mils wet (or 5 mil dry)	Fed 141/4121.1	0.96

Table 11. Bead sources for 30 bead packages.

Source	Bead Packages (30)	
	Provided	Manufactured
Potters	6 packages from 3 different plants	15
Weissker	8 packages from 3 different plants	0
Greenstar	1 package	0

The original testing matrix specified 72 different bead packages. However, this wasn't feasible given that the bead manufacturing process does not support this level of control (for different air inclusion, gradation, roundness, color, and so on).

The 15 additional manufactured samples were created in the laboratory using the following process:

1. Determine bead package gradation and roundness (Camsizer).
2. Determine percent retained on #30 and passing #100 and identify the gradation category (low, medium, or high).
3. Determine the target gradation (low, medium, or high).
4. Add/remove #30 mesh or #100 mesh (by weight) from the sample to achieve the target gradation and mix.
5. Determine new gradation and roundness (Camsizer).

Physical Characteristics

Paint: The paint properties were tested using an independent laboratory. The results are presented in Table 10.

Beads: The bead characteristics evaluated and method used for measurement are:

1. Gradation (Camsizer, Sieve Analysis ASTM D1214).
2. Roundness (Camsizer, Roundometer).
3. Color (Colorimeter).
4. Air inclusions (Image analysis).
5. Coating (AASHTO M247).

The findings are presented in the following.

Gradation and Roundness

Gradation and roundness for each of the 30 samples were measured using a Camsizer. A standard report was generated showing retained and percent passing by sieve number (#18, #20, #30, #40, #50, #80, #100, and pan) and roundness. The resulting gradation and roundness measurement information follows.

Figure 34 provides an example of the different ways the gradation measurement data are presented to reveal the variations among the 30 bead samples. The data are arranged by sieve number from #18 (largest in size) down to #100 (smallest in size) and including the pan at the bottom of the sieve. The green horizontal bar within each cell provides a graphic measure of the percent retained by the sieve. The vertical bar chart provides a traditional view of the same data by sieve

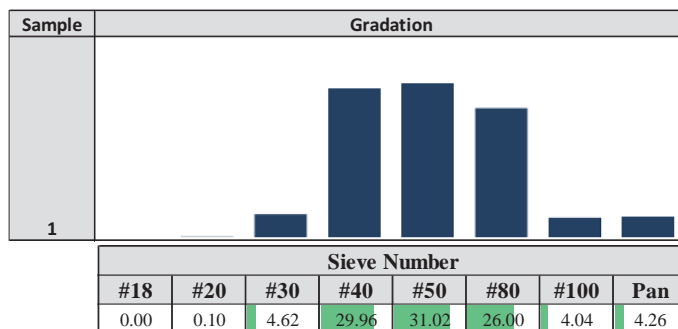


Figure 34. Gradation data presentation.

Table 12. Gradation (percent retained) by sieve number.

Sample	Sieve Number							
	#18	#20	#30	#40	#50	#80	#100	Pan
AASHTO	0	5-25	40-80	10-35	0-5			
1	0.00	0.10	4.62	29.96	31.02	26.00	4.04	4.26
2	0.01	0.27	12.48	29.88	25.69	22.76	3.96	4.95
3	0.00	0.26	9.76	29.10	26.85	25.11	3.91	5.26
4	0.02	0.49	20.21	34.02	22.05	17.00	2.65	3.56
5	0.01	0.15	7.02	30.38	25.70	24.72	5.06	6.96
6	0.00	0.14	7.06	32.36	27.79	27.08	3.34	2.23
7	0.01	0.25	10.93	29.65	26.16	27.12	3.40	2.48
8	0.03	0.42	15.65	30.24	24.15	24.37	3.03	2.11
9	0.13	0.99	12.68	30.46	28.45	24.48	1.94	0.87
10	0.16	1.32	16.39	29.84	27.22	22.73	1.69	0.65
11	0.23	1.28	9.91	25.47	33.15	26.41	2.56	0.99
12	0.38	2.04	15.85	24.25	29.69	24.56	2.39	0.84
13	0.68	3.46	21.92	23.27	26.56	21.35	2.02	0.74
14	0.09	0.13	4.88	29.99	31.70	28.23	3.57	1.41
15	0.07	0.11	4.90	30.02	29.95	26.81	3.99	4.15
16	0.32	0.49	11.04	29.59	27.92	25.78	3.50	1.36
17	0.46	0.86	16.07	29.59	25.31	23.27	3.20	1.24
18	0.00	0.02	7.30	29.45	33.68	22.61	2.76	4.18
19	0.00	0.04	11.63	31.38	34.58	21.59	0.54	0.24
20	0.00	0.05	19.34	30.61	31.16	18.25	0.42	0.17
21	0.00	0.16	10.84	35.68	26.02	23.02	2.49	1.79
22	0.16	0.96	6.99	21.92	32.18	29.47	3.70	4.62
23	0.00	0.17	6.34	29.59	35.54	26.27	1.34	0.75
24	0.04	0.38	18.67	35.33	23.62	16.85	2.46	2.65
25	0.00	0.21	7.30	32.38	35.77	22.76	1.04	0.54
26	0.02	0.35	17.86	12.17	39.35	23.11	4.66	2.48
27	0.04	0.32	17.52	11.87	38.09	23.80	5.00	3.36
28	0.03	0.37	18.28	36.43	22.26	14.72	2.25	5.66
29	0.15	0.66	19.27	27.44	32.80	17.57	1.36	0.75
30	0.16	0.65	17.81	27.64	31.82	19.12	1.64	1.16

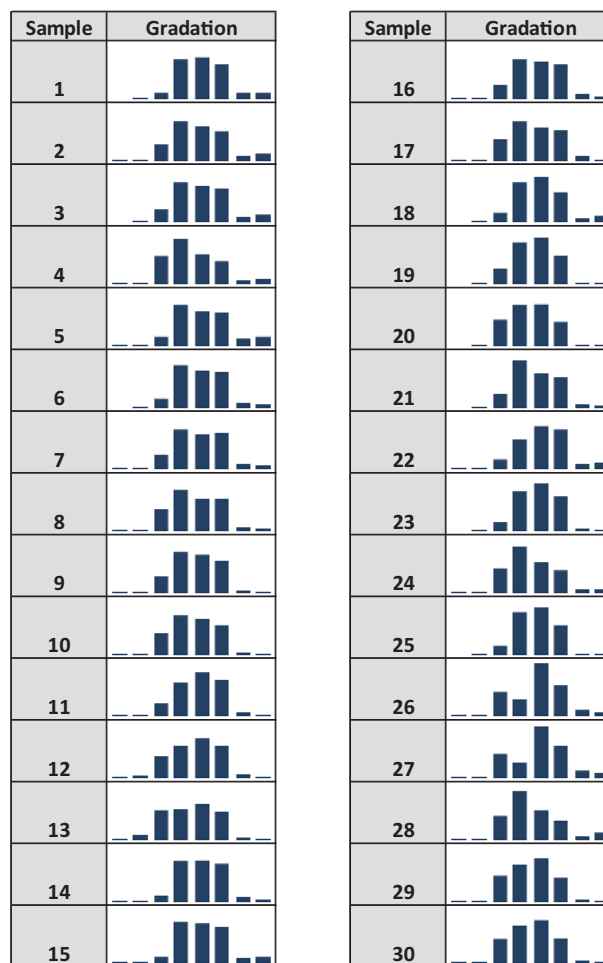


Figure 35. Gradation (percent retained) bar chart.

number. These formats deliver a visual interpretation of bead concentrations by size.

Table 12 shows the laboratory Camsizer results, in terms of percent retained, for each of the 30 samples by sieve number. Figure 35 shows the same data in a traditional bar chart (beginning with sieve #18 on the left, down to the pan on the far right).

In addition to the Camsizer, the research team conducted a mechanical sieve analysis (ASTM D1214) for a 100-g sample (from bead package 3) to verify the Camsizer gradation results in the lab. Table 13 shows that the results from each method are similar. Based on these results, the Camsizer was determined to be consistent in determining gradation and was used as the standard method for this research project.

Table 14 shows the percent rounds measurements made using the laboratory Camsizer. The range was found to be between 68% and 90%; all gradations except sample 4 met or exceeded the roundness specification (minimum 70%) for AASHTO M247 Type I beads.

Five additional samples were sent out to a separate manufacturing facility to test for roundness and gradation as a second verification of the laboratory Camsizer results. The factory

measurements included a mechanical sieve, a Camsizer, and a roundometer. Table 15 shows the factory and laboratory measurements for five different bead samples. A discussion of findings follows:

- **Factory Camsizer versus laboratory Camsizer:** The gradation measurements for both were consistent.

Table 13. Mechanical versus Camsizer gradation (lab).

Sieve	Sample 3	
	Mechanical	Camsizer
	% Retained	% Retained
18	0.00	0.01
20	0.08	0.22
30	10.24	9.07
40	32.98	28.01
50	26.05	28.87
80	24.30	24.80
100	4.08	4.12
Pan	2.46	4.90

Table 14. Percent rounds by sample (laboratory Camsizer).

Sample	% Rounds
1	74
2	71
3	73
4	68
5	82
6	82
7	80
8	79
9	80
10	80
11	79
12	81
13	80
14	77
15	77
16	75
17	74
18	81
19	81
20	83
21	78
22	79
23	79
24	70
25	79
26	90
27	90
28	71
29	88
30	88

- **Mechanical sieve gradation versus Camsizer gradation:** Measurement values were consistent for all sieve sizes with the exception of the percent passing the #100 sieve, which had minor differences.
- **Roundometer versus Camsizer:** The percent rounds comparison showed mixed results, which could be explained given the subjective element of the roundometer test.

Color

Glass bead color was measured using a colorimeter (Konica-Minolta CR-400). The Konica colorimeter measures reflected light to compute the color in terms of parameters L , a , and b . The colorimeter is calibrated using a white color tile. Targets are set to compute the delta E . A different target is set for each type or size of product. A delta E of more than 2 means the general population can see a difference between the sample and the target. The bead samples were simply poured in their entirety into a glass flat-bottomed Petri dish and placed on top of the col-

orimeter to be measured. Each measurement took less than 10 s. The depth of material was at least $\frac{1}{4}$ in. The CR-400 device is shown in Figure 36.

Table 16 shows the laboratory color measurements by bead sample. A description of each measurement parameter follows:

- L is the luminance or lightness component, which ranges from 0 to 100. (The higher the L value, the whiter the bead.)
 - Letters a (from green to red) and b (from blue to yellow) are the two chromatic components, which range from -120 to 120 .
 - Delta E represents the total color difference (must be greater than 2 to be visible to the human eye).

Each L measurement includes a horizontal bar to visualize the color variation by sample. Sample 24 was used as the target value for the delta E measurements. The delta E values greater than 2 are highlighted in red, given that when the value exceeds 2.0, the color difference is visible to the human eye.

Image Analysis for Air Inclusions

The research team developed a tool to quantify air inclusions in glass beads using image analysis. Figure 37 shows an image of beads in oil taken at $30\times$ magnification, with bead sizes reported in microns.

The objective of the analysis was to quantify the number of beads that had air inclusions and the area of air inclusions compared to the total area of beads. Figure 38 shows preliminary results from the image analysis tool. This tool was used to quantify air inclusions for each sample as part of the laboratory testing.

Quantifying Air Inclusions

The percent of air inclusion was measured for each sample using image analysis. The digital images were taken with the beads in oil under $30\times$ magnification. These images were then processed to calculate the percent of air inclusions by sample. Several digital image examples are shown in Figure 39, with the dark dots representing air inclusions within a bead.

The image analysis procedure takes the original image (as shown in Figure 39) and splits it into several smaller images with fewer beads. Those images are then analyzed using gray-scale image analysis and filtering techniques to determine the areas with air inclusions. The total area of beads is then calculated and the percent air inclusions determined by dividing the total area of air inclusions by

Table 15. Mechanical sieve/roundometer versus Camsizer for gradation/rounds (factory).

Sieve	Sample 6			Sample 12			Sample 14		
	Factory		Lab	Factory		Lab	Factory		Lab
	Mechanical	Camsizer	Camsizer	Mechanical	Camsizer	Camsizer	Mechanical	Camsizer	Camsizer
	% passing	% passing	% passing	% passing	% passing	% passing	% passing	% passing	% passing
#16	100.00	100.00	100.00	100.00	100.00	100.00	100.00	100.00	100.00
#20	99.94	99.93	99.86	98.10	97.80	97.58	99.76	99.82	99.78
#30	95.33	94.04	92.80	83.58	81.27	81.73	97.59	96.78	94.90
#50	32.41	33.66	32.65	30.26	29.86	27.79	36.66	36.33	33.21
#100	0.98	1.62	2.23	0.28	0.42	0.84	0.36	0.86	1.41
Rounds %	80.55	83.60	81.80	76.55	79.70	80.50	68.00	78.00	77.10

Sieve	Sample 26			Sample 29		
	Factory		Lab	Factory		Lab
	Mechanical	Camsizer	Camsizer	Mechanical	Camsizer	Camsizer
	% passing	% passing	% passing	% passing	% passing	% passing
#16	100.00	100.00	100.00	100.00	100.00	100.00
#20	99.93	99.73	99.63	99.67	99.32	99.19
#30	83.80	82.69	81.77	79.33	80.98	79.92
#50	30.82	32.04	30.25	21.36	21.31	19.68
#100	0.00	1.52	2.48	0.25	0.53	0.75
Rounds %	82.66	88.90	89.60	81.13	89.30	88.30

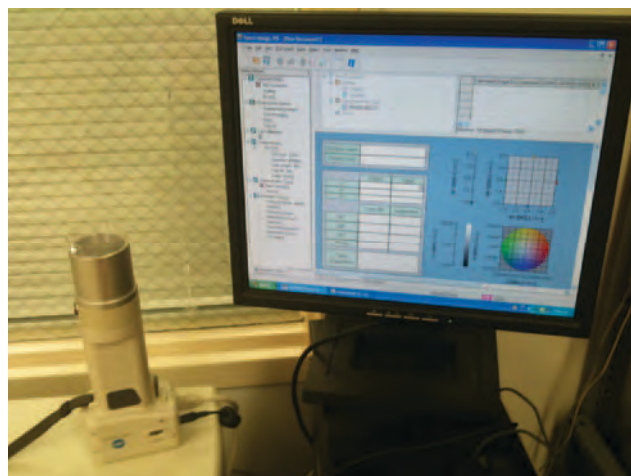


Figure 36. CR-400 colorimeter.

the total area of beads. Figure 40 shows examples of split images and results from the image analysis process. Table 17 shows the results of the air inclusion testing for 28 out of 30 samples. (No bead samples were available to conduct the air inclusion test for samples 6 and 14.) Air inclusion among the samples ranged from 0.95% to 7.78%.

Coating

Glass beads were tested for dual coating performance in accordance with AASHTO M247 test methods. The test method determines the presence of moisture resistance coating by detecting silicon and the presence of adhesion-promoting coating by detecting silane; however, the quantity of coating is not determined. All samples were found

Table 16. Color measurements by bead sample.

Sample	Color Parameters			
	L	a	b	Delta E
1	28	-1.64	2.28	2.39
2	31	-1.49	1.83	2.19
3	28	-1.39	2.52	2.88
4	29	-1.80	2.33	2.09
5	26	-1.36	2.60	4.72
6	30	-1.48	2.29	1.62
7	30	-1.51	2.09	1.85
8	29	-1.50	2.29	2.23
9	33	-1.72	2.07	3.57
10	33	-1.79	2.14	3.32
11	32	-1.82	1.79	2.82
12	33	-1.88	1.91	3.17
13	34	-1.67	1.56	4.55
14	34	-1.88	0.76	4.71
15	32	-1.75	0.92	3.55
16	33	-1.86	0.56	4.56
17	33	-1.99	0.57	4.40
18	33	-1.97	1.57	3.51
19	35	-2.12	1.44	5.74
20	36	-2.19	1.25	6.20
21	29	-1.47	2.82	1.26
22	32	-1.96	1.99	2.62
23	37	-0.19	4.27	6.78
24	29	-1.86	4.00	1.04
25	36	-0.20	4.35	6.35
26	30	-1.71	4.23	0.62
27	29	-1.66	4.36	1.36
28	29	-1.59	4.28	1.14
29	38	-0.12	3.98	7.79
30	36	-0.12	4.07	6.15

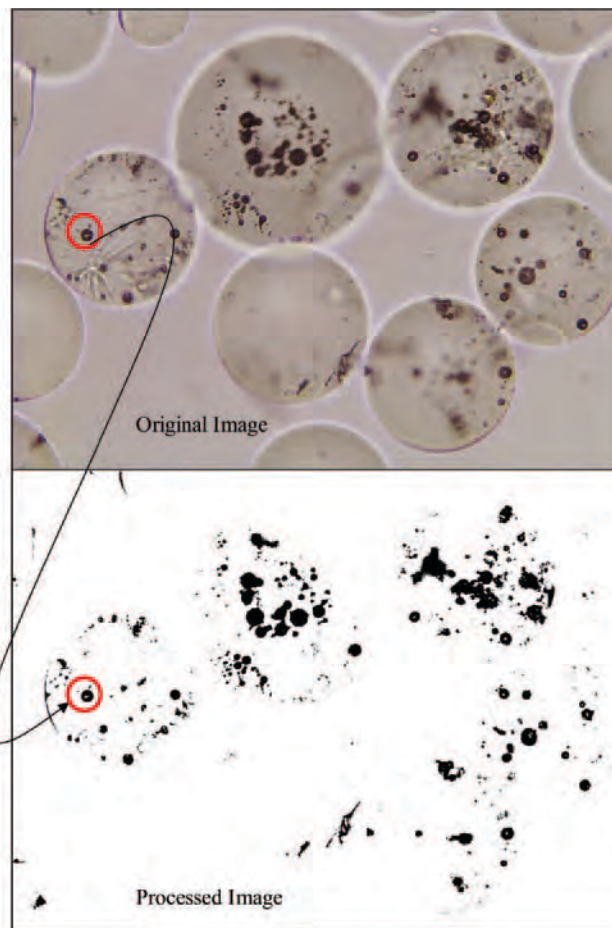


Figure 38. Results from image analysis tool.

to have dual coating. Figure 41 shows an example of both procedures.

Drawdown Sample Preparation

Paint: The Sherwin-Williams TM2152 White paint was mixed and then placed within several smaller airtight containers to be used for the drawdowns.

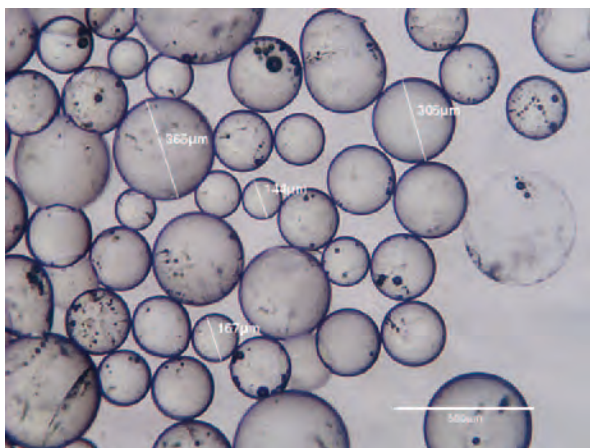


Figure 37. Beads in oil at 30x magnification.

Beads: Bead samples were prepared for the drawdowns using the following procedure:

1. Beginning with a 50-lb bag for each bead package, a 16:1 splitter was used to obtain a 3-lb sample.
2. Each 3-lb sample was further reduced (four times) using a 1:1 splitter to obtain a small enough sample (roughly 80 g) to be used in the lab for the drawdowns.
3. Using the 1:1 splitter and gram scale, a 17-g sample was created for each bead package. (These were labeled and used for each drawdown.)

Drawdown Procedure

The drawdown procedure was as follows:

1. Equipment: bead delivery box, wet film applicator to deliver 15 mil of paint, bucket of water, and a 24-in.-long by 6-in.-wide glass plate.
2. Drawdown steps:
 - a. Labeled the sample plate using the sample number and direction of application.

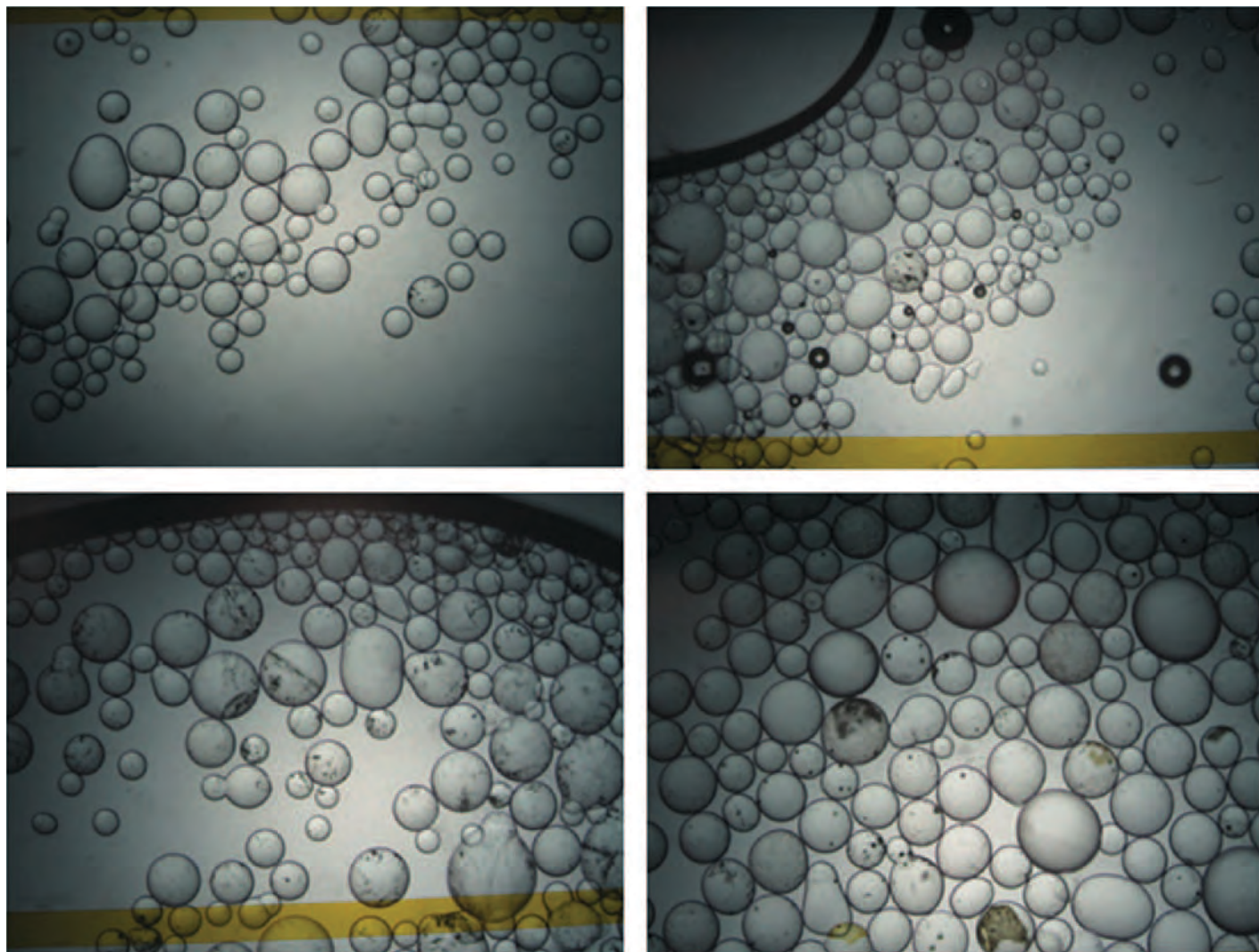


Figure 39. Digital images of beads in oil.

- b. Evenly distributed the beads into the bead delivery trough.
 - c. Applied paint using the wet film applicator using a wet mil thickness gauge to verify delivery of 15 mil wet.
 - d. Dropped the applicator in water to clean.
 - e. Positioned the bead delivery box over the sample plate and dropped the beads.
 - f. Removed the sample plate and placed in a drying rack for 24 hours.
 - g. Repeated for each bead package.
3. Quality control:
 - a. One control panel, using the same bead package, was created for each day when drawdown panels were made using the same drawdown procedure.
 - b. Duplicate (or repeat) plates were also created.

The procedure to complete each drawdown plate is depicted in Figure 42.

Environmental Lab Conditions

Laboratory temperature and humidity were recorded throughout the testing process. The readings were conducted adjacent to the location where the drawdown plates were made. The temperature ranged between 68°F and 74°F, and the relative humidity was between 32% and 50%. The readings were taken over multiple days and times.

Retroreflectivity Measurements

The measurement procedure was as follows:

1. After 24 hours, a soft bristle brush was used to lightly brush the excess beads off of each sample plate.
2. Using a handheld 30-m geometry device (LTL-X), retroreflectivity was measured at five random locations in the

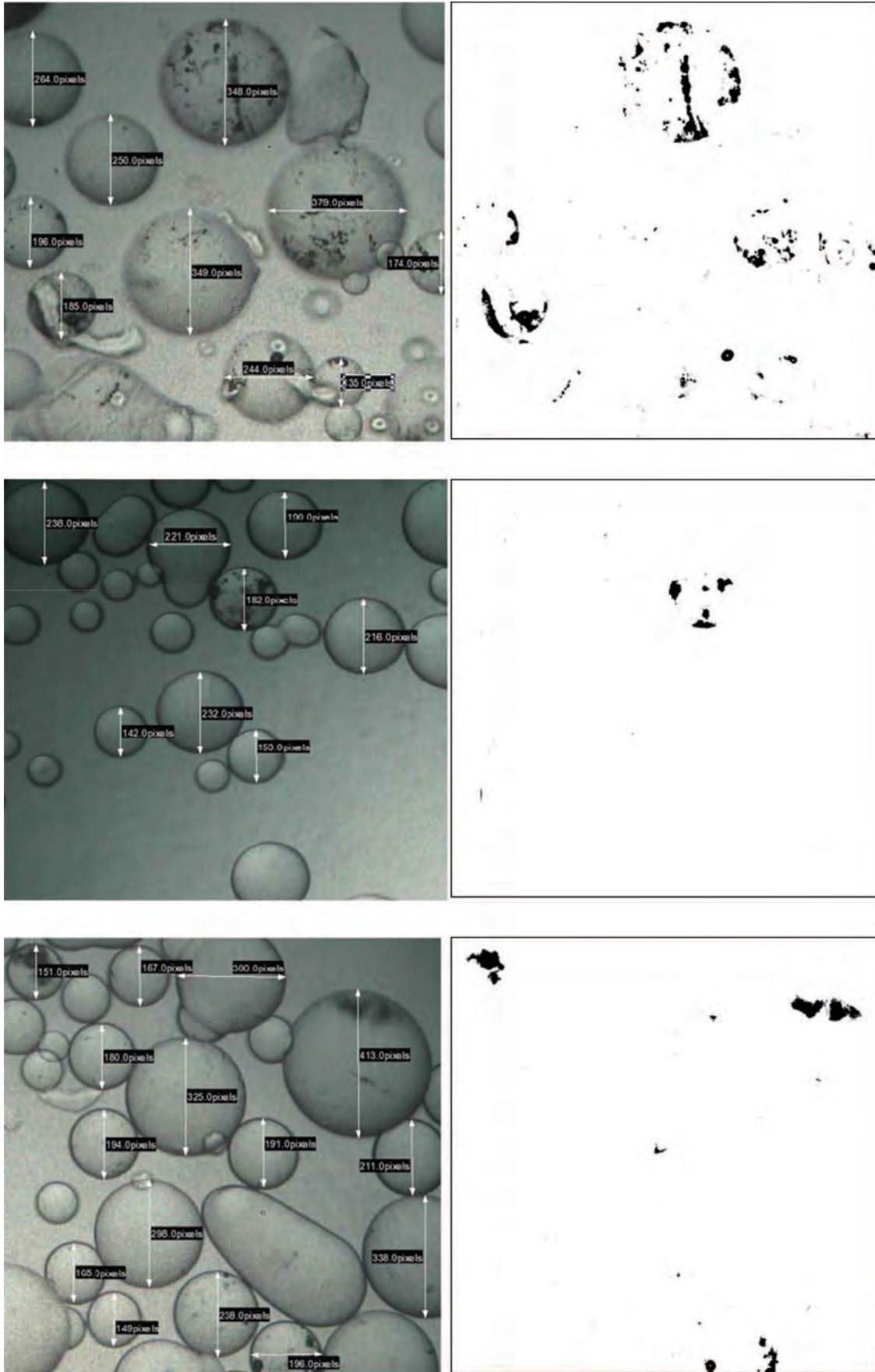


Figure 40. Air inclusions using image analysis.

Table 17. Air inclusion by bead sample.

Sample	% Air Inclusion
1	1.94
2	1.85
3	1.25
4	3.42
5	1.93
6	N/A
7	2.16
8	0.95
9	4.54
10	5.87
11	3.21
12	2.89
13	3.80
14	N/A
15	4.05
16	7.78
17	3.46
18	4.09
19	2.91
20	2.65
21	7.12
22	4.22
23	5.40
24	4.50
25	2.37
26	5.94
27	5.94
28	3.96
29	2.43
30	2.58

same direction as the paint application (as identified on the sample plate).

- All readings were recorded and average retroreflectivity for each sample plate was calculated.

Table 18 shows the average retroreflectivity for each sample. The retroreflectivity values ranged from a minimum of

290 mcd to a maximum of 680 mcd. Accordingly, the experimental design goal of having a wide range of retroreflectivity values was accomplished.

Bead Embedment and Distribution

After 24 hours, each sample plate was evaluated for bead embedment and distribution. Bead distribution was found to be satisfactory in all cases. Bead embedment was satisfactory in the majority of cases, with a few being either slightly over- or under-embedded. Figure 43 shows an example of the digital images that were taken for each sample plate to document both bead embedment and distribution. The results support the conclusion that the bead drop box provides satisfactory bead distribution and embedment for the laboratory testing.

Results

This section presents the results from the laboratory testing. The objective of the laboratory test was to assemble bead packages that give the research team a wide range of characteristics (gradation, roundness, color, and air inclusions), which will result in a wide range of retroreflectivity values while at the same time meeting the AASHTO M247 (Type I) specifications. The following tables and figures show the overall results from the laboratory test. Table 19 shows the overall results and recommendations for the field testing.

Figure 44, Figure 45, Figure 46, and Figure 47 show the relationships between retroreflectivity and rounds, color, gradation ranking, and percent air inclusions, respectively. Gradation ranking was determined by taking the rank of the sum of percent retained on sieves #30 and above and also the rank of the sum of the percent retained on sieve #100 and below. The higher the sum of #30 and above, the higher the ranking, and

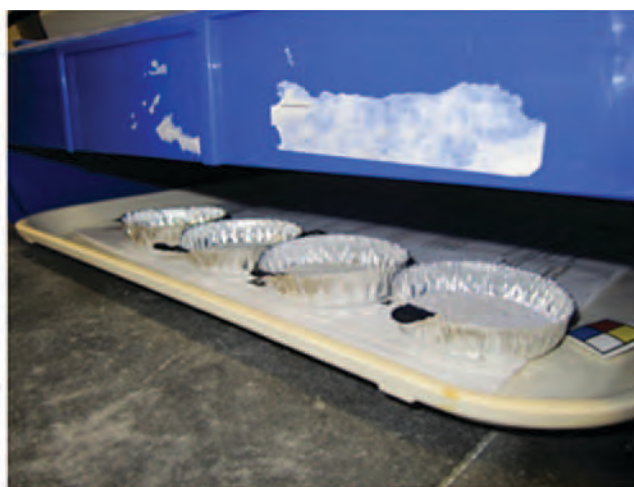


Figure 41. Moisture and adhesion coating testing.

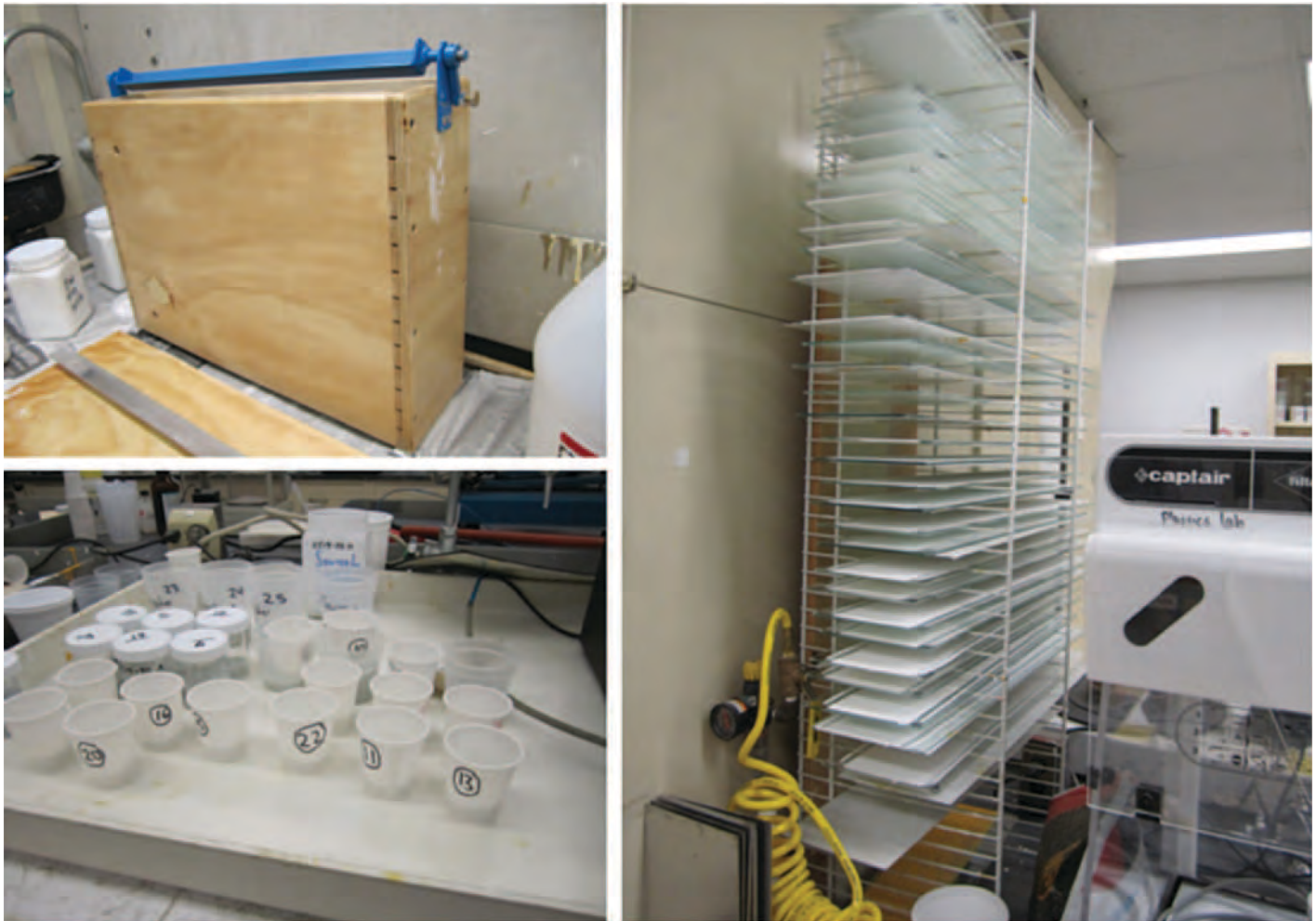


Figure 42. Drawdown procedure.

the higher the sum of the #100 and below, the lower the ranking. The two ranks were added to determine the overall ranking of each bead package. Figure 48 shows the overall relationship between retroreflectivity and the physical bead properties.

The results show that the research team was able to achieve the objectives of the laboratory test. The 30 bead packages had a wide range of percent rounds (68% to 90%), a good color range (26 to 38 in terms of L values), a range of air inclusions (0.95% to 7.78%), and very different gradations shown by the gradation ranking. The resulting retroreflectivity ranged from a minimum of 290 mcd to a maximum of 680 mcd. The original request for proposals discussed a range of more than 200 mcd while still meeting the specification, and the results from the laboratory tests confirm that such ranges exist.

The results also show that a direct relationship between retroreflectivity and bead physical properties was not found, even though, in most cases, a general trend can be seen. The combination of all of the properties together (Figure 48) can start to shed some light on the interactions that take place

between retroreflectivity and various physical properties. These results confirmed to the research team that the drawdown approach is the proper method to determine the potential retroreflectivity of a bead package rather than the different tests of bead physical attributes.

Field Testing

The field testing portion of the research was conducted at the Texas A&M University Riverside Campus, which has concrete and asphalt sections for application of the field stripes. These test areas do not receive traffic, so there was no vehicular interaction with the markings during the 24-hour dry time. In total, 15 different bead packages (as recommended from the laboratory testing—see Table 19) were applied using a Graco LineLazer IV 5900 with an EZ Bead glass bead applicator and LineDriver ride-on drive system. The installation process, calibration of the equipment, measurement of the markings, and drawdown samples from the field testing are described in the following.

Table 18. Retroreflectivity by sample.

Sample	Retroreflectivity (mcd)
1	344
2	437
3	395
4	358
5	432
6	439
7	451
8	456
9	451
10	460
11	435
12	472
13	509
14	290
15	336
16	350
17	356
18	423
19	403
20	465
21	456
22	358
23	445
24	491
25	447
26	540
27	549
28	459
29	680
30	644

Calibration

The installation of small quantities of 15 different bead packages for the field testing phase of this research required striping equipment that could facilitate the small bead quantities and provide an easy means of switching bead types. The Graco system met the needs of being able to handle small quantities of beads accurately, and the small hopper size simplified removing and replacing the beads.

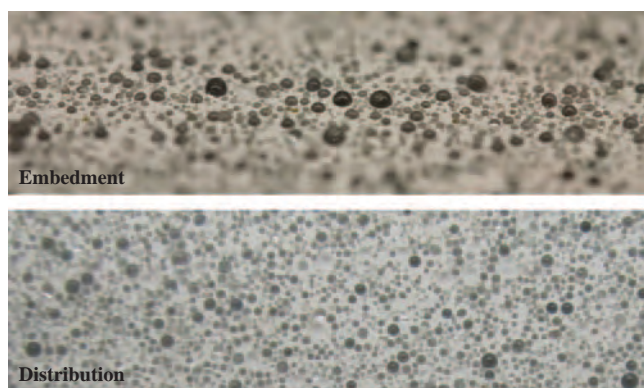


Figure 43. Bead embedment and distribution.

The drawback to the Graco system was the maximum speed that the device was able to travel while applying the pavement markings. It was found during testing that the maximum speed the striper would be able to go while still providing 15 mil of wet paint would be around 3 mph, which is less than the speed at which a typical long line striping paint truck would apply markings. This trade-off was necessary to be able to test the large number of bead samples, which was a key component to testing the proposed laboratory test method. However, a field implementation testing task was added to the research project to evaluate the test methodology using full-sized striping equipment.

The Graco striper was calibrated following procedures in ASTM D713-90, Standard Practice for Conducting Road Service Tests on Fluid Traffic Marking Materials. All calibrations of the Graco striper were conducted on tar paper so that the calibration process would not result in as many lines that would later need to be removed. All test lines and installed lines were 4 in. wide.

The paint wet mil thickness was calibrated first, given that the application thickness of the paint and speed of the striper need to be determined before calibrating the bead drop rate. The nozzle used on the striper was the largest that the research team had available to maximize the flow so that the speed could be as fast as possible. The system pressure and speed were set by measuring the weight of paint applied in several trial runs.

A test line (paint only) was then applied at approximately 3 mph. A metal sample plate of known weight was used to apply the paint stripe. This sample was then immediately weighed to determine the weight of the paint delivered. Using equation 1 in ASTM D713-90, the wet mil thickness of the line was calculated. This process was repeated until a final wet mil thickness of approximately 15 mil was achieved.

After the paint wet film thickness was calibrated, the bead drop rate was calculated. The bead dropper was set for a 4-in. drop width, so there was minimal loss of beads. Initially, the bead drop weight was measured and adjusted by capturing beads as they fell out of the applicator over a 10-s period. Using the speed of the striper, the application rate could be determined. Once the bead drop rate was approximately 8 lbs per gallon, another sample line was installed. This time, both paint and beads were applied. A sample plate was again taken and immediately weighed. The difference between this paint and bead sample and the previous paint-only sample was the weight of the applied beads. Using equation 2 in ASTM D713-90, the glass bead drop rate could be calculated. The final glass bead application drop rate was approximately 8 lbs per gallon. Some images from this process are shown in Figure 49.

Table 19. Overall laboratory results.

Sample	Gradation and Rank	% Rounds	Color (L)	% Air	R _L Avg	Use Field Testing?	
1	Low	7	74	28	1.94	344	No (manufactured lab sample)
2	Med	19	71	31	1.85	437	No (manufactured lab sample)
3	Med	12	73	28	1.25	395	Yes
4	High	40	68	29	3.42	358	No (manufactured lab sample)
5	Low	6	82	26	1.93	432	No (manufactured lab sample)
6	Med	19	82	30		439	Yes
7	Med	24	80	30	2.16	451	No (manufactured lab sample)
8	High	32	79	29	0.95	456	No (manufactured lab sample)
9	Med	39	80	33	4.54	451	Yes
10	High	45	80	33	5.87	460	No (manufactured lab sample)
11	Med	33	79	32	3.21	435	No (manufactured lab sample)
12	High	44	81	33	2.89	472	Yes
13	High	54	80	34	3.80	509	No (manufactured lab sample)
14	Low	19	77	34		290	Yes
15	Low	9	77	32	4.05	336	No (manufactured lab sample)
16	Med	32	75	33	7.78	350	No (manufactured lab sample)
17	High	37	74	33	3.46	356	No (manufactured lab sample)
18	Low	17	81	33	4.09	423	No (manufactured lab sample)
19	High	43	81	35	2.91	403	Yes
20	High	57	83	36	2.65	465	No (manufactured lab sample)
21	Med	30	78	29	7.12	456	Yes
22	Low	14	79	32	4.22	338	No (manufactured lab sample)
23	Med	31	79	37	5.40	445	Yes
24	High	41	70	29	4.50	491	Yes
25	Med	36	79	36	2.37	447	Yes
26	High	31	90	30	5.94	540	Yes
27	High	25	90	29	5.94	549	Yes
28	Med	33	71	29	3.96	459	Yes
29	High	54	88	38	2.43	680	Yes
30	High	47	88	36	2.58	644	Yes
Min		6	68	26	0.95	290	No = 15 Sample Packages
Max		57	90	38	7.78	680	Yes = 15 Sample Packages

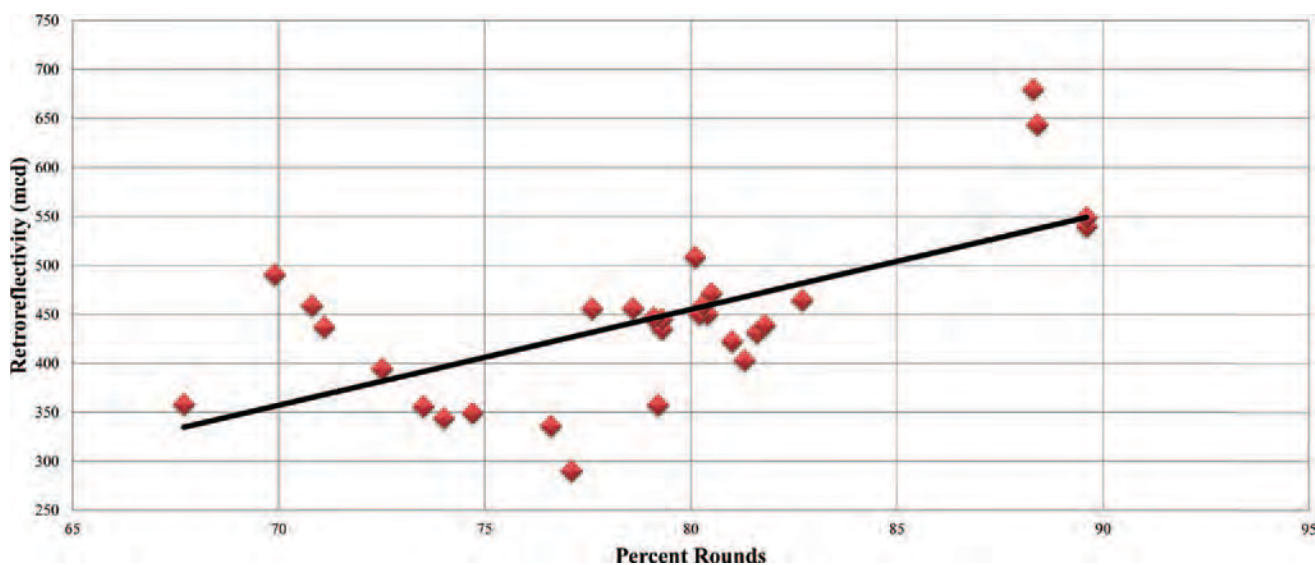


Figure 44. Retroreflectivity versus percent rounds.

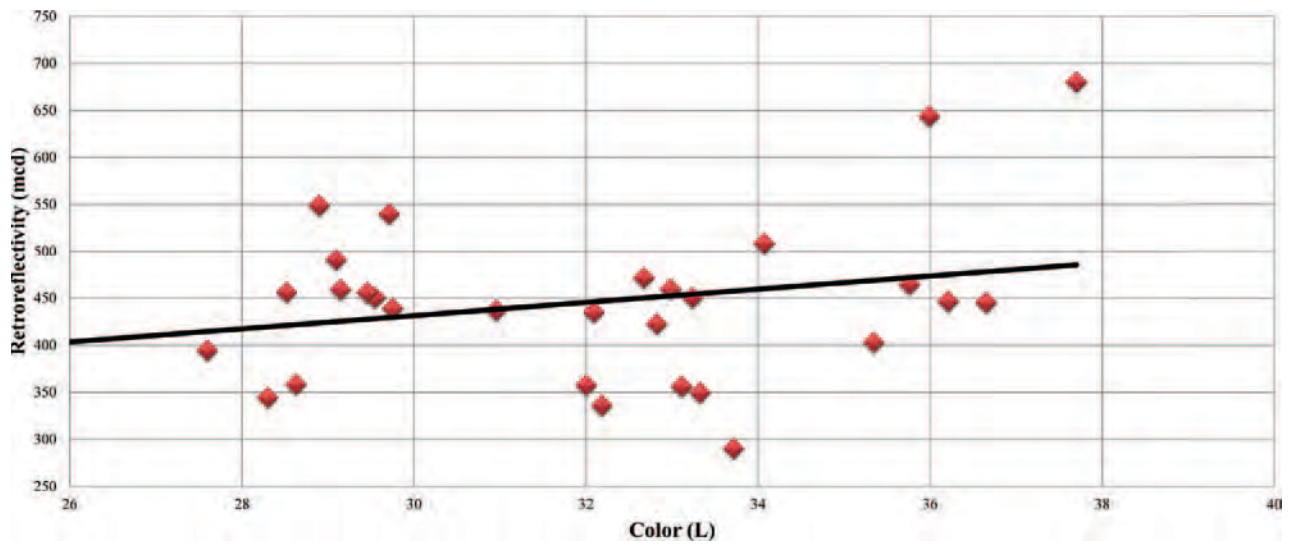


Figure 45. Retroreflectivity versus color (L).

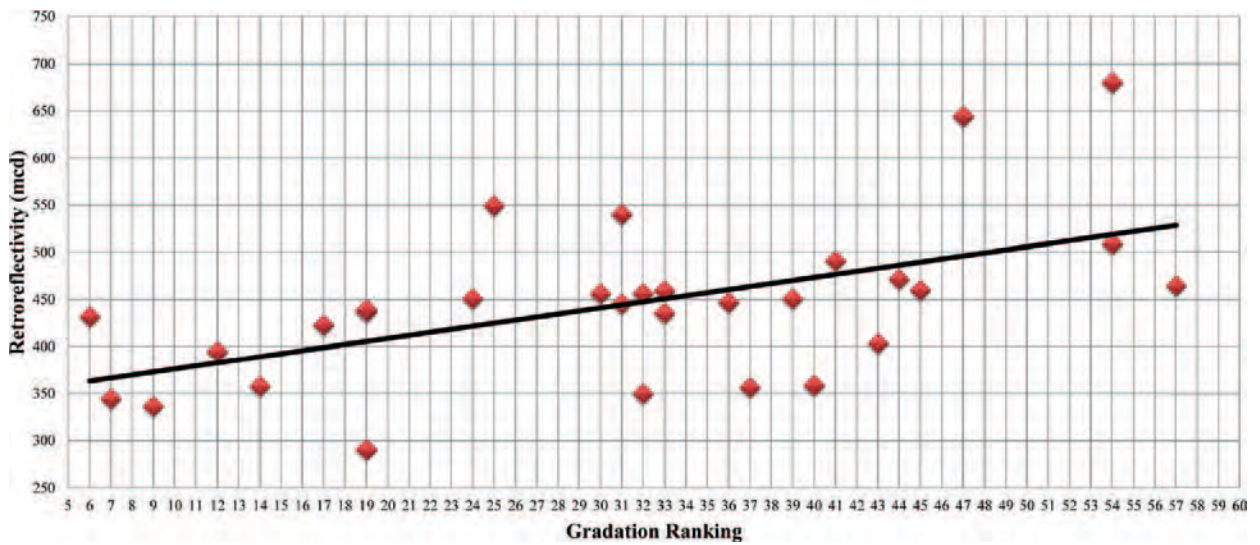


Figure 46. Retroreflectivity versus gradation ranking.

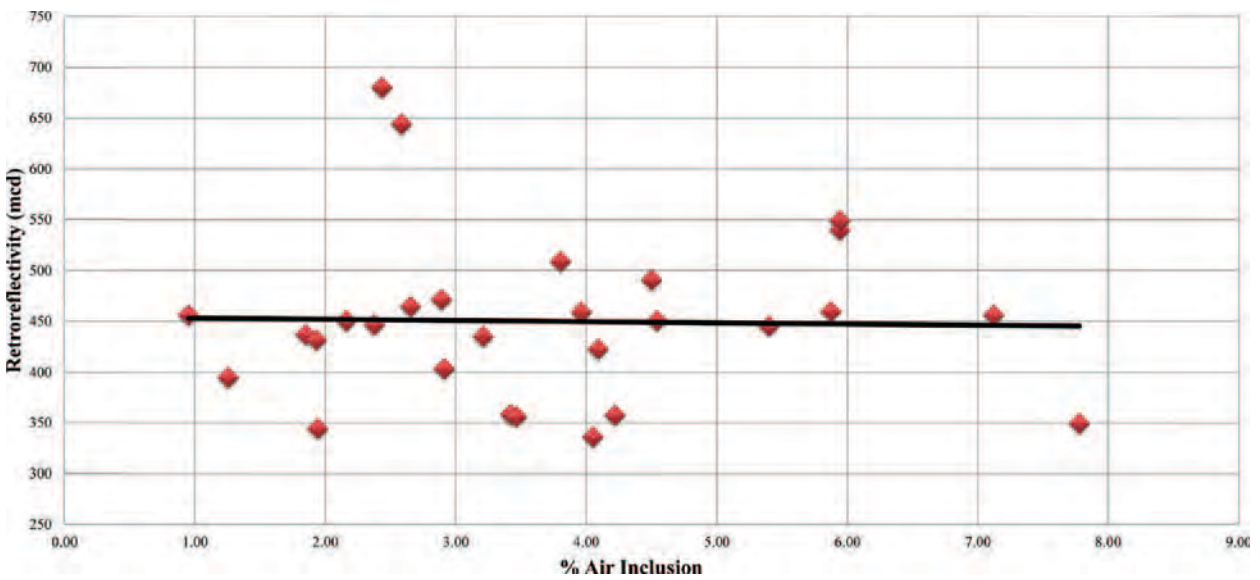


Figure 47. Retroreflectivity versus percent air inclusion.

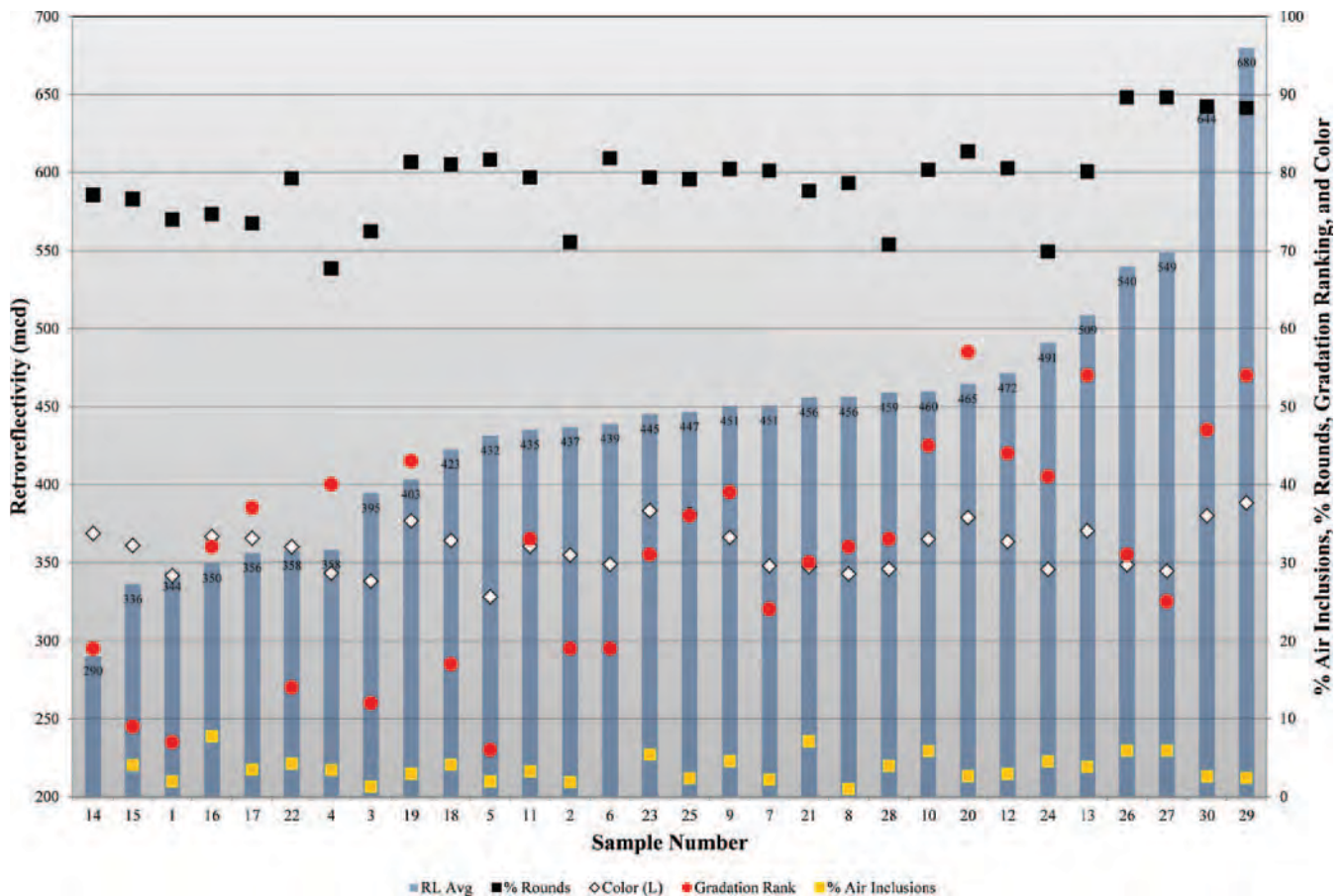


Figure 48. Retroreflectivity versus overall bead physical properties.

Installation

After calibration of the Graco striper, the pavement markings were applied to the road surfaces. Prior to the pavement marking application, the areas where the markings were to be applied were swept and blown off to remove any dirt or debris that could affect the pavement markings. Each of the 15 bead packages was applied to the concrete and asphalt surfaces. Each bead package was applied over a 45-ft-long section of each road surface. After one bead package was applied, the bead application system was completely drained, and the next bead package was loaded. All of the 15 bead

packages were applied on the same day within the environmental tolerances of the paint system used. Figure 50 shows the installed markings on the concrete and asphalt test deck surfaces.

Measurement

After the pavement markings had been applied and allowed to cure for 24 hours, the research team swept the markings to remove any loose beads that could interfere with the readings and began taking retroreflectivity measurements. A handheld retroreflectometer was used to measure the length of the



Figure 49. Calibrating the Graco striping equipment.

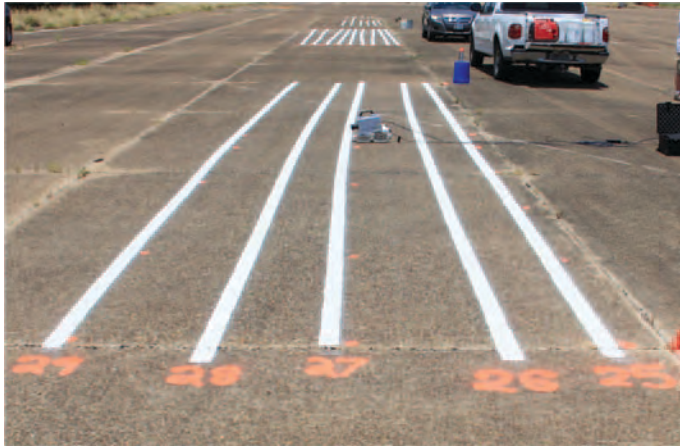


Figure 50. Installed markings—concrete (left) and asphalt (right).

45-ft section except for the last few feet on each end. In total, 16 measurements were made in the application direction for each marking based on the results of the proof-of-concept testing. Table 20 lists the resulting retroreflectivity readings averaged for 16 readings per sample on both the asphalt and concrete surfaces.

Laboratory Versus Field Testing

A comparison of retroreflectivity readings for the 15 bead packages was completed based on the laboratory and field testing results.

Analysis

This section summarizes the statistical analysis completed in comparing the laboratory and field retroreflectivity data.

Table 20. Field retroreflectivity readings.

Sample ID	Retroreflectivity	
	Field Asphalt	Field Concrete
3	301	380
6	334	380
9	323	382
12	323	369
14	281	326
19	271	345
21	323	361
23	329	376
24	386	376
25	332	397
26	455	462
27	417	474
28	350	365
29	403	434
30	403	453

The statistical analysis was completed using JMP base version 8.0.1. Designations used in the analysis are:

- RL: Retroreflectivity value (mcd), and
- ID: Numbers that identify each bead package.

Field Markings (Asphalt)

Figure 51 shows the retroreflectivity measurements from the field on asphalt surfaces as compared to the same bead packages (ID) in the laboratory. This comparison results in an R^2 of 0.73 and Equation 1:

$$FieldAsph = 138 + 0.44LabMean \tag{1}$$

Field Markings (Concrete)

Figure 52 shows the retroreflectivity measurements from the field on concrete surfaces as compared to the same bead packages (ID) in the laboratory. This comparison results in an R^2 of 0.68 and Equation 2:

$$FieldConc = 217 + 0.37LabMean \tag{2}$$

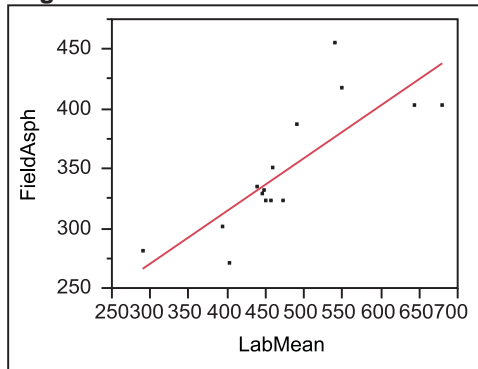
Field Markings (Surface Type)

Figure 53 shows the differences in retroreflectivity means among the asphalt, concrete, and laboratory plate surfaces. This also provides the differences in standard error and upper/lower confidence levels.

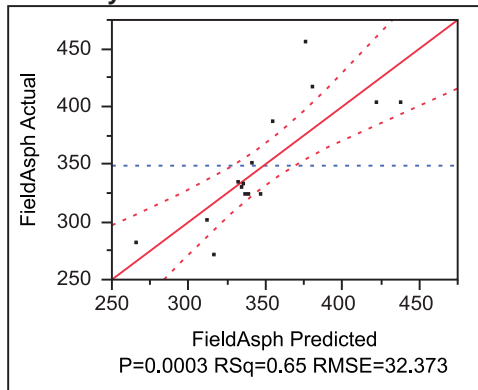
Table 21 contrasts the differences between retroreflectivity values in the laboratory and field. With two exceptions on concrete, all of the field values were lower than what was found in the laboratory, which is intuitive given that the laboratory represents ideal conditions. Retroreflectivity values for the markings on concrete were closer to the laboratory values (averaged 17% lower) as opposed to asphalt (averaged 26% lower).

Asphalt

Response FieldAsph
Whole Model
Regression Plot



Actual by Predicted Plot



Summary of Fit

RSquare	0.6508
RSquare Adj	0.623939
Root Mean Square Error	32.37282
Mean of Response	348.7333
Observations (or Sum Wgts)	15

Analysis of Variance

Source	DF	Sum of Squares	Mean Square	F Ratio
Model	1	25390.936	25390.9	24.2280
Error	13	13623.997	1048.0	Prob > F
C. Total	14	39014.933		0.0003*

Parameter Estimates

Term	Estimate	Std Error	t Ratio	Prob> t
Intercept	138.11134	43.59901	3.17	0.0074*
LabMean	0.4411856	0.089632	4.92	0.0003*

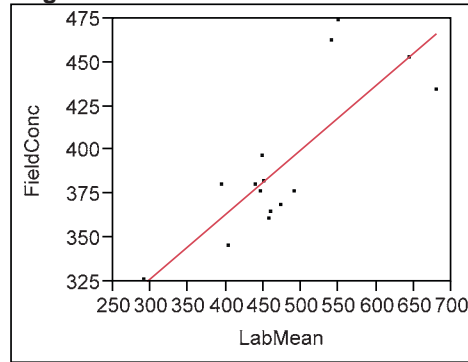
Figure 51. Field markings (asphalt).

Concrete

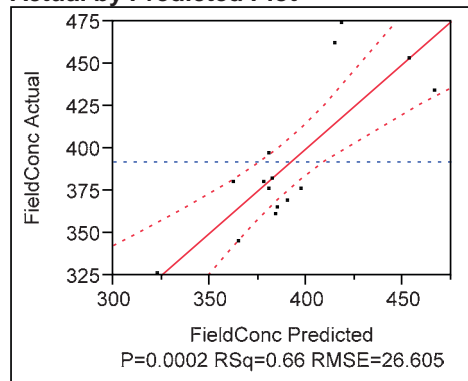
Response FieldConc

Whole Model

Regression Plot



Actual by Predicted Plot



Summary of Fit

RSquare	0.65687
RSquare Adj	0.630475
Root Mean Square Error	26.60548
Mean of Response	392
Observations (or Sum Wgts)	15

Analysis of Variance

Source	DF	Sum of Squares	Mean Square	F Ratio
Model	1	17615.931	17615.9	24.8865
Error	13	9202.069	707.9	Prob > F
C. Total	14	26818.000		0.0002*

Parameter Estimates

Term	Estimate	Std Error	t Ratio	Prob> t
Intercept	216.56462	35.83167	6.04	<.0001*
LabMean	0.3674809	0.073664	4.99	0.0002*

Figure 52. Field markings (concrete).

Surface

Least Squares Means Table

Level	Least Sq Mean	Std Error	Lower 95%	Upper 95%	Mean
Asphalt	295.90464	4.1978142	287.66904	304.14024	348.662
Concrete	339.28768	4.1980838	331.05155	347.52380	391.858
Plate	438.24229	4.4029456	429.60425	446.88033	494.390

LSMeans Differences Tukey HSD

g=0.050 Q= 2.34652

LSMean[j] By LMean[j]

Mean[i]-Mean[j]	Asphalt	Concrete	Plate
Std Err Dif			
Lower CL Dif			
Upper CL Dif			
Asphalt	0	-43.383	-142.34
		2.36063	2.72288
		-48.922	-148.73
		-37.844	-135.95
Concrete	43.383	0	-98.955
	2.36063		2.72462
	37.8438	0	-105.35
	48.9223	0	-92.561
Plate	142.338	98.9546	0
	2.72288	2.72462	
	135.948	92.5612	0
	148.727	105.348	0

Level		Least Sq Mean
Plate	A	438.24229
Concrete	B	339.28768
Asphalt	C	295.90464

Levels not connected by same letter are significantly different.

Figure 53. Statistical differences by surface type.

Table 21. Laboratory versus field retroreflectivity.

ID	Retroreflectivity			Difference between Lab and Actual			
	LabMean	FieldAsph	FieldConc	LabMean to FieldAsph		LabMean to FieldConc	
3	395	301	380	-94	-24%	-15	-4%
6	439	334	380	-105	-24%	-59	-13%
9	451	323	382	-128	-28%	-69	-15%
12	472	323	369	-149	-32%	-103	-22%
14	290	281	326	-9	-3%	36	12%
19	403	271	345	-132	-33%	-58	-14%
21	456	323	361	-133	-29%	-95	-21%
23	445	329	376	-116	-26%	-69	-16%
24	491	386	376	-105	-21%	-115	-23%
25	447	332	397	-115	-26%	-50	-11%
26	540	455	462	-85	-16%	-78	-14%
27	549	417	474	-132	-24%	-75	-14%
28	459	350	365	-109	-24%	-94	-20%
29	680	403	434	-277	-41%	-246	-36%
30	644	403	453	-241	-37%	-191	-30%
Average				-26%		-16%	
Min				-41%		-36%	
Max				-3%		12%	

CHAPTER 3

Field Implementation

The field implementation portion of the research was conducted at the Texas A&M University Riverside Campus on both concrete and asphalt sections and on the same general areas where the field testing occurred.

A single bead package of AASHTO M247 Type I beads (provided by the contractor) was applied using a full-sized paint line striping truck. The beads and paint were the standard materials that the striping company typically uses within the state (waterborne paint and M247 beads). The beads used for the field implementation were not the same as any bead package used within the previous tasks.

The installation process, the calibration of the equipment, and the measurement of the markings and drawdown samples from the field implementation are described in the following.

Calibration

The field implementation testing was conducted to compare the laboratory and field retroreflectivity values while using a full-sized striping truck and equipment for field installation (see Figure 54).

The striping truck was calibrated following procedures in ASTM D713-90, Standard Practice for Conducting Road Service Tests on Fluid Traffic Marking Materials. Calibrations were conducted on a concrete road surface, and all markings were placed at a 4-in. width.

The paint wet mil thickness was calibrated first given that the application thickness of the paint and speed of the striper needed to be determined before calibrating the bead drop rate. A metal sample plate of known weight was used to collect paint, which was immediately weighed to determine the weight of the paint that was applied. Using equation 1 in ASTM D713-90, the wet mil thickness of the line was calculated. The first pass of the striper was at what the contractor considered their normal striping application parameters; however, this yielded less than the desired 15 wet mils. The size of the paint application nozzle used on the striper was increased, and the

striper speed was reduced. After several trial runs, the speed was set at approximately 7 mph, which produced the desired 15-mil wet thickness.

After the paint thickness was calibrated, the bead drop rate was calculated. The bead dropper height was set for a 4-in. width, so there was minimal loss of beads. Initially, the bead drop weight was measured and adjusted by capturing beads as they fell out of the applicator over a 10-second period. Using the speed of the striper, the application rate could be determined. The initial bead tip was replaced with a larger one to get a higher bead drop rate. Once the bead drop rate was approximately 8 lbs per gallon, another sample line was installed. This time both paint and beads were applied. A sample plate was again taken and immediately weighed. The difference between this paint and bead sample and the previous paint sample was the weight of the applied beads. Using equation 2 in ASTM D713-90, the glass bead drop rate was calculated. The final glass bead application drop rate was established at approximately 8 lbs per gallon.

Installation

After calibration of the striping truck, the pavement markings were applied to the road surfaces. Prior to the pavement marking application, the areas where the markings were to be applied were swept and any dirt or debris that could affect the pavement markings was blown off. The first installation section was an old area of the concrete that had not been touched. It was approximately 300 ft long. The second installation section was an area of the concrete that had been cleaned recently with a high-pressure water-blasting system (Figure 55). The second installation section was approximately 0.1 miles long.

The crew then went to install the third section on an asphalt area of pavement, but the striping truck began to experience problems. The issue could not be resolved at the time. After the crew was able to go to the shop and repair the truck, the installation resumed. Not knowing if the repair had an impact



Figure 54. Calibrating the full-sized long line paint striper.

on the paint application, the paint system was recalibrated following the procedure discussed previously. To check for any differences, a third section was installed on the prepared concrete for approximately 0.1 miles. The fourth and fifth sections were approximately 300 ft each and were installed on an asphalt surface.

Measurement

After the pavement markings had been applied and allowed to cure for 24 hours, the research team swept the markings and began taking retroreflectivity readings. The markings were swept to remove any loose beads that were still on the marking that could interfere with the retroreflectivity readings. Each application section was divided into two measurement sections. The measurement sections were 45 ft long each. A handheld retroreflectometer was used to measure the entire length of each section. In total, 16 measurements were made in the application direction of each marking.

Drawdown Work

Following the field implementation, drawdown plates were made using the field-applied materials. The paint collected from the full-sized striper was used to create two drawdowns. The standard paint that had been used for all other aspects of this research was also used to create two drawdowns. The beads for all four drawdown samples were those collected from the full-sized striping truck during the field implementation. After 24 hours of drying, the panels were brushed and measured. Five measurements were recorded in the direction of application on each drawdown sample (Figure 56).

Drawdown Lab Plates

The drawdown sample plate was 24 in. by 6 in. A wet film thickness of 15 mil of paint was applied along the plate. The glass beads from the field implementation were applied immediately to the paint.



Figure 55. Installed markings on cleaned concrete.

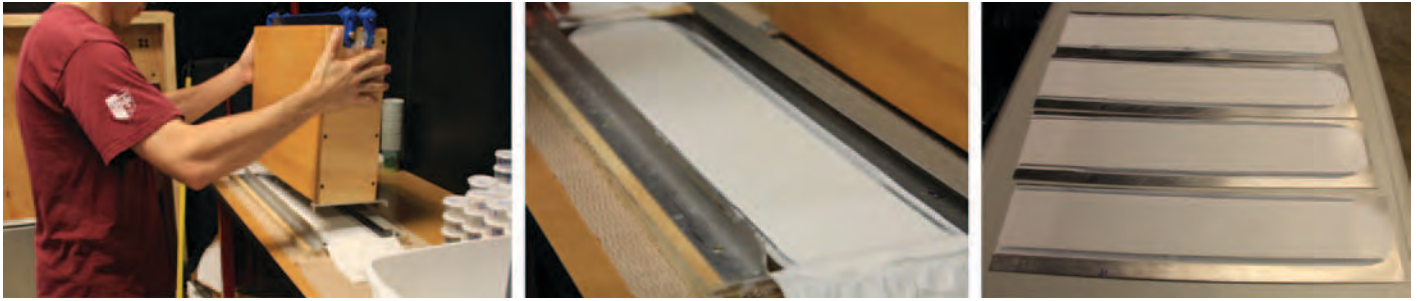


Figure 56. Making the drawdown panels.

Paint. Two paint samples were used:

Paint #1: standard drawdown paint (Sherwin-Williams TM2152).

Paint #2: waterborne paint used by the contractor during the field implementation.

Sample. Two drawdowns were made for each paint type.

Measurements. Handheld retroreflectivity measurements were taken approximately 24 hours after creating the drawdown plates. The plates were brushed prior to measurement to remove any loose beads. Five retroreflectivity measurements were taken in the direction of application using a handheld retroreflectometer, with the results shown in Table 22.

Statistical Analysis

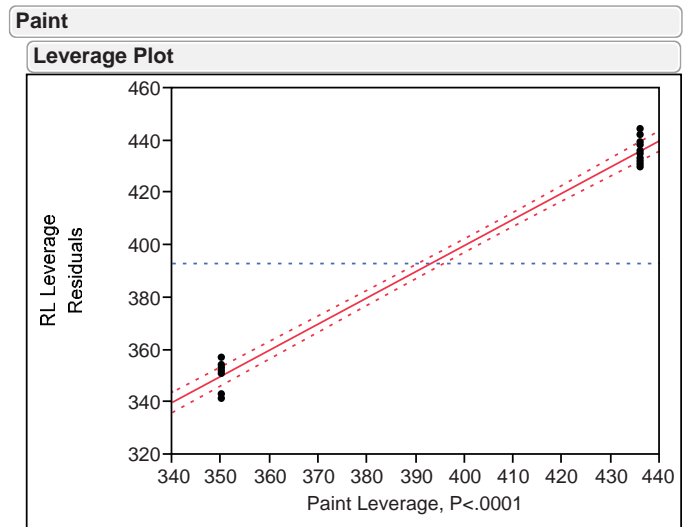
This section summarizes the statistical analysis completed in comparing the laboratory and field retroreflectivity data for the field implementation task. The statistical analysis was completed using JMP base version 8.0.1.

Drawdown Plates

In Figure 57, a leverage plot for paint type is shown to visually present the significance of this effect. The blue line

Table 22. Field implementation drawdown retroreflectivity readings.

Retroreflectivity Readings (mcd)	
Drawdown Plate	
#1 – Standard Paint	#2 – Contractor Paint
442	437
436	432
440	433
437	438
431	434
Average	436



Least Squares Means Table

Level	Sq Mean	Std Error	Mean
1	433.95000	2.0640836	436.000
2	348.05000	2.0640836	350.100

LSMeans Differences Student's t

g= 0.050 t= 2.10982

LSMean[i]	LSMean[j]	
	1	2
Mean[i]-Mean[j]		
Std Err Dif		
Lower CL Dif		
Upper CL Dif		
1	0	85.9
	0	2.3834
	0	80.8715
	0	90.9285
2	-85.9	0
	2.3834	0
	-90.929	0
	-80.871	0

Level	Sq Mean
1 A	433.95000
2 B	348.05000

Levels not connected by same letter are significantly different.

Figure 57. Retroreflectivity versus paint type (laboratory drawdown).

in this plot presents the estimated mean retroreflectivity value without including paint as an effect. The red line presents the estimated mean, in the current model, including the paint effect. Model residuals when paint is included (the distances from the observation points to the red line) are much smaller compared to what they would have been if paint were not included in the model (the distances

from the observation points to the red line). Student's *t*-test results show that the retroreflectivity values of the drawdowns prepared with paint A were 86 mcd higher on average than the retroreflectivity values of the drawdowns prepared with paint B.

In Figure 58, a similar leverage plot prepared for sample effect shows that sample was not a significant effect. Student's

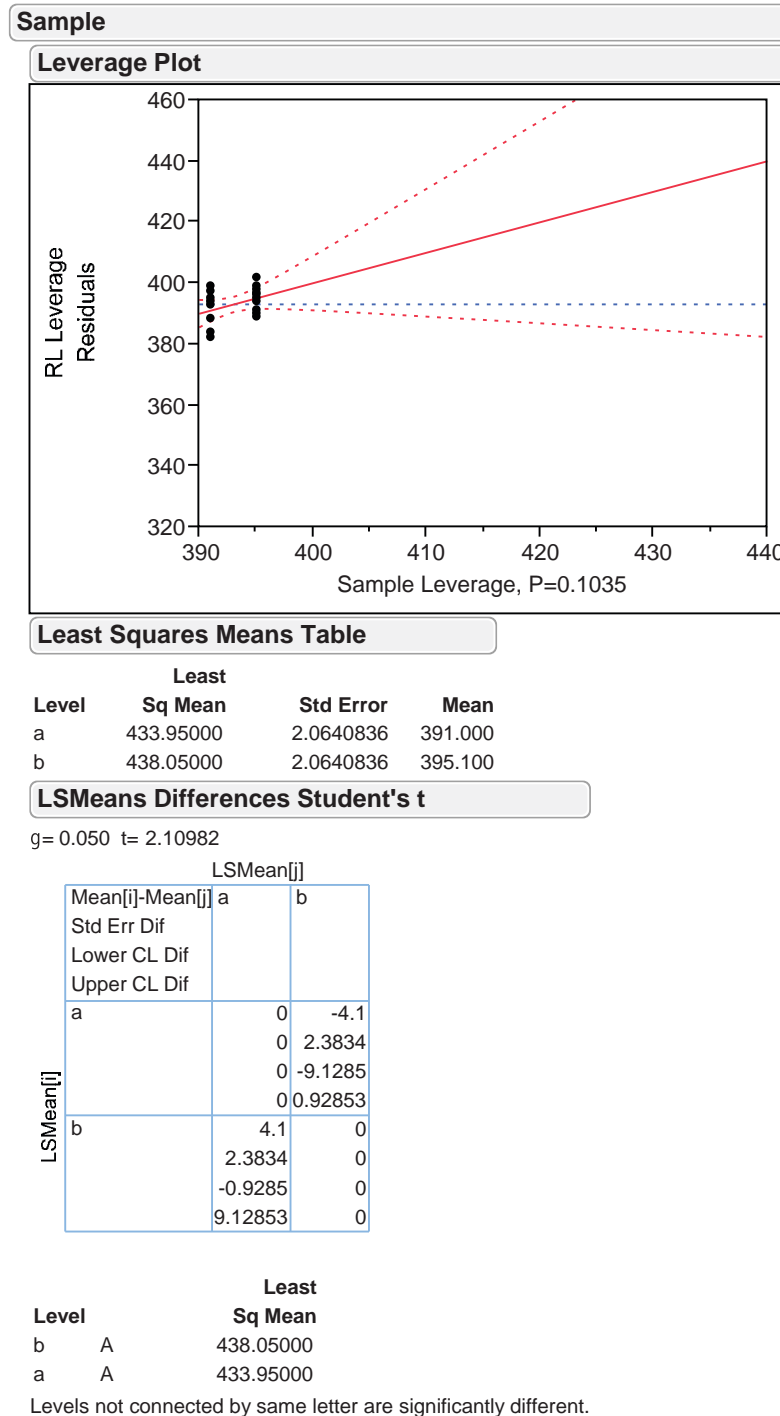


Figure 58. Retroreflectivity versus sample (laboratory drawdown).

Table 23. Field implementation field retroreflectivity readings.

Retroreflectivity Readings (mcd)			
Concrete		Asphalt	
Measurement 1	Measurement 2	Measurement 1	Measurement 2
362	373	323	310
352	376	311	303
342	372	301	314
345	365	328	316
364	374	323	305
357	364	296	319
349	359	312	312
349	356	326	309
368	369	331	311
367	355	338	313
350	356	330	288
360	372	349	295
371	368	339	285
380	363	340	306
380	362	322	295
374	367	357	301
Average	363	316	

t-test results show that no significant differences between mean retroreflectivity values were observed for different samples.

Field Stripes

Paint. Spray tip size and truck speed were adjusted to get desired thickness. Paint was sprayed 4 in. wide.

Paint was sprayed onto sample plate without beads and weighed. Final tests indicated an application rate of 14.3 mil.

Beads. There were 1,090 g collected in 10 s. Most beads fell on line when applied, achieving a bead drop rate of 7.9 lbs per gallon.

Truck Speed. Truck speed was adjusted to get optimal paint thickness, bead distribution, and embedment. The optimal speed was found to be 7 mph.

Surface of Sections.

Section 1 = concrete that had been prepared by high-pressure water blasting.

Section 2 = asphalt.

Measurements. Handheld retroreflectivity measurements were taken twice, approximately 24 hours after the

field stripes were installed. The stripes were swept prior to measurement to remove any loose beads. Sixteen retroreflectivity measurements were taken in the direction of application using a handheld retroreflectometer (see Table 23).

Analysis. Figure 59 compares the least square means of the two surfaces (sections). Student's *t*-test results show that the mean retroreflectivity values of concrete and asphalt surfaces are significantly different.

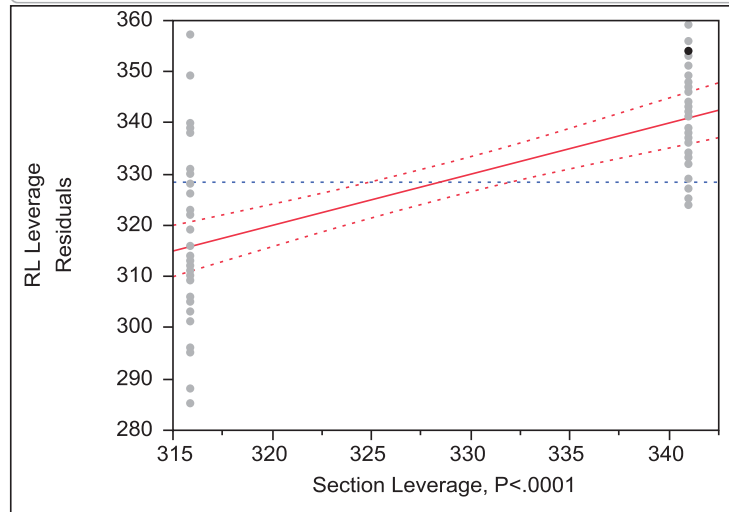
Results

Using the drawdown retroreflectivity measurements and the field measurements from the field implementation, we can compare the predicted field retroreflectivity versus the observed retroreflectivity. Table 24 shows this information, beginning with an average retroreflectivity for the drawdown samples of 436 mcd.

Once the materials were applied in the field, the observed retroreflectivity values for asphalt and concrete were 316 mcd and 363 mcd, respectively. As shown, the difference between the predicted versus observed retroreflectivity values was only 14 mcd for asphalt and 15 mcd for concrete. This verifies that the developed drawdown procedure can predict the retroreflectivity potential of a bead package.

Section

Leverage Plot



Least Squares Means Table

Least			
Level	Sq Mean	Std Error	Mean
1	341.00000	2.4196253	341.000
2	315.87500	2.4196253	315.875

LSMeans Differences Student's t

α= 0.050 t= 1.99897

		LSMean[j]	
Mean[i]-Mean[j]		1	2
Std Err Dif			
Lower CL Dif			
Upper CL Dif			
LSMean[i]	1	0	<u>25.125</u>
		0	<u>3.42187</u>
		0	<u>18.2848</u>
		0	<u>31.9652</u>
2		<u>-25.125</u>	0
		<u>3.42187</u>	0
		<u>-31.965</u>	0
		<u>-18.285</u>	0

Least		
Level		Sq Mean
1	A	341.00000
2	B	315.87500

Levels not connected by same letter are significantly different.

Figure 59. Retroreflectivity versus field surface type.

Table 24. Predicted versus actual field retroreflectivity.

Surface	Average Retroreflectivity			
	Drawdown	Field	Predicted (Field)	Difference
Asphalt	436	316	330	14
Concrete		363	378	15

Where: predicted retroreflectivity on asphalt = 138 + 0.44 * drawdown retroreflectivity (mcd)
 predicted retroreflectivity on concrete = 217 + 0.37 * drawdown retroreflectivity (mcd)

CHAPTER 4

Drawdown Interlaboratory Study

Background

The variability of the developed drawdown test method was investigated using a modified interlaboratory analysis. This included five different laboratories (two university, two private, and one DOT), which used the same set of beads (four samples) and the same paint to independently conduct the drawdown test. Two of the labs (private) used a different blade that produced a 12-mil wet thickness compared to the required 15-mil wet thickness. The ILS was conducted for the five labs and the three labs that used the same wet thickness separately.

Precision Analysis for Five Labs

The analysis of results is based on ASTM E691-11, Standard Practice for Conducting an Interlaboratory Study to Determine the Precision of a Test Method. A one-way analysis of variance (within- and between-laboratories) was carried out separately for each bead package. The data and calculated statistics for five labs are presented in Table 25.

Calculation of the Statistics

Rbar: Average of four retroreflectivity readings (Run1–Run4) for each bead and agency combination:

$$Rbar = \sum_1^n Run_i / n$$

where *n* = the number of runs (4).

s: standard deviation of four retroreflectivity readings (Run1–Run4) for each bead and agency combination:

$$s = \sqrt{\sum_1^n (Run_i - Rbar)^2 / (n-1)}$$

BeadBar: average of retroreflectivity readings for five labs, for a bead:

$$Beadbar = \sum_1^p Rbar_i / p$$

where *p* = number of laboratories in the ILS.

d: cell deviation:

$$d = Rbar - BeadBar$$

sRbar: standard deviation of the cell averages:

$$sRbar = \sqrt{\sum_1^p d^2 / (p-1)}$$

Precision Statistics

The fundamental precision statistics of the ILS are the repeatability standard deviation and the reproducibility standard deviation. The other statistics are calculated from these standard deviations (ASTM E691-11).

Repeatability standard deviation, *S_r*:

$$S_r = \sqrt{\sum_1^p s^2 / p}$$

Reproducibility standard deviation, *S_R*:

$$S_R = \sqrt{sRbar^2 + S_r^2 (n-1) / n}$$

r: 95% repeatability limit:

$$r = 2.8 * S_r$$

R: 95% reproducibility limit:

$$R = 2.8 * S_R$$

Consistency Statistics, *h* and *k*:

h: the between-laboratory consistency statistic:

$$h = d / SRbar$$

Table 25. Interlaboratory study for retroreflectivity, test results for five labs.

Bead	Agency	Run1	Run2	Run3	Run4	Rbar	s	BeadBar	d	sRbar(s _x)	Sr	SR	h	k	r*	R*	r*/BeadBar	R*/BeadBar
6	Lab A	403	385	377	350	379	22.18	398.37	-19.67	18.08	16.87	23.25	-1.09	0.95	47.24	65.09	12%	16%
6	Lab B	424	390	376	400	397	19.99	398.37	-1.02	18.08			-0.06	0.86				
6	Lab C	416	410	385	431	410	19.15	398.37	12.03	18.08			0.67	0.82				
6	Lab D	378	385	396	375	384	9.21	398.37	-14.87	18.08			-0.82	0.4				
6	Lab E	416	419	417	435	422	8.95	398.37	23.53	18.08			1.3	0.39				
14	Lab A	293	292	283	276	286	7.93	300.43	-14.33	11.31	8.75	13.61	-1.27	0.58	24.51	38.12	0.08	0.13
14	Lab B	314	309	309	295	307	8.01	300.43	6.27	11.31			0.55	0.59				
14	Lab C	295	295	302	296	297	3.45	300.43	-3.53	11.31			-0.31	0.25				
14	Lab D	309	304	294	280	297	12.44	300.43	-3.88	11.31			-0.34	0.91				
14	Lab E	317	304	327	315	316	9.44	300.43	15.47	11.31			1.37	0.69				
24	Lab A	421	416	420	383	410	18.46	433.72	-23.67	38.76	33.93	48.64	-0.61	0.38	95	136.19	0.22	0.31
24	Lab B	399	441	440	419	425	19.86	433.72	-8.92	38.76			-0.23	0.41				
24	Lab C	483	440	428	379	433	42.8	433.72	-1.22	38.76			-0.03	0.88				
24	Lab D	423	322	428	434	402	53.41	433.72	-32.07	38.76			-0.83	1.1				
24	Lab E	502	492	481	524	500	18.31	433.72	65.88	38.76			1.7	0.38				
29	Lab A	574	571	561	560	567	7.01	570.28	-3.58	98.83	33.18	102.9	-0.04	0.07	92.9	288.18	0.16	0.51
29	Lab B	604	634	605	599	611	15.86	570.28	40.27	98.83			0.41	0.15				
29	Lab C	637	654	661	585	634	34.47	570.28	63.77	98.83			0.65	0.33				
29	Lab D	446	345	358	456	401	57.94	570.28	-169.2	98.83			-1.71	0.56				
29	Lab E	651	613	623	669	639	25.68	570.28	68.77	98.83			0.7	0.25				

*95% repeatability and reproducibility limits.

Table 26. Summary of precision statistics for five labs.

Bead	S_r	S_R	h	k	r	R	$r/\text{BeadBar}$	$R/\text{BeadBar}$	BeadBar	$S_r/\text{BeadBar}$	$S_R/\text{BeadBar}$
6	16.87	23.25	-1.09	0.95	47.24	65.09	12%	16%	409.88	4.12%	5.67%
14	8.75	13.61	-1.27	0.58	24.51	38.12	8%	13%	306.50	2.85%	4.44%
24	33.93	48.64	-0.61	0.38	95	136.19	22%	31%	452.30	7.50%	10.75%
29	33.18	102.92	-0.04	0.07	92.9	288.18	16%	51%	627.88	5.28%	16.39%

k : the within-laboratory consistency statistic:

$$k = s/S_r$$

Summary of Results

We present a summary of precision statistics in Table 26. The magnitudes of the precision statistics vary across different beads. The test results within and between labs are quite consistent for bead 14, while we observe more variation for other beads.

The repeatability limit, r , is “the value below which the absolute difference between two individual test results obtained under repeatability conditions may be expected to occur with a probability of approximately 95%” (ASTM E177-10). We observe that average retroreflectivity values within labs can vary up to 24.5 mcd for bead 14 and up to 95 mcd for bead 24 with a probability of 95%.

The reproducibility limit, R , gives a similar measure for between-lab consistency. The absolute difference between average retroreflectivity values between labs can vary up to 38 mcd for bead 14 and up to 288 mcd for bead 29 at the 95% confidence level. To obtain a normalized measure of precision, we divide the repeatability and reproducibility limits by average bead retroreflectivity and present the values in Table 26. The calculated ratios suggest that average retroreflectivity can vary to up to 22% of the average bead retroreflectivity within labs and up to 51% between labs. Figure 60 shows the relationship between the repeatability standard deviation (S_r) and the reproducibility standard deviation (S_R).

The statistics h and k , which are measures of consistency between and within labs, respectively, are plotted for agency-bead combinations in Figure 61 and Figure 62. For all labs and beads, these two statistics are within the critical limits; therefore, no laboratory is singled out in behavior. The average

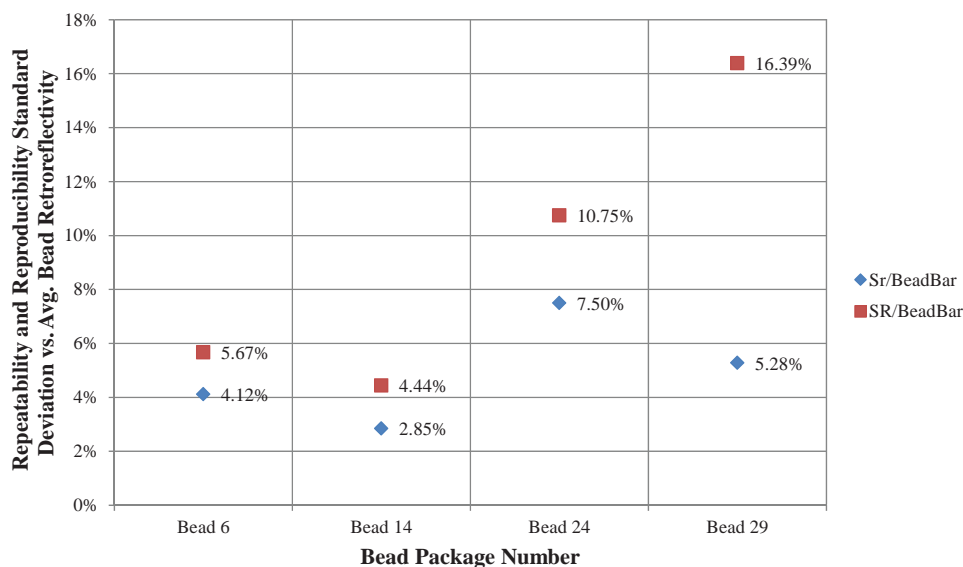


Figure 60. Standard deviation versus average retroreflectivity of the four bead packages.

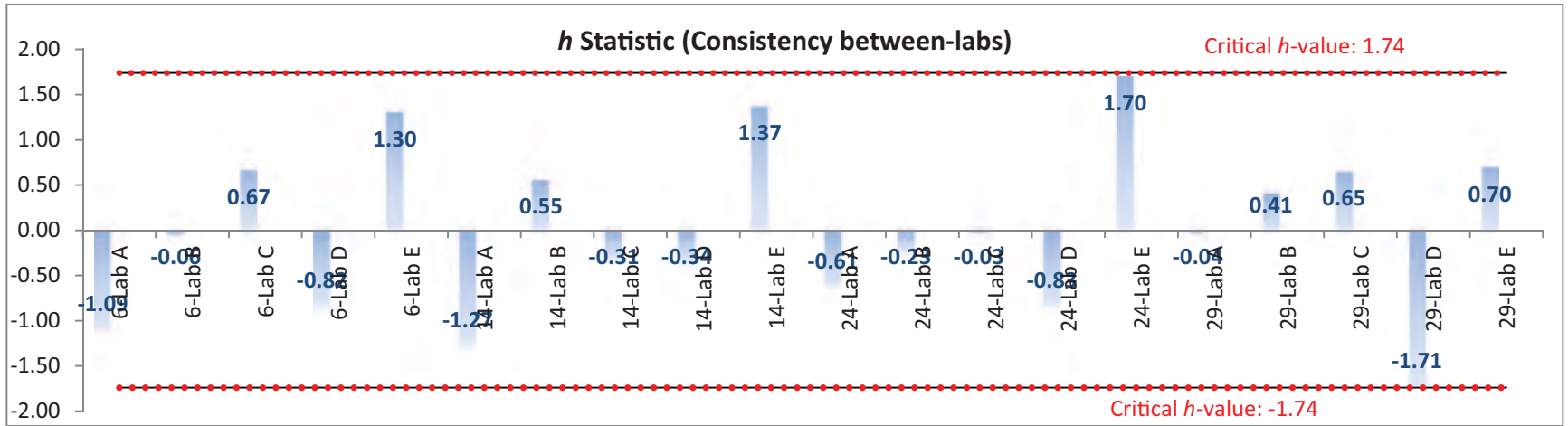


Figure 61. Plot of h statistic for five labs.

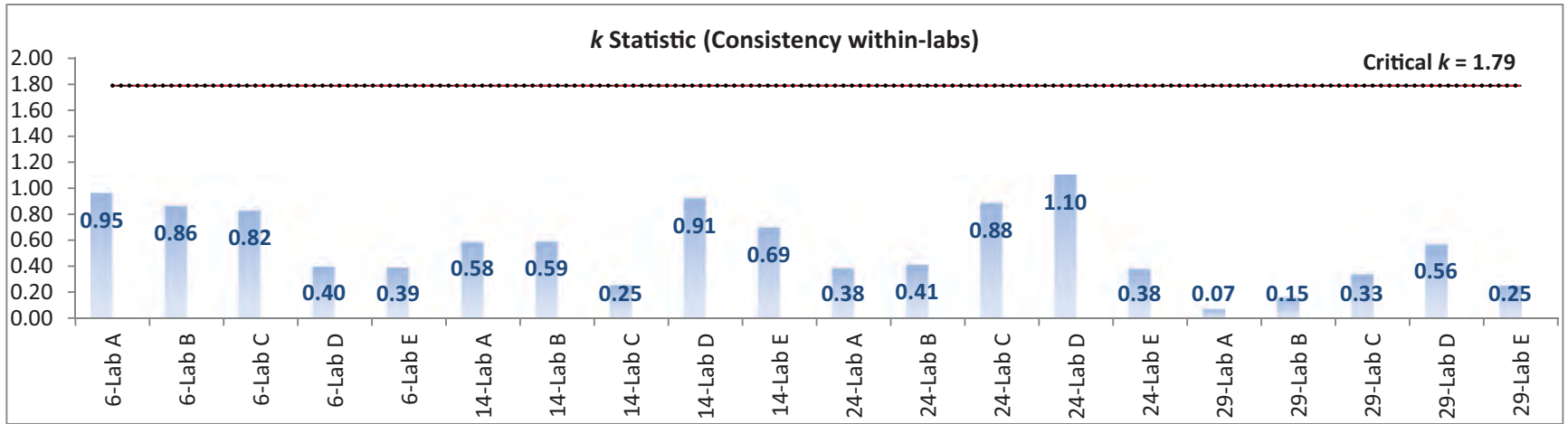


Figure 62. Plot of k statistic for five labs.

Table 27. Summary of precision statistics for three labs.

Bead	BeadBar	Sr	SR	h	k	r*	R*	r*/BeadBar	R*/BeadBar
6	409.88	16.80	19.04	-1.02	1.05	47.03	53.31	11%	13%
14	306.50	7.42	11.47	0.02	0.70	20.78	32.12	7%	10%
24	452.30	29.22	48.30	-0.67	0.41	81.82	135.25	18%	30%
29	627.88	26.45	27.50	-1.14	0.58	74.06	77.00	12%	12%

*95% repeatability and reproducibility limits.

retroreflectivity values are consistent within and between labs based on consistency statistics.

Precision Analysis for Three Labs

The same methodology in the ILS for five labs presented in the previous section was followed for the ILS for three labs. Calculated statistics and related data are presented in Table 27.

Figure 63 and Figure 64 present the plots of consistency statistics, and we observe consistency within and between labs given that all values are within the critical limits. A summary of precision statistics is given in Table 28.

The results are more precise within and between labs for these three labs as compared to the five labs. The maximum repeatability and reproducibility limits are 82 and 135 respectively, compared to 95 and 288 for the five labs.

Table 28. Interlaboratory study for retroreflectivity, test results for three labs.

Bead	Agency	Run1	Run2	Run3	Run4	Rbar	s	BeadBar	d	sRbar(s _x)	Sr	SR	h	k	r*	R*	r*/BeadBar	R*/BeadBar
6	Lab B	424	390	376	400	397	19.99	409.88	-12.53	12.28	16.8	19.04	-1.02	1.05	47.03	53.31	11%	13%
6	Lab C	416	410	385	431	410	19.15	409.88	0.52	12.28		19.04	0.04	1.01				
6	Lab E	416	419	417	435	422	8.95	409.88	12.02	12.28		19.04	0.98	0.47				
14	Lab B	314	309	309	295	307	8.01	306.5	0.2	9.5	7.42	11.47	0.02	0.7	20.78	32.12	7%	10%
14	Lab C	295	295	302	296	297	3.45	306.5	-9.6	9.5		11.47	-1.01	0.3				
14	Lab E	317	304	327	315	316	9.44	306.5	9.4	9.5		11.47	0.99	0.82				
24	Lab B	399	441	440	419	425	19.86	452.3	-27.5	41.14	29.22	48.3	-0.67	0.41	81.82	135.25	18%	30%
24	Lab C	483	440	428	379	433	42.8	452.3	-19.8	41.14		48.3	-0.48	0.89				
24	Lab E	502	492	481	524	500	18.31	452.3	47.3	41.14		48.3	1.15	0.38				
29	Lab B	604	634	605	599	611	15.86	627.88	-17.33	15.22	26.45	27.5	-1.14	0.58	74.06	77.00	12%	12%
29	Lab C	637	654	661	585	634	34.47	627.88	6.17	15.22		27.5	0.41	1.25				
29	Lab E	651	613	623	669	639	25.68	627.88	11.17	15.22		27.5	0.73	0.93				

*95% repeatability and reproducibility limits.

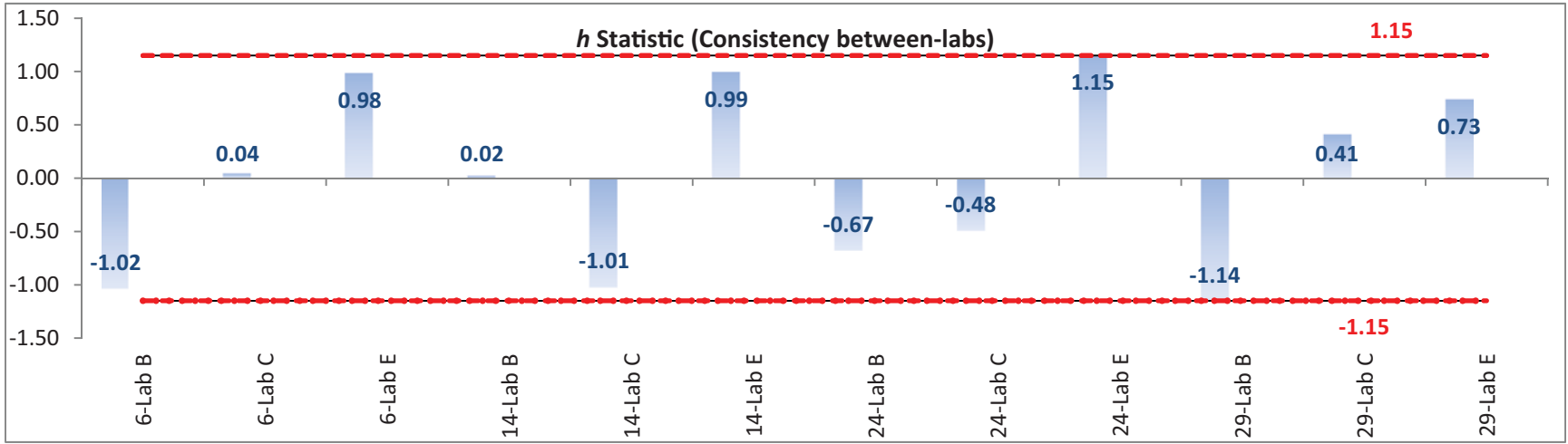


Figure 63. Plot of h statistics for three labs.

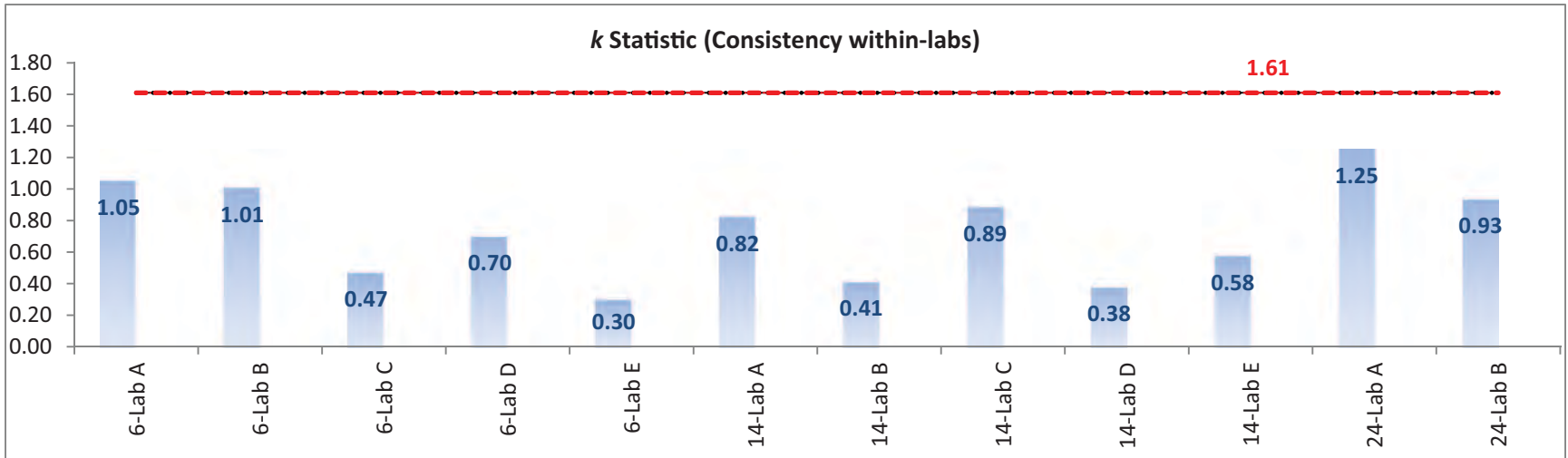


Figure 64. Plot of k statistic for three labs.

CHAPTER 5

Findings and Recommendations

Findings

This project focused on developing a recommended laboratory test to predict the initial retroreflectivity of pavement markings in the field based on the quality of the glass beads. The test was to be rapid (i.e., preparation and testing complete in 24 hours or less), repeatable and reproducible, cost-effective, practical (i.e., suitable for routine use in a state materials testing laboratory), and verified and validated through measurements of the initial retroreflectivity of pavement markings applied in the field.

The following information highlights the key findings and accomplishments in achieving the study objectives:

- Obtained bead samples that cover a wide range of retroreflectivity values, all of which meet the specification for AASHTO M247 beads.
- Conducted sufficient laboratory tests to measure the physical bead properties of each bead sample, including additional features such as color and percent air inclusion, which are not covered within the AASHTO M247 specification.
- Evaluated the relationships these bead properties have with retroreflectivity and determined that, although trends exist, no definitive relationship can be defined.
- Showed that a drawdown procedure can result in satisfactory bead distribution and embedment, which supports quantifying potential bead retroreflectivity.
- Developed a drawdown test method, which was proven to be repeatable and reproducible based on an interlaboratory study of five labs.
- Developed and validated a statistically significant relationship between laboratory and field retroreflectivity based on roadway surface type (hot-mix asphalt and concrete pavements).
- Developed a drawdown testing procedure that meets the project objectives and validated the procedure through a proof-of-concept study, laboratory study, ILS study, and field implementation (using a long line striping truck).

The recommended drawdown testing procedure is described in the following.

Proposed Drawdown Test Procedure

The test procedure developed in this research follows in the format of a proposed AASHTO standard method of test.

Standard Method of Test for Producing Drawdown Panels and Measuring the Coefficient of Retroreflected Luminance (RL) of Pavement Markings in a Laboratory Panel

1. Scope
 - 1.1 This test procedure is used to determine the retroreflectivity of AASHTO M247 Type I highway beads. Beads are dropped on top of a uniform thickness of paint, and retroreflectivity is determined with a reflectometer.
2. Referenced Documents
 - 2.1 ASTM standards
 - D7585-10, Standard Practice for Evaluating Retroreflective Pavement Markings Using Portable Hand-Operated Instruments (Replacing D6359).
 - E691, Practice for Conducting an Interlaboratory Study to Determine the Precision of a Test Method.
 - E1710, Test Method for Measurement of Retroreflective Pavement Marking Materials with CEN-Prescribed Geometry Using a Portable Retroreflectometer.
 - 2.2 Other standards
 - Alternate Bead Sampling Method AASHTO TP97-11.
 - CEN-EN 1436, Road Marking Materials—Road Marking Performance for Road Users.
 - AASHTO M247.
 - FED SPEC TT-P-1952E.

3. Terminology

3.1 *Coefficient of retroreflected luminance, R_L* —the ratio of the luminance, L , of a projected surface to the normal illuminance, E , at the surface on a plane normal to the incident light, expressed in candelas per square meter per lux [(cd·m⁻²)/lx]. Because of the low luminance of pavement markings, the units commonly used are millicandelas per square meter per lux [(mcd·m⁻²)/lx].

3.2 *Portable retroreflectometer*—an instrument that can be used in the field or laboratory for measuring the coefficient of retroreflected luminance, R_L .

4. Significance and Use

This test procedure is used to predict the retroreflectivity of AASHTO Type I glass beads in waterborne paint using a laboratory simulation of a field striping operation. Measured quantities of glass beads are dropped on top of a repeatable, uniform thickness of paint on top of a glass panel. When the paint is dry (after 24 hours), the retroreflectivity is measured using a 30-m geometry portable reflectometer.

One of the characteristics of a pavement marking is the coefficient of retroreflected luminance, R_L . Under identical conditions of headlight illumination and driver viewing, larger values of R_L correspond to higher levels of visual performance at corresponding geometry.

5. Apparatus

- 5.1 For waterborne paint, water for cleanup.
- 5.2 A 4-in. drawdown bar; thickness capability from 15–30 mils (375–750 microns).
- 5.3 Flat substrate, 6 in. by 24 in., made of 1/8-in. glass, aluminum, or slate.
- 5.4 Support fixture to hold substrate firmly in place during drawdown.
- 5.5 Balance to 0.01 g accuracy.
- 5.6 Splitters to obtain representative glass bead sample (large 16:1, small 1:1).
- 5.7 Weighing dishes and containers for beads and paint.

5.8 Bead drop box (see Figure 65) with dimensions of approximately 5½ in. by 19½ in. by 14 in. (producing a 4-in. by 18-in. stripe) filled with 10 layers of ¼-in. screening spaced 1 in. apart, with a support bar to hold beads in swivel mounted on top.

5.9 Reflectometer, 30-m geometry based on retroreflective measurements made with portable hand-operated instruments in compliance with test method E1710.

5.10 Paint film thickness gauge, 5–30 mil (125–750 microns).

5.11 Magnifying glass to check glass bead embedment.

6. Sampling

A representative sample of glass beads should be taken following AASHTO M247 procedures. The sampling shall be random in the following ratios: 100 lbs (45 kg) of sample (in full bags) per 10,000 lbs (4,535 kg) shipped. Upon arrival, material shall be reduced in a sample splitter to a size of approximately 2.2 lbs (1 kg).

7. Calibration

The drawdown procedure must be calibrated to ensure that the correct thickness of paint is applied. The reflectometer must be calibrated in accordance with the manufacturer's instructions. The retroreflectivity is dependent on the paint formula in addition to the glass bead quality. Use a control paint to compare glass bead retroreflectivity (Sherwin-Williams TM2152 White).

7.1 Paint thickness calibration procedure

- Choose a drawdown bar opening (to achieve 15 mil of paint, start with a 30-mil blade opening).
- Pour enough paint into the drawdown bar to ensure coverage over the full 18-in. panel, approximately 100 mil (Figure 66).
- Draw the drawdown blade in a smooth manner down the plate.
- Immediately place the drawdown blade into water to make cleanup easier.

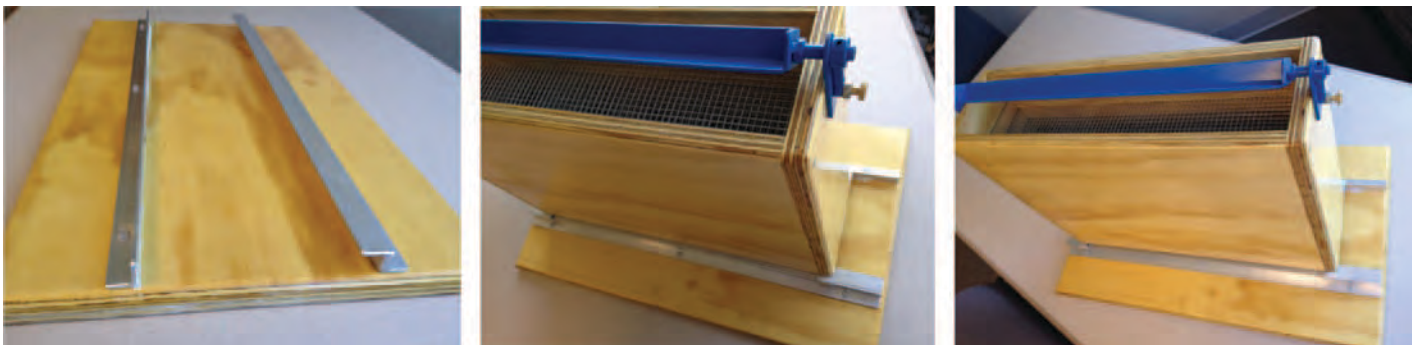


Figure 65. Bead drop box.



Figure 66. Paint drawdown process.

- Stick the paint film thickness gauge into the wet paint and read the paint thickness.
- Use a different mil thickness accordingly. (If 30 mil open yields 20 mil wet, use a smaller mil opening like 25 mil to achieve the desired 15-mil wet paint.)
- Repeat previous steps to check the resulting wet paint thickness.

7.2 Retroreflectometer calibration

- Follow manufacturer recommendations.

8. General Procedure

- 8.1 Use a large splitter to get a 2.2-lb (1-kg) bead sample and then a small splitter to get final sample sizes

(Figure 67). Split sample to approximate weight for area of paint coverage on substrate. For a 4-in. by 18-in. stripe at 15 mil with 8 lbs per gallon of beads: 17 g. This rate is equivalent to 0.236 g of beads per 1 square in. of paint.

- 8.2 Pour beads from weighing dish evenly onto the bead support bar on top of the drop box; see Figure 68.
- 8.3 With panel in support fixture, place the 30-mil (750-micron) edge of the drawdown bar on top of the panel. (This should produce a 15-mil wet thickness. Check with thickness gauge.)
- 8.4 Weigh out waterborne paint required. Stir paint thoroughly and pour into the drawdown bar. Note: Steps 4 through 7 must be completed within 20 seconds to avoid having the paint change viscosity on curing.
- 8.5 Pull the drawdown bar across the length of the panel at a consistent speed to spread a uniform layer of paint. Place a paper towel at the end of the panel to catch excess paint. A straight edge along the length of the panel insures properly applied paint.
- 8.6 Immediately after sliding the drawdown bar and after the paper towel is removed from the support fixture, place the bead drop box over the panel and dump the beads.
- 8.7 Lift the bead drop box a few inches directly above the panel and bump it to dislodge any retained beads. Clean drawdown bar with water immediately.
- 8.8 Store panel in horizontal position for 24 hours.
- 8.9 After 24 hours, use a soft bristle brush to remove any loose beads on the surface of the panel using three light strokes in one direction. Check embedment to make sure paint is covering about 60% of the bead height.



Figure 67. Large splitter 16:1 (left) and small splitter 1:1 (right).

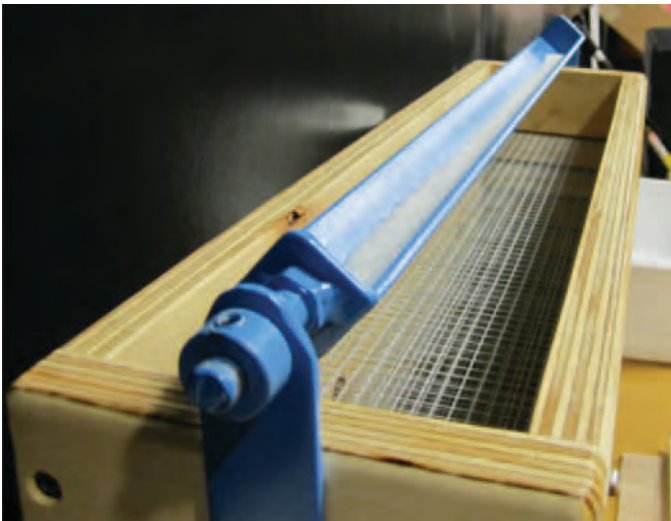


Figure 68. Drop box bead support bar.



Figure 69. Drawdown blade.

8.10 Determine retroreflectivity (using the appropriate instrument instructions) by taking five readings on each panel in the direction in which the paint was applied. Make sure the reflectometer and panel are on a flat, even surface.

8.11 Calculate the average of the readings and report.

9. Test Report

Test report should include the following:

- 9.1 Date.
- 9.2 Operator.
- 9.3 Paint used.
- 9.4 Lot number of glass beads tested.
- 9.5 Bead supplier, plant.
- 9.6 Weight of glass beads used in drawdown.
- 9.7 Paint thickness desired.
- 9.8 Drawdown blade used.
- 9.9 Time of drawdown production.
- 9.10 Temperature.
- 9.11 Humidity.
- 9.12 Time of retroreflectivity readings.
- 9.13 Average retroreflectivity reading.
- 9.14 Observations: bead embedment and coverage, lumps in paint, uniformity.

10. Factors That May Affect Measurements

- 10.1 Over embedment of glass beads will lower retroreflectivity.
- 10.2 Glass beads falling out of paint will lower retroreflectivity.
- 10.3 Paint quality will affect retroreflectivity.
- 10.4 Adding water to paint will lower retroreflectivity.

10.5 Lumps in paint will result in uneven paint thickness and will affect embedment.

10.6 Laboratory environment. (The relationships developed using this protocol are based on a temperature range of 68°F to 74°F and a relative humidity range of 32% to 50%.)

11. Appendix

11.1 Working with waterborne traffic paint

- Paint must be covered at all times, minimizing the time the container is open to prevent paint skinning on the inside cover of the paint can.
- Waterborne paint is designed to skin and dry to the touch very quickly. This necessitates working very quickly when performing this test to allow the glass beads to embed properly in the paint. If the beads are not dropped before the paint skins over, poor glass bead embedment will result.
- Paint settles quite quickly over time and has a shelf life of only 6 months.
- Paint should be stirred, never shaken. (Shaking the paint knocks dried lumps off the top of the paint can and results in lumps in the paint.)
- Paint should be screened to remove lumps.
- It is recommended that 5-gallon buckets of paint be transferred into smaller containers to ensure that, over time, each drawdown uses a consistent paint.

11.2 Drawdown blade (<http://gardco.com/pages/application/ap/8pathapp.cfm>) (see Figure 69).

References

- AASHTO. 2009. "Standard Specification for Glass Beads Used in Pavement Markings." American Association of State Highway and Transportation Officials. Washington, D.C.
- Austin, R. L., and R. J. Schultz. 2006. *Guide to Retroreflection Safety Principles and Retroreflectivity Measurements*. RoadVista, San Diego, CA.
- Australia/New Zealand Standards. 2006. "Glass Beads for Pavement Marking Materials." AS/NZS 2009–2006.
- Benz, R. J., A. M. Pike, S. P. Kuchangi, and R. Q. Brackett. 2009. *Serviceable Pavement Marking Retroreflectivity Levels: Technical Report*. Report No. 0-5656-1. Texas Transportation Institute, Texas A&M University, College Station, TX, March 2009.
- Burns, D. M., T. P. Hedblom, and T. W. Miller. 2007. "Modern Pavement Marking Systems: Relationship Between Optics and Nighttime Visibility." 18th Biennial Transportation Research Board Visibility Symposium. College Station, TX, April 2007.
- Burns, D. M., T. P. Hedblom, and T. W. Miller. 2008. "Modern Pavement Marking Systems: Relationship Between Optics and Nighttime Visibility." *Transportation Research Record: Journal of the Transportation Research Board*, No. 2056. Transportation Research Board of the National Academies, Washington, D.C., pp. 43–51.
- Carnaby, B. 2006. "Ten Years of Pavement Marking R&D to Improve Road Safety." Potters Asia Pacific. 22nd ARRB Conference—Research into Practice, Canberra Australia.
- Dale, J. M. 1967. *NCHRP Report 45: Development of Improved Pavement Marking Materials: Laboratory Phase*. HRB, National Research Council, Washington, D.C.
- Federal Specification. 2007. *Beads (Glass Spheres) Retro-Reflective*. (TT-B-1325C). U.S. Department of Transportation, Washington, D.C.
- Federal Highway Administration. 2003. *Standard Specifications for Construction of Roads and Bridges on Federal Highway Projects*. U.S. Department of Transportation, Washington, D.C.
- Gates, T. J., H. G. Hawkins, and E. R. Rose. 2003. *Effective Pavement Marking Practices for Sealcoat and Hot-Mix Asphalt Pavements*. Report No. 0-4150-4. Texas Transportation Institute, Texas A&M University, College Station, TX, August 2003.
- Graco. 2010. http://www.graco.com/Internet/T_PDB.nsf/SearchView/LineLazerIV5900Auto-LayoutSystem (accessed January 2010).
- Kalchbrenner, J. 1989. Large Glass Beads for Pavement Markings. *Transportation Research Record 1230*. TRB, National Research Council, Washington, D.C., pp. 28–36.
- McGinnis, R. G. 2001. *Pavement Marking Benchmarking*. Report FHWA-PA-2001-027-97-04. Pennsylvania Transportation Institute, Pennsylvania State University, University Park, PA, October 2001.
- Migletz, J., J. K. Fish, and J. L. Graham. 1994. *Roadway Delineation Handbook*. Publication No. FHWA-SA-93-001. Federal Highway Administration, Washington, D.C. August 1994.
- Mizera, C., O. Smadi, N. Hawkins, and W. Zitterich. 2009. "Pavement Marking Application: A Bead Gun Evaluation Study Using a High-Speed Camera." *88th Transportation Research Board Proceedings*. Transportation Research Board of the National Academies, Washington, D.C.
- NTPEP. 1989, 1990, 1991, 1992, 1993, 1994, 1995, 1996. *Summary of Results of Field and Laboratory Evaluations of Pavement Marking Materials*. Vol. 1: Field Evaluations. National Transportation Product Evaluation Program, American Association of State Highway and Transportation Officials.
- O'Brien, J. 1989. Embedment and Retroreflectivity of Drop-On Glass Spheres in Thermoplastic Markings. *Transportation Research Record 1230*. TRB, National Research Council, Washington, D.C., pp. 37–44.
- Photron. 2010. http://www.photron.com/index.php?cmd=product_general&product_id=4 (accessed January 2010).
- Rasdorf, W. J., G. Zhang, and J. E. Hummer. 2009. "The Impact of Directionality on Paint Pavement Marking Retroreflectivity." *Public Works Management & Policy*, Volume 13, No. 3. January 2009, pp. 265–277.
- Scheuer, M., T. L. Maleck, and D. R. Lighthizer. 1997. "Paint-Line Retroreflectivity Over Time." *Transportation Research Record 1585*. TRB, National Research Council, Washington, D.C., pp. 53–63.
- Smith, D. J., and X. Yin. 2005. *Waterborne Traffic Paint and Bead Combination 4th Generation*. Report No. OR 06-011. Missouri Department of Transportation. October 2005.
- Texas DOT. 2004. *Pavement Marking Handbook*. Texas Department of Transportation, August 2004.
- Virginia DOT. 2009. *2009 Pavement Marking Certification Study Guide*. Materials Division of Virginia Department of Transportation.

APPENDIX A

Explanation for Statistical Graphing

Visual Comparison of Group Means

Each multiple comparison test begins with a comparison circles plot, which is a visual representation of group mean comparisons, as shown in Figure A.1.

A reveal table follows the plot with means comparisons. The figure shows the alignment of comparison circles with the confidence intervals of their respective group means for the Student's t comparison. Other comparison tests widen or shorten the radii of the circles.

Overlap marks are shown for each diamond and are computed as (group mean \pm). Overlap marks in one diamond

that are closer to the mean of another diamond than that diamond's overlap marks indicate that those two groups are not different at the 95% confidence level.

Each pair of group means can be compared visually by examining how the comparison circles intersect. The outside angle of intersection shows whether group means are significantly different. Circles for means that are significantly different either do not intersect or intersect slightly so that the outside angle of intersection is less than 90 degrees. If the circles intersect by an angle of more than 90 degrees or if they are nested, the means are not significantly different.

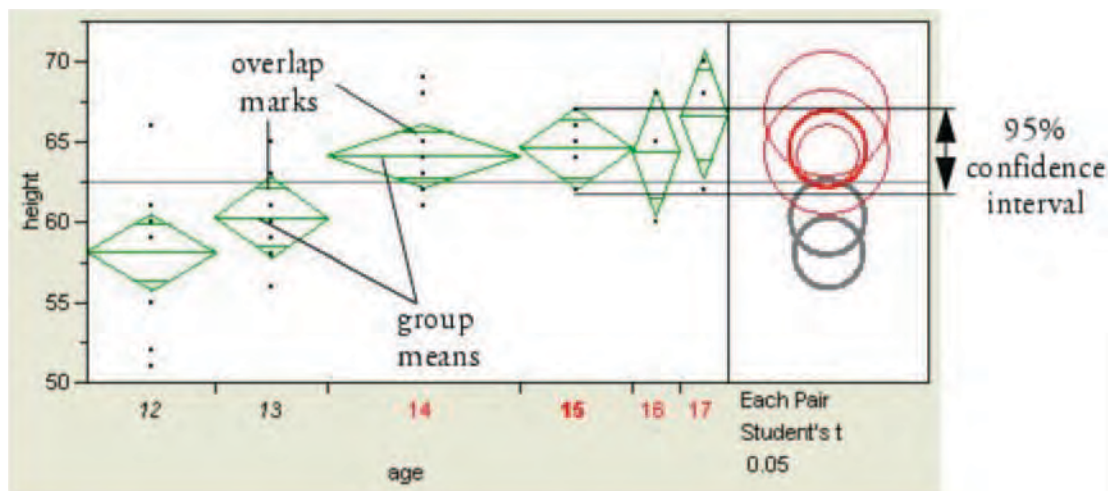


Figure A.1. Visual comparison of group means.

Abbreviations and acronyms used without definitions in TRB publications:

AAAE	American Association of Airport Executives
AASHO	American Association of State Highway Officials
AASHTO	American Association of State Highway and Transportation Officials
ACI-NA	Airports Council International-North America
ACRP	Airport Cooperative Research Program
ADA	Americans with Disabilities Act
APTA	American Public Transportation Association
ASCE	American Society of Civil Engineers
ASME	American Society of Mechanical Engineers
ASTM	American Society for Testing and Materials
ATA	American Trucking Associations
CTAA	Community Transportation Association of America
CTBSSP	Commercial Truck and Bus Safety Synthesis Program
DHS	Department of Homeland Security
DOE	Department of Energy
EPA	Environmental Protection Agency
FAA	Federal Aviation Administration
FHWA	Federal Highway Administration
FMCSA	Federal Motor Carrier Safety Administration
FRA	Federal Railroad Administration
FTA	Federal Transit Administration
HMCRRP	Hazardous Materials Cooperative Research Program
IEEE	Institute of Electrical and Electronics Engineers
ISTEA	Intermodal Surface Transportation Efficiency Act of 1991
ITE	Institute of Transportation Engineers
MAP-21	Moving Ahead for Progress in the 21st Century
NASA	National Aeronautics and Space Administration
NASAO	National Association of State Aviation Officials
NCFRP	National Cooperative Freight Research Program
NCHRP	National Cooperative Highway Research Program
NHTSA	National Highway Traffic Safety Administration
NTSB	National Transportation Safety Board
PHMSA	Pipeline and Hazardous Materials Safety Administration
RITA	Research and Innovative Technology Administration
SAE	Society of Automotive Engineers
SAFETEA-LU	Safe, Accountable, Flexible, Efficient Transportation Equity Act: A Legacy for Users (2005)
TCRP	Transit Cooperative Research Program
TEA-21	Transportation Equity Act for the 21st Century (1998)
TRB	Transportation Research Board
TSA	Transportation Security Administration
U.S.DOT	United States Department of Transportation